Lehrstuhl für Gebäudetechnologie und klimagerechtes Bauen
Technische Universität München

Robust optimization of load management potential and energy consumption

Study on refurbishment strategies for the residential building stock

Martin Gabriel

Lehrstuhl für Gebäudetechnologie und klimagerechtes Bauen

Fakultät für Architektur

Wissenschaftliche Arbeit zur Erlangung des Grades

Master of Science

an der Fakultät für Architektur der Technischen Universität München.

Betreut von

Prof. Ing. Thomas Auer

Dipl.-Ing. Manuel De Borja Torrejón, M.Sc.

Eingereicht von

Martin Gabriel

Matrikel-Nr.: 03653435

martin.gabriel@tum.de

Eingereicht am

München, den 01.03.2020

Ich versichere hiermit, dass ich die von mir eingereichte Abschlussarbeit selbstständig verfasst und keine anderen als die angegebenen Quellen und Hilfsmittel benutzt habe.

München, 17.02.2020 Martin Gabriel

Zusammenfassung

Das Ziel folgender Masterarbeit ist es, robuste Sanierungsstrategien mit Fokus auf Lastmanagementpotential und Energieverbrauch zu finden. Mittels einer vollfaktoriellen robusten Optimierung konnten konkrete Sanierungsstrategien für Wohngebäude im Bestand erstellt werden. Die Ergebnisse basieren auf mehr als 200 000. Simulationen, welche die einflussreichsten Parameter unter Betrachtung von sieben Unsicherheitsszenarien abdecken.

Folgende Kernaussagen lassen sich aus den Ergebnissen ableiten. Durch die entwickelten Sanierungsstrategien kann eine Steigerung des Lastmanagementpotentials von bis zu 122% bei gleichzeitiger Reduktion des Energieverbrauchs um 56% erreicht werden.

Als wichtigster Parameter wurde der Austausch von Radiatoren durch Fußbodenheizung identifiziert. Dieser führt zu mehr als einer Verdoppelung des Lastmanagementpotentials bei reduziertem Energieverbrauch.

Der größte Effekt kann in der Sanierung von unisolierten Bestandsgebäuden erzielt werden. Durch eine zusätzliche Dämmschicht mit einer Dicke von 4 cm, doppelt-verglasten Fenstern und einem thermischträgen Heizsystem kann das maximale Verbesserungspotential erschlossen werden. Ein noch höheres Lastmanagementpotential auf Kosten des Energieverbrauchs ist durch einen Verzicht auf eine Fassadensanierung möglich. Hier werden besonders denkmalgeschütze Gebäude als Zielgruppe identifiziert.

Die vorliegende Arbeit ist besonders für Forscher interessant, die sich mit Lastmanagementpotentialen von Gebäuden beschäftigen. Zudem kann sie als Entscheidungshilfe für Planer in der Baupraxis dienen, da konkrete Handlungsstrategien vorgeschlagen werden. Die entwickelten Erweiterungen für TRN-Lizard sowie die optimierte Parallelisierung von TRNSYS Simulationen ist für Personen relevant, die Optimierungsstudien mit TRNSYS durchführen.

Abstract

This thesis aims to develop robust refurbishment strategies for the residential-building stock. This is achieved by conducting a full-factorial robust-optimization for load-management-potential and energy-demand. The final strategies are based on data from more than 200 000. simulations, which cover the most influential design-parameters under seven uncertainty-scenarios.

The following main findings have been made in this study. The developed refurbishment-strategies increase load-management-potential up to 122% and simultaneously reduce energy consumption by 56% compared to non-optimized buildings.

The highest impact has been identified in the replacement of radiators by underfloor heating. Thus, a more than two-fold increase in load-management-potential can be unlocked at reduced energy demand.

Maximum refurbishment efficiency can be unlocked in uninsulated buildings. Upgrading the walls with an insulation layer of 4 cm, installing double glazed windows and exchanging the heating system by underfloor heating unlocks the maximum potential. An even higher load management potential can be achieved at the cost of energy demand if no refurbishment of the facade is conducted. This identifies especially listed buildings as target group.

The given study is of particular interest for researchers, who focus on the load-management-potential of buildings. Furthermore, it may act as a decision support tool for planners, since actual refurbishment strategies are provided. Additionally, the extensions implemented to TRNLizard as well as an optimized parallelization-methodology are of general interest to all researchers conducting optimization-studies with TRNSYS.

Contents

1 Introduction

30% of CO2-emissions in Germany are due to the operation of buildings [BMU, 2019]. Even though a significant emission-reduction of 44% has already been achieved between 1990 and 2018 in building operation, a further reduction of 67% is required to meet the climate goals of 2030 [BMU, 2019]. Savings can be primarily opened up in the building-stock rather than in new buildings since two-thirds of the existing buildings are still low insulated [BMU, 2019]. In the following study, refurbishment strategies are developed, which go one step beyond reducing emissions. It contributes to unlock and optimize the load managment potential of buildings by utilizing their heat storage capacity. Coupling the heating and energy sector facilitates an active contribution to the transition from fossil energy to renewables.

1.1 Background and current situation

The increasing share of renewable energies in the German electricity grid highly depends on a shift from demand-oriented power production to supply oriented power consumption. The German ministry for the environment projects a contribution of renewables of over 80% in 2050 [Nitsch et al., 2011]. The remaining power, provided by non volatile generation, is known as residual load and is needed to provide balance- and storage capacities in the grid. The expansion of renewable energies increases the demand for short term balancing power. In theory further storage capacities could supply the needed residual load, however, the restricted availability of storage options make further expansion increasingly difficult.

Up to now a major part of the residual load has yet to be provided by traditional power plants. Therefore, a further decrease of the fossil-share can only be achieved through a shift from demand-oriented to supply-oriented power production. This means that energy consumers orient their consumption on the available supply in the grid and shift load-intensive processes. This approach is also known as load management.

Load management controls energy demand by shifting loads over certain periods. Aligning the demand to the volatile energy generation allows to minimize the required amount of residual load [Hausladen, 2014]. Electrical loads are shifted to operate during peak generation hours and lessen the demand during low generation periods. Load management allows for a efficient use of the available production and grid infrastructure [Hausladen, 2014] and maximizes the utilization of renewable technologies.

Substantial load management potential has already been discovered in industrial processes [Paulus and Borggrefe, 2011] and electric vehicles [Druitt and Früh, 2012]. However, the German energy agency identified the foremost potential in the household sector [Deutsche Energie-Agentur GmbH (dena), 2012]. The main loads are constituted by electric heating and cooling, domestic hot water, and refrigeration [Deutsche Energie-Agentur GmbH (dena), 2012].

Further potential is attributed to the rising share of heat-pumps, which are increasingly used in new buildings. Unlocking the load management potentials of buildings is ascertained a significant contribution to emission reduction in literature. Therefore, load-management in buildings takes a central role in achieving the climate goals set for 2030 and 2050.

1.2 Previous studies

Several studies assessing the load management potential of buildings have already been conducted. [Deutsche Energie-Agentur GmbH (dena), 2012] examines the national load-management-potential of buildings. [Sarran et al., 2017] considers the load-shifting of thermal energy. Three studies concerning load management potential of buildings have been conducted at the Technical University of Munich.

The first study from [Hausladen, 2014] examined the fundamental load management potentials of buildings depending on their construction-typology and building-technology. It ascertained significant potentials, which can be utilized by coupling building-operations and the electric-grid. A further research project by [Auer et al., 2017] resumed the research and proved that residential buildings can play an important role in Germany's future energy system by balancing renewable energy loads. In [Jungwirth, 2014] load-management-strategies are optimized depending on a variable electricity-tariff.

The following thesis will continue the research of these studies and seek to contribute to the research with new findings. It is especially based on the methods and definitions made in [Hausladen, 2014] and [Auer et al., 2017].

1.3 Research gap

Previously mentioned studies examined load-management-potential of buildings on different scales. Each study agrees that significant load-management-potential can be unlocked in building-operation.

Therefore, further research should be conducted, which goes beyond evaluation and develops optimized strategies, which unlock load-management-potential in buildings. As stated above, the building-stock offers the greatest potential and should be of foremost consideration. Since the higher purpose is a reduction of emissions, energy-consumption should be taken into account alongside load-management-potential. Achieving robust optimization strategies is key, in order to achieve the set goals. This requires to take uncertain future conditions into account and finding an optimum, which performs well under all possible scenarios.

To summarize, a research gap has been identified in the creation of robust refurbishment-strategies, which simultaneously optimize load-management-potential and energy consumption. This is highly relevant since load management potential and energy consumption are codependent. Robustness guarantees future proof variants, even if boundary conditions are changing.

1.4 Research framework

In the following section, the study framework is derived from the research gap. It is divided into three parts: research question, research hypotheses, and research objectives. These are listed below.

The **research questions** try to reshape the identified research gap into individual answerable questions. These will be assessed in this study and answered in the end. The following questions will be addressed:

- Can an optimum be found for energy demand and load management potential?
- Can this optimum perform well under uncertain conditions?
- What are the impacts on energy demand and load management potential?

These questions lead to the following **hypotheses**, which will be tested in the course of this study and confirmed or dismissed in the conclusion.

- Robust refurbishment strategies can be defined for load management potential and energy consumption through a robust optimization.

The **Research objectives** give an overarching structure to the study and define the individual required tasks. The following objectives are set in order to test the hypothesis and answer the research questions.

- This thesis should conduct a robust optimization of energy demand and load management potential by choosing a robust optimization framework from literature and creating a TRNSYS implementation.
- Refurbishment-strategies should be developed based on a robust optimization.
- The derived optima should then be assessed regarding their improvements compared to non-optimized variants.

1.5 Overview

The following thesis can be divided in a theoretical- and a practical-part. The first can be further subdivided in fundamentals, which cover load-management, optimization and mitigation of uncertanties, and a exploration on the current state-of-research of robust-optimization in buildings.

To begin with, an exploration of the theoretical background on load management potential in building design lays the cornerstone of this thesis. It is comprised of a literature analysis of previously conducted studies with special focus on the methodology. An overview over different optimization techniques in building-simulation continues the study. Focus is laid on classifiying different optimization approaches in order to provide a basis for forthcoming chapters. An exploration of uncertainty mitigation methods concludes the fundamentals-part.

With the fundamentals being set, an in-depth exploration of the current state of research in the robust optimization of buildings follows. In this part, a selection of relevant studies is analyzed in detail and compared to each other. The findings made in this part translate directly to the framework, which defines the setup of the subsequently conducted study.

The practical part in this thesis is structured according to the stages of optimization. These are pre-processing, optimization-run, post-processing and results-analysis. In the pre-processing chapter, the model-setup as well as the parameter-choices are explained in detail. In optimization-run, the key methods applied to facilitate efficient and automatic optimization with TRNSYS are shown. The chapter post-processing deals with the post-simulation tasks required in order to bring the data into meaningful form. Finally the results are analyzed and compiled to refurbishment-strategies in the chapter results.

A final conclusion summarizes all findings of this study and evaluates if the research questions could be answered and the hypotheses proven. Furthermore, recommendations for further research are provided.

1.6 Methodology

The following section explains the applied methodology. Generally, a quantitative approach is used, which utilizes a simulation-study in order to generate test-data. Simulation setup and optimization method are derived from a literature review. A comparability to previous studies of [Hausladen, 2014] and [Auer et al., 2017] is aspired.

A literature review is used to define the set of initial parameters and intervals. The load-management-calculation methodology as well as the model setup from [Hausladen, 2014] and [Auer et al., 2017] has been adapted for this study in order to achieve comparability.

Furthermore, state-of-research optimization- and uncertainty-mitigation-methods are assessed and selected regarding their suitability. An in-depth exploration of robust-optimization studies forms the basis for choosing a simulation framework, which is divided in: design-space, scenarios, performance-indicators, robust-optimization methods, robustness-indicators and post-processing-methods.

The simulation study is based on this framework. Simulations are conducted with TRNSYS, a transient system simulation tool. The simulation for this study is implemented in the TRNSYS Grasshopper interface TRNLizard, which allows for a more modular approach and increases expandibility. All extensions that are developed are exclusively written in the programming language Python. To allow reproducability, dependencies on other Grasshopper-plugins than TRNLizard and Python were avoided. Post-processing will also be solely conducted in Python. All used Python-libraries, required for data-processing and visualization, are available in default through the Python-distribution Anaconda.

1.7 Summary

In the following section, the cornerstones of this thesis are restated:

- **Research gap**: Robust optimization of load management potential and energy consumption
- **Importance of research**: Creation of refurbishment strategies that optimize load-management potential and energy consumption under uncertain conditions

- **Research questions**:
  - Can an optimum be found for energy demand and load management potential?
  - Can this optimum perform well under uncertain future conditions?
  - What are the impacts on energy demand and load management potential?
- **Hypotheses**: Robust refurbishment strategies can be defined for load management potential and energy consumption through a robust optimization.
- **Research objectives**:
  - Conduct a robust optimization of energy demand and load management potential
  - Develop refurbishment strategies based on the robust optimization
  - Assess the improvements of the refurbishment strategies
- **Methodology**: Literature review, simulations and data-processing

Part I

Theory

2 Load management potential of buildings

The following chapter introduces the basics of load management potential of buildings. As stated by [Klobasa, 2007] and [T Rössel, F Sänger, 2012] a leading role can be attributed to buildings in the future grid infrastructure. These will act simultaneously as energy consumer, energy storage, and energy producers. In the following, an analysis of the load management potential of buildings is carried out. Special focus will be led on the studies of [Hausladen, 2014] and [Auer et al., 2017], which examined load management potential with focus on the use of thermal mass in buildings. These lay the foundation for the subsequent study.

2.1 Typologies

Load behaviour and load periods of buildings strongly depend on their typology. In [Hausladen, 2014] and [Dirlich et al., 2011] 12 main building typologies have been identified. Based on the share of typologies [Hausladen, 2014] considered residential, office, and retail buildings in a load management potential study. In [Auer et al., 2017] the focus is laid on residential, and office buildings since [Hausladen, 2014] asserted only insignificant load management potential in retail buildings, due to their neglegible amount of incorporated thermal-mass.

In [Loga et al., 2015] the residential building typology is further subdivided in: single-houses, terraced-houses, apartment-houses and large apartment-houses. However, [Auer et al., 2017] assumes that single-family houses and apartment buildings sufficiently represent the residential building stock with a total share of over 80 %.

2.2 Age classes

Within each typology, the year of construction is the decisive factor for energy consumption. With higher age, energy consumption strongly increases, particularly due to lower insulation levels. It is therefore

crucial to consider the age distribution of buildings. Additionally to age-classes, the construction-type is key to load managment potentials. Espescially the thermal-inertia induced through building weight has foremost impact.
[Loga et al., 2015] subdivide residential buildings into ten age classes. [Auer et al., 2017] considered another classification to integrate non-residential buildings. The study classifies nine residential and eight non-residential age classes.

For modelling purposes [Hausladen, 2014] and [Auer et al., 2017] group age classes by building energy standard. Thereby each group can be represented by a model with typical constructions and building systems. [Hausladen, 2014] differentiates between existing buildings (built before 2002) and new ones (EnEV 2009 standard). A more detailed consideration is made in [Auer et al., 2017]. Buildings are grouped in four energy standards:

- **Low:** represents buildings built before the 1. *Wärmeschutzverordnung* (heat-protection-regulation) in 1978.
- **Medium:** represents buildings built between 1978 and the introduction of the *Energieeinsparverordnung* (energy savings regulations) in 2002
- **High:** represents new buildings built according to the baseline *EnEV 2009* requirements.
- **Very-high:** represents new buildings built in passive-house standard

2.3 Systems

The heat generation and transmission systems play a vital role in load management. The generation system defines the end energy consumption, depending on the conversion efficiency of the system (coefficient of performance).
In order to take part in load management, electric heating and cooling is necessary. It constitutes the interface between the energy grid and the useful energy demand of the building. Depending on the age class and typology, different technologies are feasible.
A direct electric heater converts electrical energy into heat. Systems can be either water-based (electric heating element) or air-based (electric convector). Due to the direct conversion, the operation is energy-intensive. The coefficient of performance (COP) is per definition one.
A night storage heater directly converts electrical energy into heat. Due to the inbuilt storage capacity, the operating time depends on electricity prices. Night storage heaters are common in older buildings and

store heat during nighttime taking advantage of lower electricity tariffs. The stored heat is then released during the daytime.

A heat pump uses electrical energy to utilize environmental energy for heating and cooling purposes. Electric power raises the temperature level of the environmental source to a usable temperature. The ratio of the electrical input to the power of the heat source depends on the temperature difference between initial and target temperature. The ratio is expressed in the COP and usually differs between 3 and 4.5, depending on the available source. Heatpumps can utilize air, soil, and groundwater as a heat source. Reversible heat pumps can provide cooling in summer and heating in winter. In [Hausladen, 2014] an annual COP of 3 is assumed.

Compression refrigeration machines apply the same working principle as heat pumps. Ambient air is used to cool down a refrigerant. Electrical powered compression and expansion adjust the heat level. In [Hausladen, 2014] a COP of 3.5 is assumed.

Analyzing load management potential of buildings requires assumptions regarding the coverage of electrical heating and cooling systems. In [Hausladen, 2014] the load management potential is analyzed, assuming that 100% electrical cooling and heating generation is available. [Auer et al., 2017] develops different refurbishment scenarios in order to forecast the future coverage of electrical systems. Both studies consider cooling to be only available in office buildings.

Thermal inertia and the available thermal storage capacity are the decisive factors in load management potential[Hausladen, 2014]. Therefore different heat transmission systems have been considered in [Hausladen, 2014] and [Auer et al., 2017].

- **Radiators** are widespread in old buildings. Radiators have a high specific heating power due to high inlet temperatures of the heat liquid.
- **Floor heating** is common in new buildings. Floor heating has an intermediate specific-heating-power due to decreased inlet temperatures. The thermal storage capacity of the screed lowers the response velocity of floor heating systems due to higher thermal inertia.
- **Concrete core activation** is common in energy-efficient office buildings and can be used for heating and cooling purposes. The low inlet temperatures result in low specific heating and cooling power. The high activated thermal mass leads to a control free system. Concrete core activation is only assessed in [Hausladen, 2014]. [Auer et al., 2017] justifies the omission of concrete core activation with the missing retrofit potential and its consequential insignificant share in the building stock.

- **Air heating** is applied in passive-house standard residential buildings. The low heat storage capacity of air can only supply a small amount of specific power at reasonable ventilation rates.
- **Air cooling** is the most common cooling transfer system in office buildings. In buildings with high cooling energy demand, a high ventilation rate is necessary.
- **Radiant cooling** can be applied as an alternative to air cooling systems. Condensation on the cooling surface poses a constraint and limits the available power.

2.4 Existing methods

Having defined the scope [Hausladen, 2014] and [Auer et al., 2017] apply similar methods to asses demand side management potential. A model is created for each typology and system and simulated with a thermal dynamic simulation engine. The simulation is carried out on representative type days. Load management potential is assessed in an external post processing based on the simulation results.

Additionally to the type day approach [Hausladen, 2014] conducted a preliminary sensitivity analysis with constant boundary conditions (irradiation, ambient temperature, internal gains). Following parameters were examined: building envelope, thermal mass, conditioning system, ventilation system, internal gains.

[Hausladen, 2014] defines 7 type days for Munich (table 2.1) representing typical climate conditions.

type day	range	Tmean	Imean	share
very cold	<-5	-7.7	23	14
cold	-5 - 0	-1.8	43	36
cool	0 - 4.5	2.1	71	72
moderate	4.5 - 13	9.2	110	123
warm	13 - 18	15.5	175	68
hot	18 - 20	19.8	210	29
very hot	>20	21.6	270	23

Table 2.1 Classification of type days in [Hausladen, 2014]

Based on the mean temperature and irradiaton days are grouped in 7 categories. For each category the mean values are computed and a type day selected as close as possible to this value. The type days very cold, cold, and cool represent the heating period. Moderate stands for the transitional periods in spring and autumn. Warm, hot, and very hot typify summer days without heating- but with cooling demand in non-residential buildings [Hausladen, 2014].

As defined above, load management potential is the amount of energy demand that can be shifted within certain constraints. More specifically, for buildings load-management potential is the amount of power that can be activated or deactivated. The comfort-band limits the duration of the load-management measure. Thermal mass plays a vital role in load-management due to its ability to store energy. An activation of the conditioning systems charges the thermal mass. A deactivation discharges the stored heat. In [Hausladen, 2014] thermal comfort boundaries are assumed to be 20℃ - 24℃ in winter and 22℃ - 26℃ in summer. Load management measures are only undertaken within the comfort range.

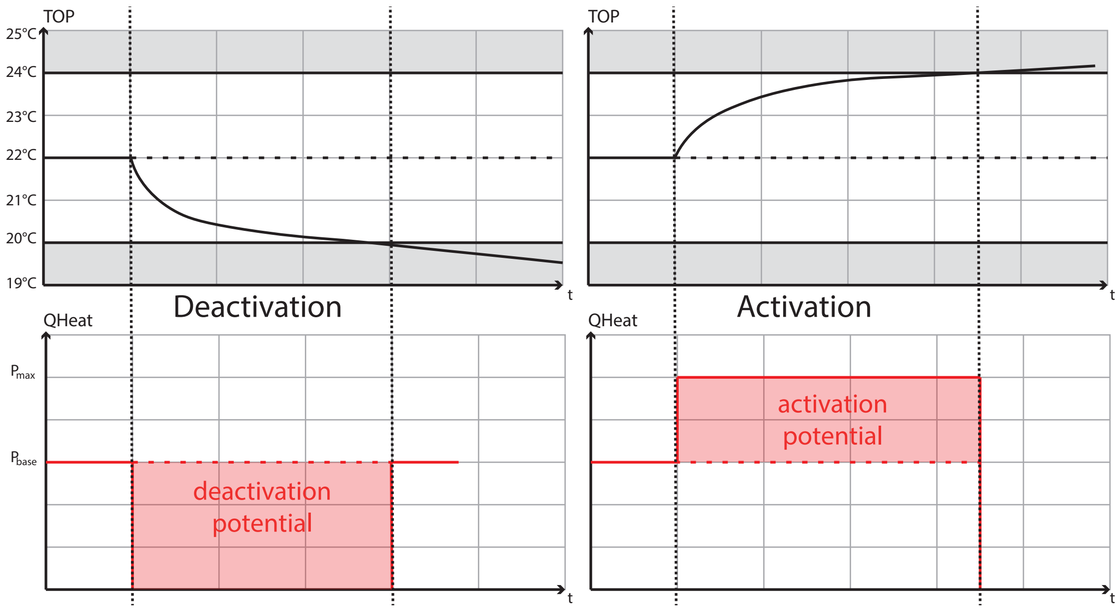

Figure 2.1 Load management calculation in [Hausladen, 2014]

Figure 2.1 shows the principle how load management potential in [Hausladen, 2014] is calculated. To assess load management potential [Hausladen, 2014] compares a base-simulation with constant heating setpoint to a load-management-simulation with a variable heating setpoint. The setpoint of the load-management-simulation will then either be lowered or increased. Consequently, power consumption and temperature in the corresponding simulation will change as well. The load-management-time in [Hausladen, 2014] is the duration the operative temperatures stay within the comfort band. After the load management strategy is initiated, the power consumption of the base-case and the load-management simulation are compared to assess the available load management potential. Since the power is time-dependent, load-management potential can not be calculated simply over the product from time and power [Hausladen, 2014]. Instead, load management potential is computed by integrating the power over the load-management-time. The load management potential can be understood as the area between the power consumption of the base-simulation and the load-management-simulation.

Therefore **Deactivation potential** depends on the maximal load-management-time and the power consumption of the base-simulation that can be switched off. **Activation potential** depends on the load-management-time and the difference between base-case power and maximal available power. If the base case is already operating near the power limit of the heating system, activation potential will be small. In a real building, conditioning power and load management time depend upon various variables. During the daytime, solar gains lead to long shut off times. However, lower demand for heating power counteracts this effect. In Figure 2.2 an exemplary deactivation potential curve from [Hausladen, 2014] is displayed. The left chart depicts the significant time dependence of deactivation potential. In that specific case [Hausladen, 2014] identifies a maximum load-management potential at 6 am since a high load-management-time of over 12 hours comes together with a high deactivation power. Except for a peak at 6 am, load-management-potential stays constant even though deactivation time varies widely.

[Hausladen, 2014] differentiates between short-term and long-term load-management potential. Short-term potential should support the grid in brief timeframes for up to two hours. Long-term potential utilizes the whole time-span in which operative temperatures are within the comfort band. Simulation models in

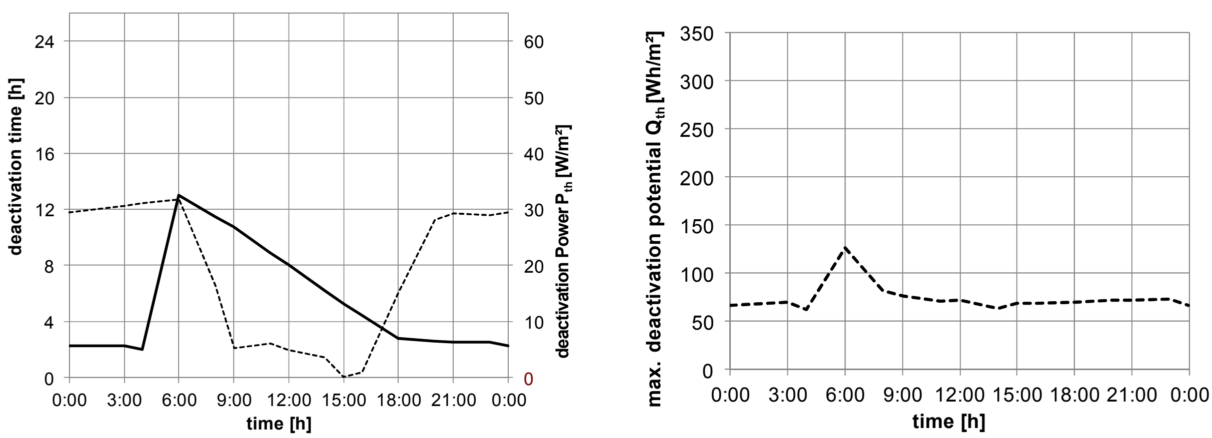

Figure 2.2 exemplaric deactivation potential [Hausladen, 2014]

[Hausladen, 2014] and [Auer et al., 2017] are reduced to one zone to keep modeling effort at bay. [Hausladen, 2014] consider a building as a group of similar units and uses that unit as study object. For example a multi-family-home can be interpreted as a accumulation of flats. A single-flat is therefore an adequate representation of the building typology. Typical values for geometry and size for each typology guarantees scalable results. In [Loga et al., 2015] a detailled assessment of the residential building-stock has been done. This data establishes a basis for the study of [Auer et al., 2017]. In [Hausladen, 2014] further sources have been consulted in order to define characteristic constructions: [Dirlich et al., 2011] [Discher et al., 2010], [BMVBS, 2009]. Further model definitions are based on DIN 18599, DIN 4108, EnEV 2009, and EnEV 2014.

2.5 Results

The following section summarizes the results of the analyzed studies. In section 2.5.1 the sensitivity of load management potential is assessed. Section 2.5.2 considers the load management potential of different typologies.

2.5.1 Sensitivity analysis

[Hausladen, 2014] examined building envelop, thermal mass, conditioning system, ventilation system, and internal gains in a preliminary sensitivity analysis. Each parameter was individually adapted to evaluate its impact. [Hausladen, 2014] concludes that constructive attributes and the conditioning system have a significant impact on load management potential. Less sensitive are parameters depending on the building usage. Nevertheless, building usage parameters are still responsible for deviations over 100%. [Hausladen, 2014] identified a maximum of load-management-potential in buildings with high thermal mass and concrete core activation systems. A building envelope constructed according to EnEV 2009 achieves maximum potential. A further increase of insulation level leads to reduced available power and a significantly impaired load management potential. [Hausladen, 2014] showed that lower insulation levels obtain good results for short time-spans. Therefore, existing buildings might be especially applicable to mitigate short-term fluctuations. On the other hand, new buildings are capable of providing long-term load management potential with little power.

2.5.2 Typology study

[Hausladen, 2014], and [Auer et al., 2017] make a typology specific analysis of load-management-potential. The objective was to assess the potential of various typologies and age-classes under instationary conditions. For each typology, age class, and system, a simulation model was developed and assessed on different type days.

Findings from the typology study underline the results of the sensitivity analysis. Transmission systems with high thermal inertia as well as high thermal mass generate maximal load management potential. Tables A.2 - A.8 in the appendix summarize the results in [Hausladen, 2014]. The office building with concrete core activation performs best in terms of overall load management potential. The high thermal mass makes it suitable to buffer thermal energy to relieve the power grid. Due to the low specific power, activation potential is predominant.

In the case of Germany residential buildings lack load management potential in summer because of the absence of cooling systems. In [Hausladen, 2014], the new apartment house performs worst due to the combination of radiator heating and high thermal insulation level. In comparison, single-family houses with a similar insulation level and floor heating provide significantly more load management potential. Following conclusions have been drawn in [Hausladen, 2014]:

- The higher power consumption of old buildings leads to higher deactivation power. However, shorter deactivation time balances the resulting load management potential.
- Switchable power dominates short-term load management potential. Load-management-time is the key factor for long-term load management.
- Load management potential in residential buildings is independent of the daytime. In non-residential buildings, a strong correlation exists due to strict utilization times.
- In most cases, residential buildings have lower short-term activation potentials. Due to higher long-term potential residential buildings prevail in mean activation potential.

2.6 Application

[Hausladen, 2014] has proven the theoretical potential for load management in buildings. Further development has been made detailing the integration between buildings and the electricity grid.

[Jungwirth, 2014] developed a model predictive control for flexible consumption of heating- and cooling energy. The study utilizes electricity price as an indicator of renewable energy share in the grid. In a sim-

ulation model, load management is implemented through a control algorithm. [Jungwirth, 2014] applies the algorithm on an exemplary office unit with concrete core activation and a heat pump system. Control objectives are electricity price and operative temperature. Integrating penalty costs for occupation times outside the comfort band guarantees a feasible solution with a minimum of comfort violations. [Jungwirth, 2014] results prove a reduction of electricity costs up to 63% using the algorithm compared to the reference application.
[Auer et al., 2017] investigates the implications that load management in buildings can prove for national power supply. Refurbishment scenarios assess the increase in electric heating systems in different frameworks. Based on these estimations, an optimized power system model has been created and assessed concerning electricity demand, the share of renewable energies, and CO2 emissions. Coupling the heat demand and the electricity systems increases electricity demand [Auer et al., 2017]. If the goals for renewable electricity coverage are met in the future, CO2 emissions can be significantly reduced compared to a non-coupled scenario.

2.7 Summary

Various studies assessed the load management potential of buildings and their further applications. The examined studies imply that a significant load management potential in buildings can be opened up with a higher share of electric heating and cooling generation. Coupling the heating sector with the electricity system creates mutual benefits, resulting in lower building operation costs and higher utilization of renewable energies. Furthermore, load management in buildings has the potential to contribute to the drastical reduction of CO2 emissions.
A sensitivity analysis showed that load management potential in buildings mainly depends on thermal mass and the heat transmission system. In a nutshell, high thermal mass and systems with high inertia result in a maximized potential. Existing buildings generally tend to have short-term load management potential with high loads to be switched. New buildings can shift smaller loads over a longer period.

3 Optimization

"Optimisation theory encompasses the quantitative study of optima and methods for finding them" - Beightler et al. in [Goldberg, 1989]

Optimization is an increasingly relevant topic in building science. According to [Nguyen et al., 2014a], publications on optimization studies more than tripled in building science between 2000 and 2010. The availability of computing power makes it feasible to conduct multiple simulations in order to find an optimum. The following sections summarize optimization fundamentals with a focus on building energy simulation.

In mathematics, optimization is defined as a method to find the best solution from the whole set of alternatives. It uses an iterative or analytical approach [Nguyen et al., 2014a]. In practice, the focus of optimization is to find the best possible solution in a feasible manner. Primarily, the solution will be an approximation of the mathematical optimum. Studies on building performance simulation developed different optimization methods. These methods can be classified in mathematical and non-mathematical optimization [Nguyen et al., 2014a] [Maderspacher, 2017]. The individual methods can be assessed depending on their accuracy, efficiency, and implementation. The following section will look into methods (section 3.1), how optimization problems are classified (section 3.2), the applied models (section 3.3), and the stages involved (section 3.4).

3.1 Classification of optimization methods

In following section different types of optimization methods are examined and classified. A distinction between mathematical optimization (section 3.1.1) methods and non-mathematical optimization methods (section 3.1.2) is proposed.

3.1.1 Mathematical optimization

Mathematical optimization finds an optimum for building models using an numerical or analytical approach. The analytical approach searches for the optimum by solving the underlying equations. Due to the complexity and number of equations an analytical approach is unfeasible in building simulation. On the contrary, numerical optimization is an iterative method. Each iteration seeks to achieve higher convergence to a solution [Nguyen et al., 2014a]. The algorithm computing each subsequent step differentiates the methods [Nguyen et al., 2014a]. In building simulation *heuristic* algorithms are foremost applied, which do not necessarily result in the global optimum, but in a close approximation [Evins, 2013]. Following common mathematical optimization methods are used in building simulation.

- **Direct search**: This method searches for an optimum through looking at the course of previous results and developing a further strategy from it. Direct search methods constitute efficient optimization methods although they have a tendency to find local optima instead of the global optimum [Evins, 2013]. Direct search has been applied in [Hooke and Jeeves, 1961] [Bouchlaghem and Letherman, 1990], [Al-Homoud, 2005] and [Al-Homoud, 2009].
- **Evolutionary algorithms**: These apply Darwins principle of the survival of the fittest. From a initital population of solutions the worst are sorted out. New options are generated through mutation of the input data. This process is repeated over several generations until an optimum has been found [Evins, 2013]. Evolutionary alogrithms have been implemented in [Tuhus-Dubrow and Krarti, 2010], [Sahu et al., 2012] and [Wang et al., 2005].
- **Gradient-based**: These are simple optimization algorithms searching to select trial points along an increasing gradient until the vertex has been reached. Due to their simplicity, they are fast converging [Nguyen et al., 2014a]. However gradient-based algorithms are highly susceptible to reaching a local optimum instead of a global. It is implemented in [Wetter and Wright, 2004].
- **Particle swarm**: These are methods that compute new trials based on the relation of current solution position and best possible solution in the swarm [Evins, 2013]. Particle-swarm optimization is applied in [Hasan et al., 2008] and [Ren et al., 2009].

Name	Utilization
Direct search	[Hooke and Jeeves, 1961] [Bouchlaghem and Letherman, 1990] [Al-Homoud, 2005] [Al-Homoud, 2009]
Evolutionary algorithms	[Tuhus-Dubrow and Krarti, 2010] [Sahu et al., 2012] [Wang et al., 2005]
Gradient-based	[Wetter and Wright, 2004]
Particle swarm	[Hasan et al., 2008] [Ren et al., 2009]

Table 3.1 Overview over mathematical optimization methods in literature

3.1.2 Non mathematical optimization

Non-mathematical optimization includes methods that do not rely on algorithms to define the points in search space. Instead, variants are either randomly selected or predefined. In order to achieve a good approximation of the optimum, sampling data has to be created over the whole input space. Consequently, non-mathematical optimization is a computational expensive optimization approach and is therefore labeled as a brute-force search method. Even though non-mathematical optimization is inefficient compared to mathematical optimization, its independence towards a mathematical algorithm guarantees a good approximation of the true optimum [Nguyen et al., 2014a]. As it does not require further verification it is commonly used to verify mathematical optimization algorithms [Hasan et al., 2008]. According to Evins, "brute force is shown to be an effective method, but with a very high computational burden" [Evins, 2013].
In building performance simulation, the design of experiment (DOE) approach is the most common implementation of non-mathematical optimization. In DOE, design parameters are changed individually in order to observe the outcome [Chlela et al., 2007]. This method is used in sensitivity analysis and optimization. The DOE simulation set leads to the optimal parameter combination. Whether all or only a fraction of all parameter combinations are assessed differentiates DOE methods [Chlela et al., 2007]:
In a full factorial experiment, a set of values is defined for each design parameter [Van Gelder et al., 2014]. Then every combinations across all values and parameters are made. If there are n values for x stages a total of n^x runs have to be conducted [Chlela et al., 2007]. Due to the exponential increase in runs, a full factorial experiment is inefficient for a high number of design parameters.
A fractional factorial experiment seeks to reduce the number of runs that are needed for a full factorial

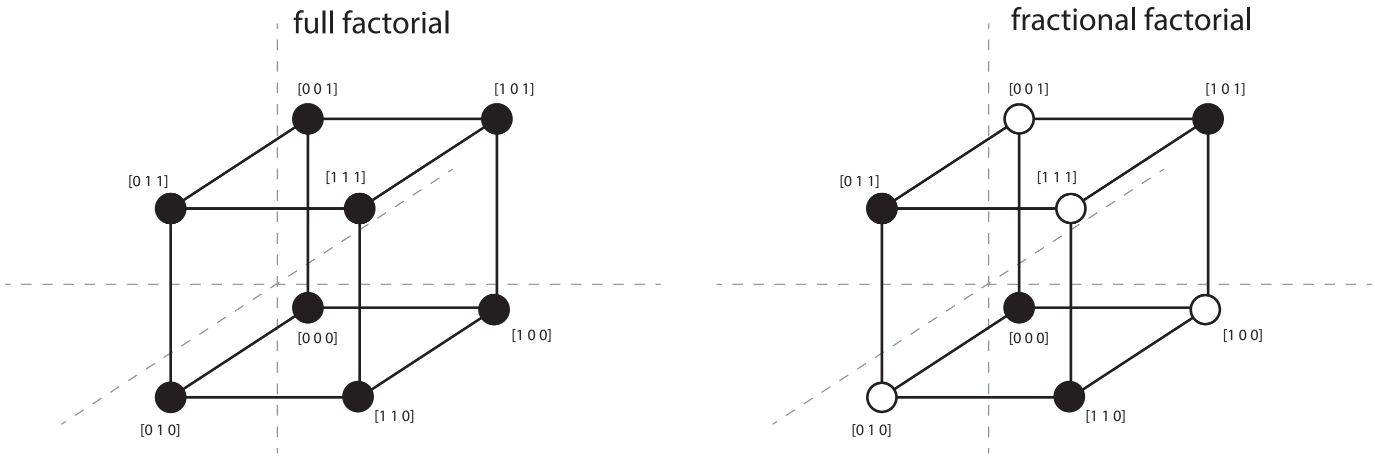

Figure 3.1 2^3 full-factorial and fractional-factorial analysis, adapted from [Macdonald et al., 1999]

experiment. It explores only a fraction of the input space. This fraction can be either determined manually by identifying technical constraints and infeasible parameter combinations or using the Taguchi method [Chlela et al., 2007]. It reduces the number of runs needed for a full factorial experiment without decreasing the significance of the result [Macdonald et al., 1999].

3.2 Classification of optimization problems

Optimization problems can be classified according to the embedded framework. Adapted from [Roy et al., 2008], [Sahab et al., 2013] and [Nguyen et al., 2014a] following categories are applicable for mathematical and non mathematical functions:

- **Number of design parameters:** Depending on the number of design parameters optimization problems are classified as *one-dimensional-* or *multi-dimensional-* optimization problems.
- **Nature of design parameters:** The nature of design parameters can be differentiated in *independent* parameters if they do not influence each other or *dependent* parameters. Independent design parameters can be *static* if they do not depend on any other factor, otherwise they are classified as *dynamic*. If parameters are subject to uncertainty the optimization problem is termed deterministic optimization. Parameters are then considered under a *probability distribution*.
- **Number of target parameters:** Depending on the number of target parameters (non mathematical) or objective functions (mathematical) optimization problems can be differentiated in *single-objective* or *multi-objective* optimization problems.

- **Presence of constraints:** Depending on the presence of constraints optimization problems are classified as *constrained* or *unconstrained*. Out of all possible solutions constraints define the feasible solutions.

3.3 Classification of optimization models

In literature review, three dominating modelling approaches to optimization in building performance simulation have been found.

3.3.1 Full-model

Full simulation models represent the most common approach to building simulation optimization [Machairas et al., 2014]. According to [Machairas et al., 2014], the most common programs are *TRNSYS, IDA-ICE, DOE2, EnergyPlus, and APACHE*. These programs are capable of modeling all relevant physical phenomena occurring in buildings. They use climate data, geometry, materials, occupancy, and parameters of the HVAC system [Machairas et al., 2014]. In order to apply optimization algorithms, script-based automation is necessary. Programs like GenOpt automate the coupling between optimization algorithms and building simulation programs [Bandara and Attalage, 2012]. This has been applied in [Hasan et al., 2008], [Hamdy et al., 2009] and [Hamdy et al., 2011]

3.3.2 Simplified-model

In a simplified simulation model, aspects of a full simulation model are reduced to a set of equations. Thus, it can be used to run time-intensive optimization methods (e.g., brute-force search) in a significantly lower duration. Due to the creation effort it is only feasible for specific problems [Machairas et al., 2014]. Commonly, the results of a simplified simulation model are used as pre-screening for a detailed analysis with a full simulation model. This has been applied in [D'Cruz and Radford, 1987] [Castro-Lacouture et al., 2009], [Marks, 1997] and [Adamski, 2007]

3.3.3 Meta-model

Meta-models are also known as surrogate models [Van Gelder et al., 2014]. They "aim at mimicking the original simulation model, but with a highly reduced calculation time" [Van Gelder et al., 2014]. Metamodels

Type	Description
Full-model	[Hasan et al., 2008], [Hamdy et al., 2009], [Hamdy et al., 2011]
Simplified-model	[D'Cruz and Radford, 1987], [Castro-Lacouture et al., 2009], [Marks, 1997], [Adamski, 2007]
Meta-model	[Wong et al., 2010], [Magnier and Haghighat, 2010], [Zemella et al., 2011]

Table 3.2 Overview over applied optimization models in literature

approximate full simulation models with statistical tools. The use of machine learning algorithms as meta-models is the most used approach. In them, a full simulation model creates the needed data to fit and test the machine learning algorithm. Artificial neural networks are the most common type of machine learning algorithms applied in building simulation [Machairas et al., 2014]. This has been applied in [Wong et al., 2010], [Magnier and Haghighat, 2010] and [Zemella et al., 2011]

3.4 Classification of optimization stages

[Nguyen et al., 2014a] identified a optimization process that is commonly applied in building performance simulation. It can be subdivided in three steps: pre-processing, optimization-run and post-processing [Nguyen et al., 2014a]. Following section will explore each of this stages in detail.

3.4.1 Pre-processing

Pre-processing can be further differentiated in three tasks: Definition of the optimization problem, parameter screening and meta-model creation.

1. **Definition of the optimization problem:** In the first step of optimization, the problems and constraints are set and the model built. Furthermore, the objective function is defined, the design variables selected and the optimization methodology chosen. Finally, a coupling between the optimization algorithm and the simulation model is established in order to automate the optimization [Nguyen et al., 2014a].
2. **Parameter screening:** Parameter screening is a optional stage in preprocessing. A sensitivity analysis can be used in order to identify the most influential parameters and filter out parameters

with an insignificant impact. Thus, the search space and, consequently, the simulation time can be reduced.

3. **Meta-model creation:** If a meta-model is used, it has to be trained and tested from simulation data.

3.4.2 Optimization-run

The optimization run is the second stage of the optimization process. During the optimization-run, three main tasks arise:

1. **Convergence monitoring:** If a mathematical optimization is conducted, each iteration has to be monitored if convergence or termination criteria are met. [Nguyen et al., 2014a].
2. **Error detection:** Detecting errors during the simulation run is crucial in order to avoid issues during post-processing and minimize time delay during the simulation. Erroneous simulations can either be repeated or discarded. It is important to track failed simulations to mitigate subsequent errors.
3. **Parallelization:** Non-mathematical optimization can be run in parallel, as successive simulations do not depend on previous results. Parallelization allows for simulation time reduction. The number of simulations in parallel depends on the number of processing-cores available.

3.4.3 Post-processing

The main task in post-processing is to interpret the simulation results. However, further optional tasks include the verification of meta-models and conducting a sensitivity analysis on the results of the optimization [Nguyen et al., 2014a]. In the last step, results are visualized to improve readability.

3.5 Summary

Following findings have been made in previous section:

- Optimization methods in building performance simulation can be classified as mathematical and non-mathematical methods
- Mathematical optimization methods are time-efficient. However, they come at an increased effort of implementation and once the optimization is done, the results have to be verified.
- The number of runs in non-mathematical optimization increases exponentially to the number of explored parameters. Parallelization and fractional factorial design mitigate simulation time.

- Optimization problems can be classified according to the number and nature of design parameters, the number of target parameters, and the presence of constraints.
- Building models for optimization can be differentiated in simplified and non-simplified models. Simplified models generalize and simplify physical phenomena. Meta-models replace the full simulation model through stochastic algorithms. These simplifications allow for a reduced simulation time.
- The process of optimization can be divided into pre-processing, optimization-run, and post-processing.

4 Mitigation of uncertainty

Uncertainty in building simulation is unavoidable. Neglecting uncertainties may lead to unpredicted results and worse performance than expected. This deviation is a commonly known phenomenon and termed *performance-gap* in literature. The performance gap represents the shortcomings of the actual performance compared to the predicted performance. Assessing and mitigating uncertainties is an important step in reducing the performance gap. Following section reviews the different concepts that can be applied in uncertainty mitigation (section 4.1), the sources of uncertainty (section 4.2) as well as methods to mitigate uncertainty (section 4.3).

4.1 Concepts

In following section key concepts of uncertainty mitigation are explored. [Kotireddy, 2018] lists following concepts:

- **Reliability** is defined as the ability to perform without failure over a predefined period under specified- as well as uncertain-conditions [(IEA) International Energy Agency, 2013]. Reliability only accounts for uncertainties in building operations. It does not account for external factors or a change in building function [Chalupnik et al., 2013]. Reliability is all about maintaining initial requirements without the need for change. Therefore restructuring in order to fulfill new requirements is no part of the concept.
- **Resilience** is defined as the ability of a building to perform outside of its original intended field of application under uncertain conditions [Chalupnik et al., 2013]. Resilience mitigates uncertainties in building operation, function, and external factors [Chalupnik et al., 2013]. Resilience is understood as passive strategy, it does not actively adapt in order to fullfill new requirements under uncertain-conditions.
- **Adaptability** in buildings stands for their ability to adapt their functions or structure to cope with uncertain conditions. It mitigates uncertainties in building operations as well as external factors.

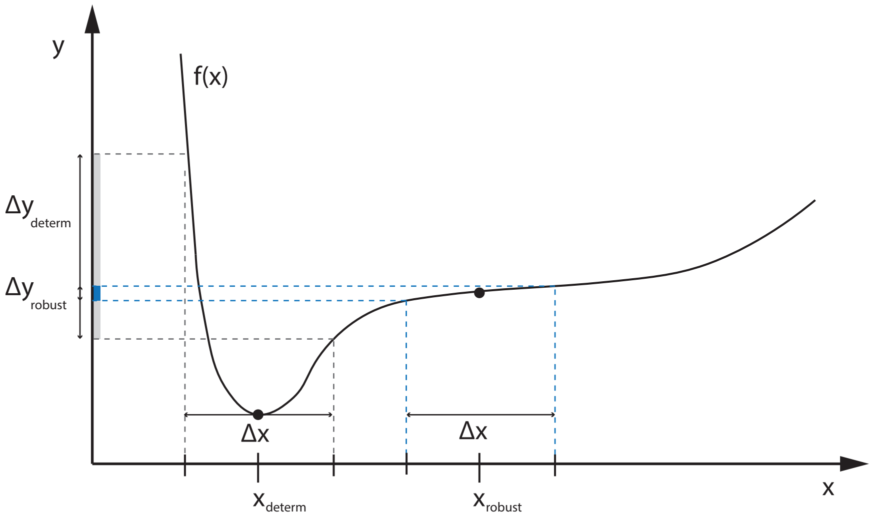

Figure 4.1 Deteminsitic and robust optimum, based on [Rhein, 2014] and [Keane and Nair, 2005]

Adaptability is an active strategy, it continuously adapts in order to meet prospective requirements [Chalupnik et al., 2013].

- **Flexibility** is defined as the building's ability to restructure easily in order to adapt to future scenarios. It allows to cope with uncertainties in building function, operation, and external uncertainties. It is an active strategy that requires future adaptation [Chalupnik et al., 2013].
- **Robustnes** is defined as the ability of a building to perform well under a wide range of uncertain conditions [Olewnik et al., 2004], [Chalupnik et al., 2013]. [Andersson, 1997] and [Bettis and Hitt, 1995] expand this definition by including environmental conditions and future scenarios. The robustness concept includes uncertainties in operation as well as external uncertainties. As it is no active strategy the initial setup has to be able to perform well over a wide range of scenarios. Figure 4.1 illustrates the concept of a robust optimum. The robust optimum is less prone to variations in the final performance under uncertainties compared to the global/deterministic optimum.

In summary, the explored concepts differ in the uncertainties they include, as well as if they require active adaption. As [Kotireddy, 2018] notes, active mitigation is not applicable in buildings. Even though adaptive construction techniques have been explored, they did not prevail. Therefore flexibility and adaptability are no suitable uncertainty mitigation concepts for buildings. Furthermore, reliability only provides basic mitigation against operational uncertainty. It is not sufficient to guarantee good performance over the whole life span as external factors may change.

Concept	Function	Operation	External factors	Active mitigation
Reliability		X		
Resilience	X	X	X	
Adaptability		X	X	X
Flexibility	X	X	X	X
Robustness		X	X	

Table 4.1 Overview over uncertainty mitigation concepts, adapted from [Chalupnik et al., 2013]

In [Anderies, 2014] robustness and resilience are compared and differentiated:
The focus in resilience is laid on a long term, large scale uncertainty mitigation. It includes catastrophic events as terrorist attacks or natural disasters. Resilience acts on an urban to national scale within a decade to century timeframe [Anderies, 2014]. The single building is integrated into a whole resilient system and is insignificant.
In robustness, the focus is laid on the single building. The considered time span corresponds with the life cycle of the building [Kotireddy, 2018].
In conclusion, robustness is more applicable in mitigating uncertainty on a small scale. Resilience, however, should be applied for an urban to regional scale. As this thesis is focused on individual houses, robustness will be further considered.

4.2 Uncertainty sources

Knowing the uncertainty sources is key in finding appropriate mitigation techniques and assess the fluctuation margin. In the following section, the main sources are listed, and their impact on the final results discussed. According to [Hopfe and Hensen, 2011], a differentiation can be made into two categories: planning uncertainties and scenario uncertainties. The first arise during the planning and building phases and remain constant over the whole lifecycle of a building. The latter arise during the usage of the building, and depend on the usage scenario and external conditions.

4.2.1 Planning uncertanties

According to [Hopfe and Hensen, 2011], [Macdonald, 2002] and [Kotireddy, 2018] planning uncertainties can be further subdivided in: design uncertainties, physical uncertainties, modelling uncertainties and numerical uncertainties. Common to all is the ability to asses them and assign them a probability distribution. The probability distributions remain constant over the whole life cycle of the building.

Design uncertainties occur during the planning phase. Due to the stepwise process of planning, uncertainties decrease with continuous design stages. Being aware of the design uncertainties and their impacts can significantly increase building performance. Providing uncertainty assessment to the planner as early as possible is therefore crucial to mitigate uncertainties. In later design stages, the implementation of changes becomes exceedingly time and cost expensive. Design uncertainties may arise from the absence of clear specifications or execution errors on the building site.

Physical uncertainties arise through the inherent fluctuations in thermophysical properties in construction materials. They are inevitable; however, they can be assessed and implemented in the design process. Main physical uncertainties according to [Macdonald, 2002] and [Kotireddy, 2018] are:

- **Thermophysical properties:** Density, Conductivity, and specific heat storage capacity are the main thermophysical properties of each material. Usually, in building simulation, each material is assigned one set of properties. However, due to differences in production, storage, transport, and assembly, thermophysical properties may vary widely [Macdonald, 2002]. Especially the moisture content is the decisive factor.
- **People gains:** Internal gains are important factors when assessing building performance. Heat gains through electrical equipment can usually be exactly quantified, however, people-gains are highly uncertain. The metabolic rate is a statistical estimation of human heat dissipation depending on the degree of activity. However, [Macdonald, 2002] shows that these values vary significantly between different persons. Furthermore, uncertainty lies in the estimation of the degree of activity.
- **Infiltration:** Several studies have shown that infiltration is of major impact on building performance [De Wit, 1997], [de Wilde and Tian, 2009] and of increasing relevance with higher insulation level. Nevertheless, determining the infiltration rate in building simulation is highly uncertain. Infiltration depends on many different factors and fluctuates depending on temperature, wind speed, and wind

direction. Due to the time consuming and error-prone manner of CFD simulations tabular values are applied in most cases . As [De Wit, 1997] and [de Wilde and Tian, 2009] showed this can lead to significant deviations between predicted and actual performance.

Model uncertainties are a result of the simplification of complex physical processes in simulation programs [Kotireddy, 2018]. An example is the simplified one-dimensional heat flux calculation applied in most building simulation software. Simplifying heat flux to only one dimension results in huge time benefits. However, heat bridges or three-dimensional component connectors cannot be taken into account. It is common practice to approximate heat flux through heat bridges by adding a certain loss factor to the entire wall.

Numerical uncertainties are due to the discretization of the simulation engine [Kotireddy, 2018]. Numerical building simulation software is based on a stepwise calculation of the heat balance. Depending on the increment, a certain uncertainty will be introduced into the model. The smaller the timestep, the lower the uncertainty.

4.2.2 Scenario uncertainties

Scenario uncertainties are inherently different from planning uncertainties. They can arise anytime during the lifespan of the building and encompass events where the probability of occurrence is unknown [Hopfe and Hensen, 2011], like usage or climate scenarios. [Hopfe and Hensen, 2011] differentiate between internal and external scenario uncertainties.

Internal scenario uncertainties originate from uncertainties in building use and operation, which include heating and cooling setpoints, lighting, ventilation, occupancy density and shading usage [Hopfe and Hensen, 2011]. These uncertainties depend heavily on the user and are practically random in their occurrence.

External scenario uncertainties originate from uncertainties in weather data or climate change [Hopfe and Hensen, 2011]. Due to the unpredictable nature of long term weather phenomena, these uncertainties are quasi-random as well.

4.3 Methods

Previously the key concepts of uncertainty mitigation and their sources have been summarized. The following section examines the different methods applied to uncertainty mitigation in building simulation.

In the literature review, four main methods have been identified: uncertainty analysis, sensitivity analysis, stochastic optimization, and robust optimization. Below the fundamentals of each method are summarized and compared.

4.3.1 Sensitivity analysis

Sensitivity analysis (SA) is used to determine the impact of parameters on the final result. It produces a ranking that shows the planner which parameters play a key role and which have only a marginal influence on the result. SA enables the planner to make informed decisions and allocate resources appropriately. Even though it is not a classical uncertainty mitigation method, it is commonly applied to determine the most sensitive paramerters and reduce their sensitivity in an iterative approach.

SA is conducted in the following steps [Wei, 2013]:

1. **Input range definition:** To begin with, the range of the input parameters has to be defined. Probability distribution and discretization are the main methods used. Probability distributions require a sampling-based simulation, such as the monte-carlo simulation (see 4.3.2). Discretization divides the input space into discrete points.
2. **Model building:** In the second step, a building energy model is created. Commonly, model creation is automated due to the high number of runs. Parametrizing the parameters in a base model allows for automated model creation. Common programs for SA are: EnergyPlus, ESP-r, TRNSYS, and DOE2 [Wei, 2013]. These programs are flexible and can be automated, due to their script-based input [Wei, 2013]. Other approaches fall back on simplified simulation models based on Matlab or VBA scripts. These can be computed quickly and can directly integrate post-processing.
3. **Simulation run:** After the setup, the models are run. This process is usually automated using a script which successively starts the simulations. The simulation run is expensive in computational time and resources. Methods like multi-core or multi-computer simulations make it possible to reduce the time [Wei, 2013].
4. **Post-Processing:** In post-processing, simulation results are gathered from the output files of all runs. Then the sensitivity analysis is conducted using the results of all runs.
5. **Visualization:** In the final step, the results are processed and visualized. Common visualization forms are scatter-plots, box-plots, tornado-plots, and spider plots [Wei, 2013].

A range of methods is available for test point selection in SA. These can be differentiated into local methods or global methods (figure 4.2).

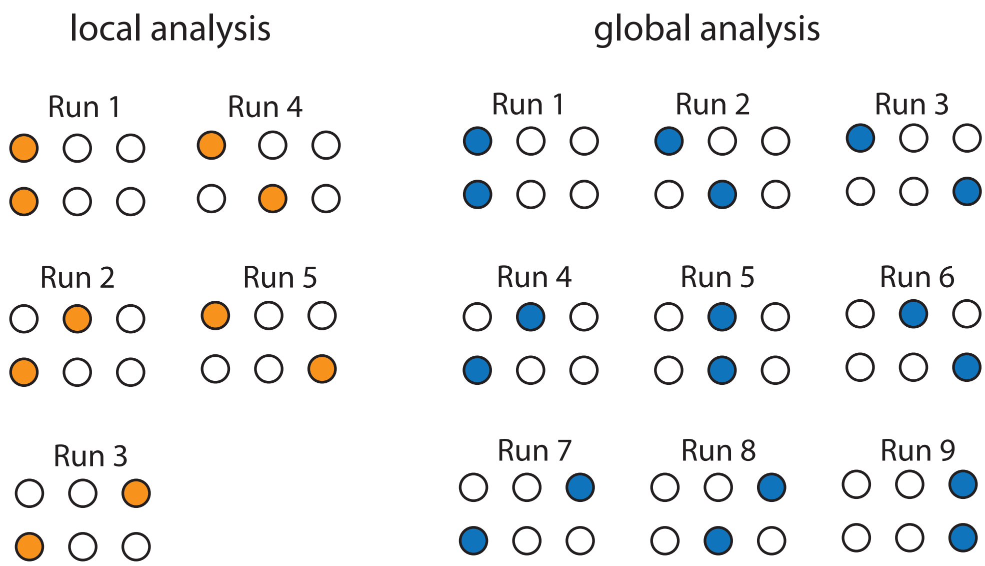

Figure 4.2 Distinction between a local and a global analysis

Local SA is commonly applied due to its simplicity and moderate computational demands. The most common method is the so-called one-factor-at-a-time (OAT) method [Wei, 2013]. In it, one factor is changed for each simulation run, while all other parameters remain unchanged. Thus, sensitivity can be determined independently for each factor with minimal computational effort. The drawback of this method is that correlations between factors are unconsidered. Depending on the nature of the parameters, this can seriously distort the result. Furthermore, the explored input space is reduced and bound to a base-case [Wei, 2013].

Global SA explores the whole input space of the input factors. Therefore results are highly reliable, as they include all factor correlations. The main drawback of global SA is the extensive computational effort required. In simple methods as full factorial (section 3.1.2) analysis, the number of runs increases exponentially with the number of parameters. Alternative methods (e.g., the regression method) have been developed to conduct a global SA in less time.

Other sensitivity analysis methods include screening-based methods, variance-based methods, and meta-model-based methods [Wei, 2013].

4.3.2 Uncertainty analysis

Uncertainty analysis (UA) focuses on determining the impact of uncertain parameters. In comparison to SA, parameters without uncertainty are neglected regardless of their sensitivity. If the most sensitive value is not susceptible to uncertainty, it is irrelevant. As stated in [Macdonald et al., 1999] and [Hamby, 1995]: *"It may be that a sensitive parameter is known to within a close tolerance, in which case uncertainty in this parameter will not lead to significant uncertainty in the predictions"*. UA is used for assessing uncertainty but not mitigating it. The approach resembles the process of SA (section 4.3.1). However, instead of an equally distributed input space, UA assigns probability distributions to each parameter.

To define the input-space, the Monte-Carlo simulation is used, which assesses probabilistic parameters through a sampling scheme. Model input samples depend on their probability distribution curve for each simulation. The most common sampling algorithm is the simple random sampling algorithm [Burhenne et al., 2010]. Other, more complex algorithms, such as Latin Hypercube sampling provide better input space coverage [Burhenne et al., 2010]. According to [Macdonald, 2009], a typical sampling size of 100 runs gives a good estimation of the uncertainty among given probability distributions.

The following steps are needed to conduct a monte-carlo-simulation [Burhenne et al., 2010].

1. For each input factor, a probability distribution is defined. Probability distributions are based on measurement data, literature review, or a Gaussian distribution if no data is available [Macdonald et al., 1999].
2. Secondly, a sample generation is generated by using a sampling algorithm. All sampling generations form a sampling set.
3. Each sample generation from the sampling set is simulated. Script-based building simulation software is preferred to automate the simulation runs (see section 4.3.1) .
4. The results are then post-processed and visualized. The data obtained from the individual results of the sampling set make it possible to create a probability assessment of the final results.

4.3.3 Robust optimization

The robust optimization (RO) approach seeks to find a robust optimum (see figure 4.1) under uncertain conditions. A scenario-based robust optimization methodology, developed in [Kotireddy, 2018] is conducted in following steps:

1. **Design space definition:** The first step in RO is the definition of the design space. Current regulation and building codes set the boundaries. Further constraints can be implemented depending on the client and their preferences.
2. **Future scenarios definition:** Secondly, uncertain parameters have to be set by defining future scenarios. [Kotireddy, 2018] suggests including occupant scenarios (e.g., number of users), us-

age scenarios (e.g., ventilation), policy scenarios (e.g., feed-in-tariffs) and climate scenarios (e.g., changing weather conditions).

3. **Performance indicator definition:** Performance indicators are the optimization objective. Depending on the decision-maker, different robustness indicators can be relevant (e.g., CO2-emissions, thermal-comfort, costs). If multiple objectives are considered, a multi-criteria performance assessment is necessary.
4. **Model building and simulation run:** Models will be created and simulated in an automated manner, similar to section 4.3.1. Mathematical or non-mathematical optimization algorithms can be applied (section 3.1.1,3.1.2).
5. **Post-processing:** Results from the simulation runs will be gathered and assessed in post-processing. In multi-objective optimization, a trade-off has to be found by using weighted objectives, a paretro frontier, or normalized robustness indicators (section 5.5).
6. **Visualization:** To visualize robustness, scatter plots are most appropriate for several performance indicators [Kotireddy, 2018]. If only a single indicator is assessed, boxplots provide a comprehensive representation of robustness.
7. **Sensitivity analysis:** In the final step, a sensitivity analysis is conducted to identify the scenarios which are most sensitive.

4.3.4 Stochastic optimization

Stochastic optimization (SO) is a method to optimize parameters under uncertain conditions. A probabilistic approach is applied, therefore probability distributions must be known for each uncertain factor.

The process of SO is comparable to that of RO (section 4.3.3). However, instead of defining scenarios, probability distributions are assigned to each parameter. The optimization problem is either a chance-constraint-problem or an ambiguously-chance-constrained-problem[Ben-Tal et al., 2009], depending on whether all uncertainties are known, or some are unknown.

[Ben-Tal et al., 2009] identified four main constraints of SO.

- The uncertain data has to be of stochastic nature. In building simulation, only specific factors can be assigned a probability distribution. More often, uncertain factors are quasi random and cannot be described by a probability distribution.
- The probability distribution of the uncertain data has to be known. Even if a parameter in building simulation is known to be stochastic, determining its probability distribution is often unfeasible. Data

for uncertain factors and their probability distributions is sparse in literature, while conducting a field test requires extensive effort and is prone to inaccuracies.

- The final result is a probabilistic optimum dependent on chance constraints. It is not applicable in conservative decision making as a residual risk remains.
- The problem is computationaly solvable. Due to the nature of the optimization algorithm, nonconvex feasible sets are often the result, making optimization difficult [Ben-Tal et al., 2009].

4.3.5 Summary

As seen in table 4.2, SO and RO are the only methods that can actively mitigate uncertainty. However, as shown in section 4.3.4, SO is severely constrained and can only be applied in specific cases where probability distributions are known. In a first assessment, RO seems best suited to mitigate uncertainty in building simulation. In the following it is individually compared to each of the other methods, to validate the assertion.

- **Sensitivity Analysis - Robust Optimization:** SA is solely an analytical tool. It measures the sensitivity of a given solution within a fixed parameter set. In contrast RO has a fixed set of uncertain scenarios; It then obtains the most feasible parameter set for all scenarios. As sensitivity analysis is a post-optimization-tool [Yu and Jin, 2012], it can not be used to achieve robust solutions.
- **Uncertainty Analysis - Robust Optimization:** UA is a post-optimization-tool. It is used to analyze the uncertainty in the given solution depending on probability distributions for each factor. Unlike RO, it can be used to asses the uncertainty of a solution but cannot be used as an optimization tool. The need to define the probability distributions is the main disadvantage, as accurate data is rarely available.
- **Stochastic Optimization - Robust Optimization:** SO and RO aim at an optimal solution under uncertainty. However, the general approaches differ. In SO, a probability distribution of each parameter has to be known. Based on this, a probabilistic optimum can be computed. The main disadvantage is the need to define probability distributions for each parameter correctly. Missing data often leads to simplified guesses [Ben-Tal et al., 2009]. In comparison, RO does not depend on probability distributions. The scenario approach allows the planner to determine the best performing option over all scenarios. Thus, it does not give a probabilistic optimum but rather a true optimum for the included scenarios.

To summarize, RO and SO prove to be the only methods that can mitigate uncertainty and not only assess it. SO is unfit for building performance simulation due to the difficulty in finding probability distributions and a probabilistic optimum. RO provides a scenario approach to uncertainty and is easy to implement. Therefore, RO is deemed to be the most fitting uncertainty mitigation approach for building simulation.

Method	**Sensitivity**	**Uncertainty**	**Distributions**	**Mitigate**
Sensitivity analysis	X			
Uncertainty analysis	X	X	X	
Stochastic optimization			X	X
Robust optimization	X	X		X

Table 4.2 Overview over uncertainty mitigation methods

4.4 Summary

Following key findings have been discussed in the previous section covering uncertainty mitigation:

- Resilience, reliability, robustness, and adaptivity have been identified as main uncertainty mitigation concepts. Robustness is the most appropriate uncertainty mitigation concept for buildings.
- Uncertainty sources are differentiated in planning uncertainties, which arise during the planning and building process, as well as scenario uncertainties, which are induced by external factors during the use of the building.
- Sensitivity analysis, uncertainty analysis, robust optimization, and stochastic optimization are the main uncertainty mitigation methods.
- Sensitivity analysis and uncertainty analysis are solely post-optimization tools applicable to evaluate the given solution.
- Stochastic optimization and robust optimization can be used to find the optimum under uncertain conditions. Due to its general applicability robust optimization is deemed the best uncertainty mitigation method for building simulation.

5 Robust optimization of buildings

> *"Robustness is the ability of a building to maintain the desired performance under uncertainties in building operation such as occupant behavior and in external conditions such as weather conditions, climate change and policy changes" [Kotireddy, 2018]*

Robust optimization is not widespread in building simulation [Nguyen et al., 2014a]. However, initial applications have been successfully conducted and published. In the following part, the state of research on robust optimization of buildings will be explored. The structure of this part follows the process of robust optimization as detailled in section 4.3.3. At first, the design space will be compared in section 5.1, section 5.2 reviews the applied uncertainty scenarios, section 5.3 the performance indicators, section 5.5 the applied robustness indicators, and section 5.6 covers the post-processing.

5.1 Design space

The range and number of design parameters define the design space. They can be classified in the following categories: insulation-, ventilation-, glazing-, geometry-, and shading-parameters.

Insulation-parameters are the thermophysical properties of the construction elements. These include thermal resistance and thermal transition resistance. Insulation-parameters are the most common parameters, applied in nearly all examined studies.

Ventilation-parameters are parameters that are involved in the active or passive air change of a building. Ventilation parameters include infiltration, mechanical air change, natural air change, and heat recovery.

Glazing-parameters are parameters that define the transparent surfaces. Thermal resistance and solar heat gain coefficient are the most important ones for thermal simulations.

Geometry-parameters comprise the geometry of the simulated building zone. Most common is the use of window to wall ratio as design parameter as well as the influence of window sill depth.

Shading-parameters are properties and control attributes of the shading system. Shading parameter include energy transmittance, control setpoints, and location.

Table 5.1 summarizes the parameter categories that are optimized in each study.

5.2 Scenarios

As seen in section 4.3.3 scenarios are the key element to robust optimization. The scenarios that are implemented are detailled in the following section. All applied scenarios are summarized in table 5.1.

5.2.1 Usage

Usage scenarios represent the potential change in utilization that can occur over a building's lifetime. Studies implement this by varying the number of occupants and equipment in a room. The following studies integrate usage scenarios in their robust optimization:

[Auer and Endres, 2017] examines the robustness of an office room under uncertain usage scenarios. Two scenarios are applied: room utilized as office space with two workplaces, room utilized as seminar room occupied by six persons and corresponding equipment. In [Auer and Endres, 2017], changing usage scenarios have a significant impact on user comfort. The energy consumption is less sensitive to usage scenarios.

In [Auer et al., 2013] usage-uncertainty is assessed by evaluating the effect additional internal gains have on building performance. The study implements an increase of internal gains by 20 W/m^2. Comfort has been found to be very sensitive to a change in internal gains [Auer et al., 2013].

Kotireddy conducts a robust optimization for residential buildings with usage scenarios in [Kotireddy et al., 2019],[Kotireddy et al., 2015] and [Kotireddy et al., 2017]. He defines four usage scenarios for the detached residential housing typology: occupation by one, two, three or four persons, covering the majority of usage scenarios for this typology in the Netherlands [Kotireddy et al., 2017]. Kotireddy finds that especially high insulated houses are sensitive to usage scenarios [Kotireddy et al., 2015].

Apart from these studies, usage scenarios are not applied, even though significant influence has been identified in [Kotireddy et al., 2017]. In order to conduct a holistic robust optimization, usage scenarios should be included.

5.2.2 Occupant behavior

Occupant behavior is considered in many studies and is an important topic in research. A performance gap between simulation and actual performance can often be traced back to occupants behaving differently than the planner envisioned. Therefore, occupant scenarios have high importance in robust optimization studies and are considered in half of the examined publications.

[Buso et al., 2015a] examines the effect of occupant behavior on the energy performance of office buildings in three different climates. Scenarios for the users' interaction with windows and shading are analyzed.

[Auer et al., 2013] assesses two occupational scenarios. Two types of users are compared, on the one side a user, who never ventilates the building, on the other side, a user, who constantly ventilates the building. Energy consumption is found to be very sensitive to the infiltration rate, especially in highly insulated buildings.

Several studies on robust optimization by Kotireddy [Kotireddy et al., 2019],[Kotireddy et al., 2015] and [Kotireddy et al., 2017] include occupant behaviour scenarios. He differentiates between three occupant types: energy-saving consumer, average energy consumer, and energy-wasting consumer. Based on this classification, Kotireddy develops scenarios for different heating setpoints, lighting and appliances use, internal gains, and ventilation rate. It is found that especially high insulated houses are sensitive to occupant behavior [Kotireddy et al., 2015].

[Van Gelder et al., 2014] considers occupant behavior uncertainties in ventilation, infiltration, and set-point temperature scenarios. [O'brien, 2013] analyses the occupant behavior on shading control.

5.2.3 Climate change

Changing weather patterns and temperatures due to climate change will have a major impact on building performance and energy usage. However, most simulations are conducted with a standard test reference year created from statistical data of the previous decades. The following studies, however, integrate climate scenarios in their robustness optimization.

[Maderspacher, 2017] optimizes the robustness of residential houses. Due to uncertain future climate conditions, he includes climatic scenarios to mitigate uncertainty. [Maderspacher, 2017] consideres different climate conditions by temperature difference to the current test reference year.

[Endres et al., 2019] explores the potential of low-tech office buildings. [Endres et al., 2019] and [Auer et al., 2013] include uncertain weather conditions through a future climate scenario as an alternative to the test reference year. [Endres et al., 2019] concluded that climate data is one of the key factors in the simulation and has a significant impact on the comfort and energy consumption.

In [Chinazzo et al., 2015a], the impact of climate uncertainty is explored in detail. He conducts a robustness assessment with 18 different weather scenarios based on different weather stations and algorithms for 2020, 2050, and 2080. The results of [Chinazzo et al., 2015a] show that the fluctuations induced through different weather files are much larger than the variations caused by improved construction.

Kotireddy examines climate uncertainty through four different climate scenarios. In [Kotireddy et al., 2019], [Kotireddy et al., 2015] and [Kotireddy et al., 2017] a change in air circulation patter and global temperature is considered in four scenarios. Kotireddy discovers the results to be less sensitive to climate uncertainties than to occupational behavior and usage uncertainties. [Kotireddy et al., 2015]

5.2.4 Technological failures

Over the lifetime of a building, technological failures are prone to happen. Experience shows that maintenance in existing buildings is often neglected and broken systems are often left unrepaired.

In [Auer et al., 2013], the uncertainty of technological failure is considered. A scenario is conducted which evaluates the building's performance with defect shading. It is found that, especially in a highly insulated building, a defect shading has a high impact on comfort. Buildings with high thermal mass are more robust towards technological failures than lightweight constructions.

5.2.5 Policy changes

Future Politics, regulations, and costs are inherently uncertain. Therefore, following studies consider policy changes in a robust optimization.

[Maderspacher, 2017] considers the cost change of energy carriers in uncertainty scenarios. The influence of the cost of energy carriers is important when considering total running costs. Especially poorly insulated houses are sensitive to energy carrier cost change.

In [Van Gelder et al., 2014], nominal energy price evolution is reflected in three scenarios. Nominal energy price has been identified as the most important parameter on net present costs, followed by sunscreen type and infiltration rate [Van Gelder et al., 2014].

5.3 Performance indicators

The Performance indicators are the target parameters of the optimization problem. The choice of a performance-indicator determines the focus of the study. In a multi-objective optimization, optimization is based on several performance indicators. Table 5.1 summarizes the performance indicators used in robust optimization research. The main areas of focus are comfort, energy, CO2-emission, and costs. Most studies examine multiple performance indicators.

The most investigated performance indicator is net- or final-energy. Second to this is the consideration of comfort in four out of ten studies. Two studies remain that take costs into account. CO2-emission is only examined in a isolated case.

5.4 Robust optimization methods

The type of optimization methods and how they are applied is examined in the following section. A differentiation in mathematical and non-mathematical optimization is made.

5.4.1 Mathematical

A detailed examination of mathematical optimization can be found in section 3.1.1. In this section, the application of mathematical optimization in robust optimization of buildings is explored.

Maderspacher performs a particle swarm optimization to optimize the robustness of residential buildings [Maderspacher, 2017]. Convergence is searched for in the median value and quantile difference of the result set of an uncertainty analysis, which is performed through a monte-carlo analysis. Maderspacher applies a meta-model to reduce simulation time. In [Maderspacher, 2017] it is derived that neuronal-networks are most suitable for the robust optimization of buildings.

[Kotireddy et al., 2019] uses a genetic algorithm coupled with TRNSYS in order to optimize robustness. A second simulation loop is integrated for each generation, performing a full factorial analysis of the scenarios. Alternatively, Kotireddy conducts the same study replacing the full factorial scenario analysis with a sampling scheme in order to reduce simulation time. It is noted in the study that latin-hypercube sampling with a sampling size of 100 provides a good approximation of the full factorial analysis [Kotireddy et al., 2019]. Kotireddy concludes that through applying a genetic algorithm combined with latin-hypercube sampling, over 99% of simulation runs can be saved in comparison to a full factorial study.

Mathematical optimization is seldom applied in robust optimization of buildings. However, the reduction of simulation runs and thus computational time opens up a great potential to run more complex studies. The main drawback of mathematical optimization is the complex integration and the need for a verification of the results.

5.4.2 Non mathematical

A detailed examination of non-mathematical optimization can be found in section 3.1.2.

In [Auer et al., 2013], a full-factorial study is performed for design parameters combined with an one-at-a-time analysis for scenarios. In order to parametrize the TRNSYS simulations, the open-source tool TRNLizard [Frenzel and Hiller, 2014] was used. TRNLizard connects the visual programming tool Grasshopper with the TRNSYS engine [Frenzel and Hiller, 2014].

[Buso et al., 2015b] use IDAICE for robust optimization. In order to model probabilistic occupant behavior, a monte-carlo random sampling is integrated.

[Van Gelder et al., 2014] proposes a robust optimization methodology for non-mathematical optimization. Gelder et al. utilize a sensitivity analysis in order to screen sensitive parameters, which will be further analyzed. The filtered parameters are then used to train a meta-model to decrease simulation time. After the meta-model is verified, a full factorial study is conducted. For each uncertain scenario, a monte carlo analysis is applied to retrieve the values according to the probability distributions.

Full factorial optimization is the most applied method in robust optimization of buildings. It is easy to implement and self-verifying. However, the exponential rise in simulation runs with an increasing number of parameters makes it only of limited use for complex optimization problems. Meta-models enable extended use of full-factorial analysis due to their time-efficiency.

5.4.3 Summary

From table 5.1, it is evident that full factorial optimization is dominating in current robust optimization studies. Meta-models and mathematical-optimization play only a subordinate role. Sampling strategies are frequently applied in order to assess parameters with uncertain nature. TRNSYS is the most applied simulation program in the analyzed studies. This can be traced back to its versatile script-based input.

5.5 Robustness indicators

The used robustness indicators are decisive for the optimization result. However, depending on the interpretation of robustness, different indicators have been used in literature. Following section will explore the range of indicators applied, as well as their advantages and disadvantages.

5.5.1 Performance spread

The spread of results is the most simple form of robustness indicator. For each variant, the spread of the results is calculated. The smaller the spread, the higher the robustness against uncertainty. However, spread is not able to make a statement about the performance of a variant. Performance spread is suitable for finding the variant with minimal variations under all conditions. Since it is unlikely that all scenarios will occur, it is not the variant with the best overall performance. Performance spread is a worst-case approach that guarantees constant behavior even under extreme conditions [Kotireddy et al., 2017]. This approach is applicable for very conservative decision making, e.g., the stability of a bridge. Extreme outliers tend to distort the results of performance-spread. Calculating performance-spread only between the 5th to the 95th percentile may solve this problem.

5.5.2 Standard deviation and relative standard deviation

Standard deviation is a statistical value that indicates the variance around the mean value. Similar to a low spread, a low standard deviation indicates high robustness to uncertainty. Standard deviation is not suitable to compare the absolute performance of all variants.

Since the unit of standard deviation is equal to the unit of the variable, variables with different units can not be compared. Relative standard deviation solves this problem by normalizing the value by its mean. Thus, the robustness of a variant with several performance indicators can be combined to one value.

Standard deviation and relative standard deviation are worst-case approaches. Minimizing these indicators for all results means losing performance in most scenarios.

5.5.3 Weighted median spread

The weighted-median-spread indicator determines a balance between robustness and optimality of a solution. The median is the middle value in the results set and therefore gives a good estimation of overall performance. Compared to previous indicators it also takes the performance of the given variant into account.

Depending on the weighting factor, this indicator can shift between robustness-oriented or performance-oriented orientation. Laying a focus on the spread, results in a worst-case approach that is suitable for conservative decision making. If the focus is put on the median, a more performance-oriented variant will be chosen, which will be prone to certain risks.

5.5.4 Best-case and worst-case method

The best-case and worst-case method evaluate the performance of the worst result of a variant compared to the overall best result. The performance difference will be compared between all results. The variant with the lowest robustness indicator performs closest to the overall optimum under uncertain conditions.

Like the performance spread method, the best-case and worst-case method aims to achieve maximum robustness for all scenarios. This approach maximizes robustness at the expense of performance.

5.5.5 Minimax-regret

The minimax-regret method minimizes the maximum performance regret. For each scenario, the difference between the local best-case is calculated for each variant. The resulting performance difference is then summed up over all scenarios. The variant with the lowest performance regret is selected as a robust optimum.

The minimax-regret method is a more performance-oriented approach. It is less focused on minimizing spread, than on being as close as possible to the local optimum for all scenarios. The optimization result is less conservative and is applicable to a decision-maker who can accept certain risks.

5.5.6 Summary

Table 5.1 summarizes the used robustness indicators. Performance spread is the most applied, as it is the most straightforward approach to robustness optimization. However, its sole focus on spread limits its field of application to very conservative decision making. Weighted median spread is second in utilization. It enables the planner to choose a weighting factor between performance and robustness depending on the acceptable risk. Solely Kotriddery applies the best-case and worst-case method as well as the min-max-regret method. Standard deviation and relative standard deviation are seldomly used and behave similarly to performance spread when it comes to robust optimization.

In summary, the choice of the robustness indicator depends primarily on the risk tolerance of the decision-maker. The performance spread method is only applicable if performance variations should be avoided at all costs. The best-case-worst-case method applies to conservative decision making. The weighted-median-spread method, as well as the min-max-regret method, guide risk-tolerant decision making.

The figure on the following page shows an exemplary application of the robustness indicators. Three variants are assessed for three uncertainty-scenarios. The barplot on the end of each row visualizes the result of the robustness indicator.

Notably, in the case of performance spread *Variant A* is chosen as most robust, even though its results are worse than all other variants. This can be attributed to the sole focus on result-spread and clarifies the drawbacks of this indicator.

In the case of weighed-median-spread, *Variant B* and *Variant C* perform best, since the indicator establishes a balance between performance and result spread. However, as shown later in this study, weighted-median-spread tends to generate a ranking with minimal variation, which reacts strongly to minor changes in the input functions.

The min-max-regret indicator is the only one, which identifies *Variant C* to be the most robust variant. Even though *Variant C* exhibits the highest spread, it performs best in scenario one and two, and only slightly below the optimum in scenario three. The min-max-regret indicator is practically oriented and compares results only within each scenario. Spread is allowed, as long as performance is best.

The best-worse indicator identifies *Variant B* to be most robust. Since its worst scenario is performing best among all variants. Major drawback of this indicator is its sole focus on the worst-performing item in each variant, the distribution, spread and median play no role. Extreme outliers significantly distort the result and lead to wrong conclusions.

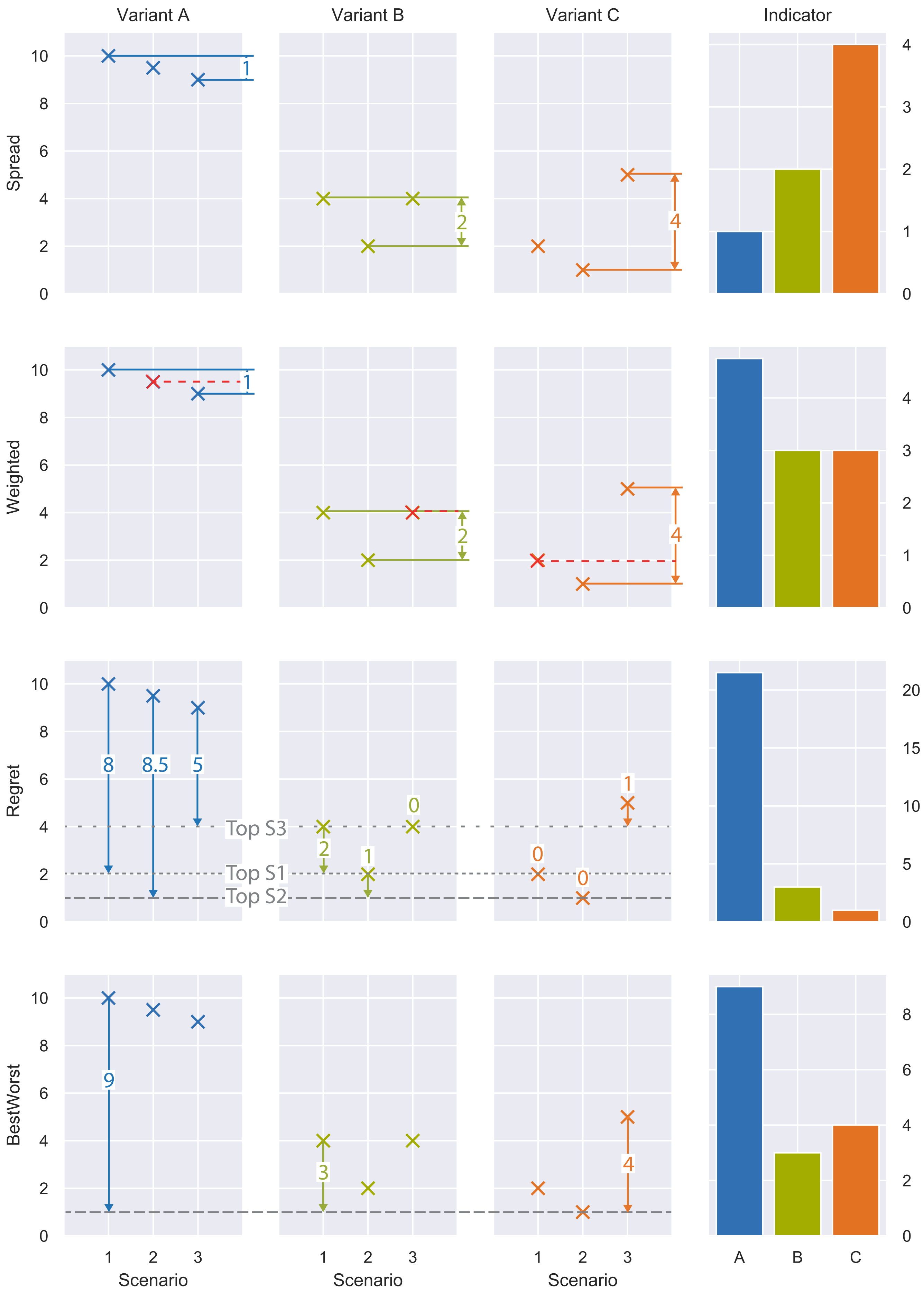

Variant A
Variant B
Variant C
Indicator
Spread
Weighted
Regret
BestWorst
Top S3
Top S1
Top S2
Scenario
Scenario
Scenario
A
B
C

5.6 Post-processing

Post-processing is the final stage in robust optimization. It is performed after the completion of the simulations. Post-processing aims at compiling the results into one dataset. Visualization, multi-criteria trade-off, and verification are further stages in post-processing. Depending on the mode of optimization (mathematical or non-mathematical), post-processing steps may differ.

5.6.1 Compiling results

Compiling the raw data from the simulations is an indispensable step in order to convert the data into a processable form. Result data is usually separated in individual files for each simulation run. The data in each file represents the results for every simulation time step for several outputs. Due to the number and size of each file, compiling the data cannot be done manually but has to be automated.

Automation is done with programming languages that are capable of processing large datasets. Most common in robust optimization of buildings is the use of *Python, R or MATLAB*.

5.6.2 Multi-criteria trade-off

Single-objective optimizations are more tractable than multi-objective optimization. However, considering multiple performance indicators is widespread in robust optimization of buildings. Therefore, a trade-off has to be made to find an optimum for both indicators. In following section, different multi-criteria trade-off methods are explored.

Individual-treatment of multiple performance indicator is a common practice. It is applied in [Auer et al., 2013], [Auer and Endres, 2017] and [Endres et al., 2019]. Robustness indicators are calculated separately for each performance indicator and optimized individually. Individual-treatment of performance indicators allows a more in-depth analysis of the influence on each performance indicator. However, individual optimization of each performance indicator may lead to non-optimal solutions due to opposing effects.

Constraints help to optimize one key performance indicator within certain limits of other indicators. Constraints are used to filter infeasible results from the result set. In robust optimization of buildings, this is especially applicable when it comes to regulations. For example, staying below certain overheating-hours a year. However, constraints are mainly applicable if one main and several subordinated performance indicators exist.

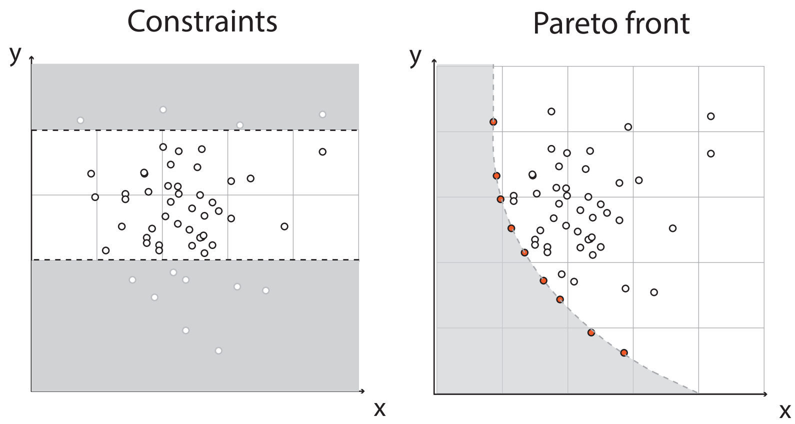

Figure 5.1 Constraints and Pareto-front

The **Cost-function method** allows comparing different performance indicators by assigning costs to each indicator. Multiple performance indicators are merged into one cost factor, which can then be assessed through robustness indicators. The assigned costs are the decisive factor as they influence the weighting of the performance indicators.

A **Paretro-front** is defined as the set of solutions where no better solution exists for the optimization of two objective functions [Maderspacher, 2017]. Figure 5.1 illustrates this in a scatter-plot with two performance indicators. The pareto-front is the weighted sum of two objectives functions where variable weights define the points [Maderspacher, 2017]. Thus the pareto results span the set of possible optima depending on the focus of the decision-maker.

Normalization is applicable for multiple performance indicators with different units. Normalization serves to make different units comparable by scaling them according to their relative maximum and minimum values. Normalizing results in values between 0 and 1, which can be used to calculate robustness indicators. The results of the robustness indicators are then summed up, and the design with the lowest score is the most robust. If the importance of the performance indicators is not equal, weights can be integrated in the totaling function.

5.6.3 Visualization

Visualization makes the results comprehensible and allows the identification of correlations. The following section will discuss different visualization techniques that have been applied in robust optimization of buildings.

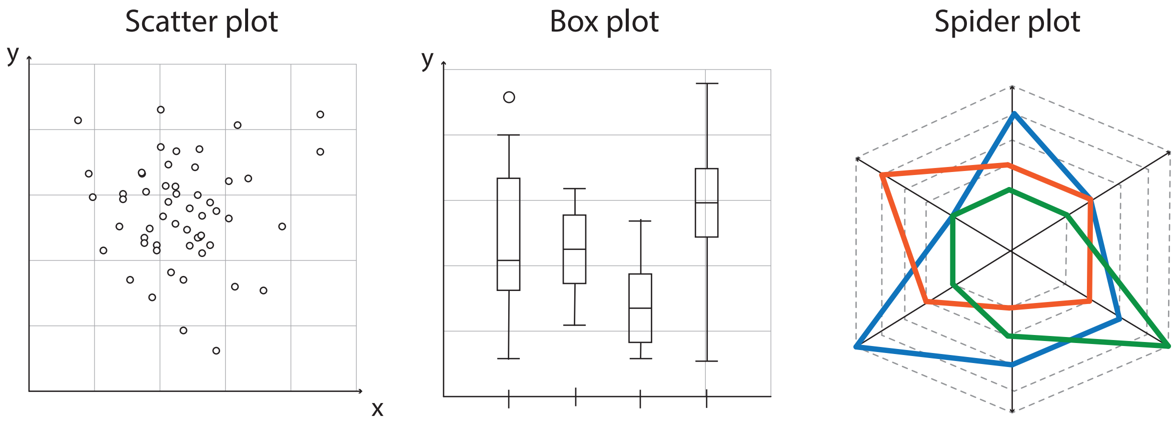

Figure 5.2 Overview over suitable plots in robust optimization

Scatter-plots plot points into a coordinate system. The axes represent different performance-indicators, the points coordinate the result. Scatter-plots are suitable for multiple performance indicators. A two-dimensional scatter-plot can accommodate two performance indicators, a three-dimensional scatter-plot three. Optionally a fourth dimension can be integrated through the size of the scatter-points. In robust optimization, scatter-plots are used to show the whole set of results in one plot. This allows for easy identification of well-performing variants. However, it is difficult to identify individual combinations in a scatter plot. Color legends and different forms can remedy this through grouping points depending on their parameters and scenarios.

Box-plots group runs and show the distribution of the results in a box and whisker representation. The box represents the range of results that lie within the first and the third quartile. The line inside the box marks the median of the results. The whiskers mark the range of results that lie within the 2.5%-percentile and 97.5%-percentile. Thus, 95% of the results lie within the whiskers. Individual points mark outliers that are outside of 95% of the distribution of the results. Box-plots are an intuitive way to assess performance robustness. The smaller the box, the shorter the whiskers and the lower the median, the better the result. However, box-plots are solely one dimensional and have to be separately plotted for each performance indicator. Multiple plots make a multi-criteria assessment difficult. Furthermore, box-plots depend heavily on the grouping.

Spider-plots are a special form of plots that show the performance of one result regarding multiple performance indicators. They can represent multiple dimensions of indicators and compare different variants to each other. For each variant, the relative performance of each indicator is marked. Each performance indicator is normalized and plotted as point onto an axis. The resulting points are then connected and span an area. Variants are differentiated between each other using different colors. If each performance indicator is equally important, the enclosed area can be seen as the optimality of the result regarding multi-criteria trade-off. Due to the form of presentation, the number of variants shown in a single spider plot is limited. Otherwise, the plot becomes overloaded and incomprehensible.

Bar-plots are simple plots that indicate a value through the height of a bar. In [Endres et al., 2019] and [Auer and Endres, 2017], bar-plots are used to show the standard deviation caused by a group of parameters. Ordered by height, the bar-plots represent the influence of each parameter. Analog to box-plots, bar-plots can only visualize a single performance indicator and are therefore unsuitable for multi-criteria assessment.

Table 5.1 summarizes the visualization techniques applied in the considered studies. The application of scatter-plots is widespread and used in nearly every study that assesses multiple performance indicators. Box-plots are especially useful if only one performance indicator is used and are applied in [Buso et al., 2015b] and [Chinazzo et al., 2015b]. Bar-plots and spider-plots are rarely used in robust optimization of buildings.

5.7 Summary

The literature review allows for following statements:

- Most studies focus on insulation and glazing parameters
- Occupant- and climate-scenarios are the most applied uncertainty-scenarios.
- All except one study apply either comfort or energy metrics as a performance indicator. Several studies consider both in multi-objective optimization.
- The full-factorial-optimization method is used in eight out of ten studies. Mathematical optimization is only applied in two publications.
- The performance-spread, followed by the weighted-mean indicator are common robustness indicators.
- A Paretro-front or weighting factors are applicable for a multivariate trade-off.
- Scatter-plots or box-plots are applied in every examined study.

Study	Design space						Scenarios					Perf. indicators					Optim. methdos					Robust. indicators						Post-processing				
	Ins	Mass	Vent	Glaz.	Geo.	Shad.	Usage	Occ.	Climate	Tech.	Policy	Comfort	Net-energy	Final-energy	CO2	Costs	Full-factorial	mathematical	meta-model	sampling	Programm	Spread	STD	RSTD	Weighted	Best-Worst	Regret	Scatter	Box	Spider	Bar	Multiobjective
[Auer and Endres, 2017]	X	X	X	X	X		X					X					X				X		X					X			X	
[Maderspacher, 2017]	X			X		X			X		X			X		X		X	X	X	X				X			X		X		X
[Buso et al., 2015b]		X		X		X		X					X				X			X				X					X			
[Endres et al., 2019]	X			X	X				X					X			X				X		X					X			X	
[Auer et al., 2013]	X			X	X		X	X	X	X			X	X	X		X				X	X							X			
[Chinazzo et al., 2015b]	X	X		X		X			X					X			X					X							X			
[Kotireddy et al., 2015]	X		X	X	X	X	X	X	X			X	X	X			X				X				X			X				X
[Van Gelder et al., 2014]	X		X	X		X		X			X		X			X	X		X	X					X			X				
[Kotireddy et al., 2017]	X	X	X	X	X		X	X	X			X	X	X			X				X	X				X	X	X				X
[Kotireddy et al., 2019]	X	X	X	X	X		X	X	X			X	X	X				X		X	X	X				X	X	X				

Table 5.1 Overview analyzed studies

5.8 Intermediate result

The following section will wrap up the findings from the previous chapter. Based on these findings, a research gap has been identified, which is addressed in the following study. The literature review forms the basis for the study-framework, which is set up in section 5.8.2.

5.8.1 Research gap

Based on the literature review, a research gap has been identified in the field of robust optimization of buildings. All in all, uncertainty mitigation in building simulation is underrepresented in research and practice considering its importance. The reviewed studies apply the robust optimization methodology in order to mitigate the uncertainty of different performance indicators. However, even though load management of buildings has great potential in a renewable energy system, the reviewed studies do not take uncertain scenarios into account. Furthermore, the reviewed studies on load management potential of buildings do not consider energy consumption, even though it is highly relevant when assessing the feasibility of load management potential. Therefore, a research gap has been identified in the assessment and optimization of load management potential and energy consumption under uncertain scenarios.

5.8.2 Study framework

Based on the findings obtained in the previous part, this section will build the framework for the robust optimization study.

Uncertainty mitigation method: Different methods of uncertainty mitigation have been explored in section 4. It has been determined that robust optimization is the best fit for uncertainty mitigation in building simulation. Therefore, a robust optimization will be conducted in the following study.

Design space: The design space defines the setup of the simulation. In order to uphold comparability, the simulation framework of [Hausladen, 2014] and [Auer et al., 2017] will be adopted and modified in order to facilitate a robust optimization. [Hausladen, 2014, Auer et al., 2017] distinguish between building typologies (section 2.1) and age classes (section 2.2). The more detailed approach of [Auer et al., 2017], differentiating four age classes, is chosen. For building typologies, the focus will be led on residential housing since it represents the most significant share in total area and heating energy consumption [Auer et al., 2017]. More specifically, apartment houses will be investigated since they hold the highest relative share of existing residential buildings.

Scenarios: The scenario definition has a significant impact on the outcome of the robustness analysis. Covering most uncertainties is key to achieve a robust optimum. Therefore, the following scenarios will be assessed: usage-, occupancy-, climate-, and a technological-scenario. The policy scenario is excluded since it has been exclusively applied to cost analysis in previous studies and costs are not regared in this study. The chosen scenarios cover 80% of all possible scenarios assessed in literature and therefore lay a solid foundation for the robust optimization study.

Performance indicators: Load management potential constitutes the primary performance indicator in the following study. The calculation of load management potential will be according to the method developed in [Hausladen, 2014]. Additionally, energy demand will be analyzed, as a research gap has been identified in the interplay of load management potential and energy demand. Furthermore, energy-demand is one of the most used performance indicators in the reviewed studies next to comfort indicators. Due to the calculation method of load management potential, comfort will always be achieved and thus is excluded.

Robust optimization methods: Even though it requires extensive computational effort, full-factorial optimization is by far the most used method in the reviewed studies. Especially its intuitive approach and self-proofing results are the main advantages of full factorial optimization. It is therefore chosen as optimization method in this study.

Robustness indicators: Even though performance spread is the most used robustness indicator, it has been shown that it is not suitable to compare differences in absolute performance. Therefore, the median-weighted-spread and min-max-regret method are chosen. Both allow the assessment of performance as well as robustness and result in a less conservative solution than the best-case - worst-case approach.

Post-processing: Scatter- and box-plots are the most suitable visualization technique for robust optimization and will be applied in study. A multivariate trade-off between load management potential and energy consumption will be made utilizing a Paretro-front as well as a weighted objective function.

Part II

Robust optimization study

6 Pre-Processing

Based on the research gap and framework defined in the previous part, a robust optimization study will be performed on load management potential and energy consumption. The study aims to derive refurbishment strategies for the residential building stock. The following part is structured in the steps required for a robust optimization: pre-processing (chapter 6), optimization-run (chapter 7) and post-processing (chapter 8). In the course of this study different terms are introduced that are crucial to understand the procedure of load management potential and robust optimization. Therefore, a glossary is created in section A.1, which summarizes key terms, their definition and abreviation.

The following chapter treats the model setup and parameter selection. The fundamental framework has already been defined in section 5.8.2. Therefore the focus is laid on parameter selection and model setup. Section 6.3 explains the steps taken to screen and select the design parameters. In section 6.4, the choice of uncertainty parameters is explained and section 6.2 details the creation of the model.

6.1 Load management potential calculation

The calculation of load management is based on the methodology of [Hausladen, 2014]. In the following section the steps taken to implement the methodology in the simulation framework are explained. It is partially based on work in the author's activity as a research assistant at the chair of building technology and climate responsive design at the technical university of Munich and based on the approach in [Auer et al., 2017].

6.1.1 Simulation

Each LMP simulation consists of three runs: base-simulation, deactivation-simulation, and activation-simulation. These are repeated for each analyzed timestep. A settling time of 168 hours guarantees equal starting conditions by charging the thermal mass. From the time the LMP-strategy is activated

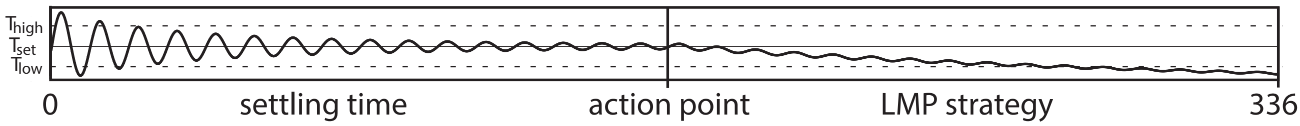

Figure 6.1 LMP simulation

(action-point), a maximum of 168 hours is allowed for the deactivation- and activation-strategy. All in all, each LMP simulation consists of 336 hours.

Depending on the load management strategy, the heating power is either cut off (deactivation) or maximized (activation). In TRNSYS, this is achieved through an equation that modifies the setpoint temperature depending on the simulation time. If the hour 168 is reached, the temperature setpoint is changed from 22℃ to 12℃ (deactivation) or 32℃ (activation).

In the base-simulations, the setpoint is held constant for the entire 336 hours. As multiple LMP simulations are conducted in this study, base-simulations are combined to a single full year simulation for each variant, thus reducing simulation time.

To summarize, a deactivation and activation-strategy are simulated for each timestep and variant. Additionally, for each variant, a full-year base-simulation is done. Evaluating the LMP for one variant and one type-day requires 49 simulations, which are comprised of 24 activation-simulations, 24 deactivation-simulations, as well as one base-simulation.

6.1.2 Calculation

The LMP calculation for one variant is performed for each strategy and timestep. The power difference between base-simulation and load-management-simulation is compared, originating from the activation point. For each subsequent hour of the LMP-simulation, the operative-temperature is monitored. The difference between the power-consumption of the LMP-simulation and base-simulation is evaluated and logged. This process is repeated for each hour until the operative-temperature of the LMP-simulation does no longer meet the comfort-requirements. The overall power difference up to this timestep equals to the load management potential for this specific action-point. Thus, deactivation-simulations will result in a negative LMP and activation-simulations in a positive LMP. The results for activation- and deactivation-potential are stored in a matrix, with a line for each action-point.

6.2 Model creation

In the following section, the creation of the model is described. Models are built and simulated with TRNSYS. The inputs are parametrized to ensure automation. Since the TRNSYS Studio application lacks parametrization ability, TRNLizard is utilized in this study.

TRNLizard is an interface between TRNSYS and the graphic programming environment Grasshopper [Frenzel and Hiller, 2014], which is written in Python. It allows sending geometries and parameters to the TRNSYS simulation engine by creating simulation files based on predefined templates. The simulations for the pre-written simulation files are launched via a command-line argument [Frenzel and Hiller, 2014]. Currently, the functionality of TRNLizard is yet subordinate to that available in TRNSYS Studio. However, its open-source implementation allows experienced users to develop new tools and functions. All in all, TRNLizard provides a solid modeling environment for parametrized building energy simulations. In this study, TRNLizard is modified and extended to facilitate parametric load management potential calculations. In the following sections, the various changes made to the original software are detailed.

[Some of the following components have been developed in the author's activity as a research assistant at the chair of building technology and climate responsive design at the technical university of Munich. The aim is to create a library of components that supplement TRNLizard by an LMP calculation. Therefore dependencies on other tools than TRNLizard and Python are avoided.]

6.2.1 Basic setup

In the following, the basic model setup is described. The geometry, orientation and boundary conditions are adpoted from [Auer et al., 2017]. All subsequent simulations are based on the model as described. No parameters concerning the geometry are modified in the course of the parametric study, to uphold comparability to previous studies.

The chosen zone models a typical flat in an apartment-house, with windows oriented towards east, west and south. Identical flats are situated in the north as well as above and below the examined unit. The floor area of 110 m^2 as well as a window to wall ratio of 14% are representative of the chosen typology [Auer et al., 2017, Loga et al., 2015].

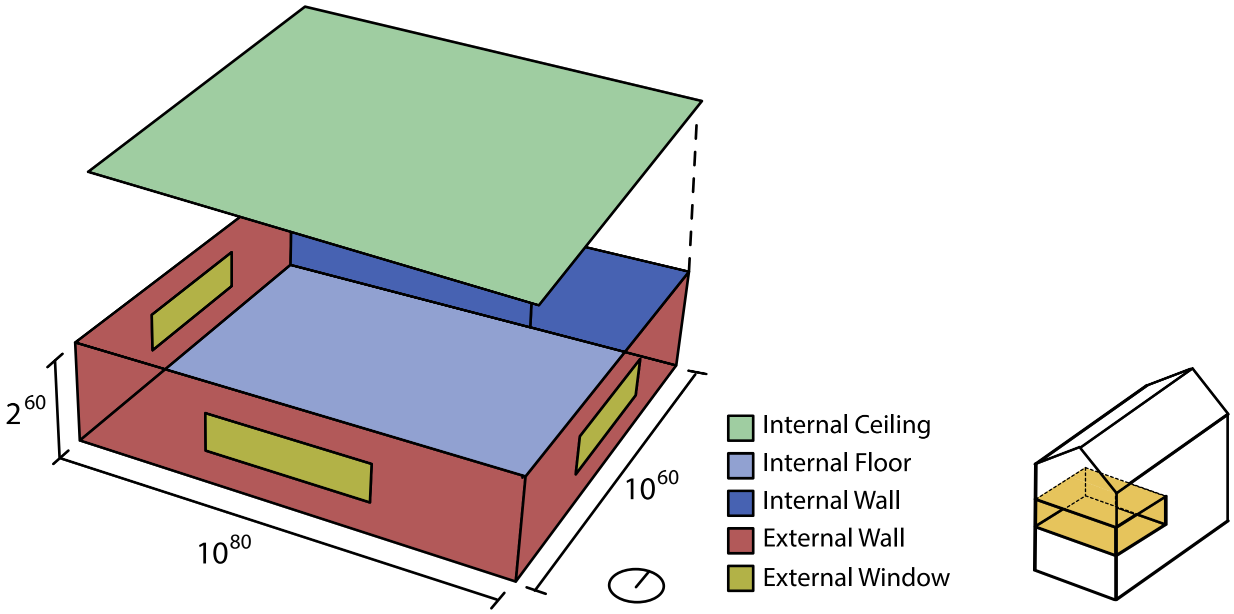

Figure 6.2 Basic model setup

6.2.2 Adaptions

Load management calculations are performed, as explained in [Hausladen, 2014]. Some adaptations had to be made to facilitate LMP simulations in TRNLizard. These are listed below.

In the basic version of TRNLizard, simulations could only be started and stopped daily. Since short simulation time-spans of exactly 336 hours are needed for load management calculation, adaptions are made to the existing code. The modified version allows defining the start and stop-moment of simulations based on the exact HOY, rather than on a daily basis.

TRNLizard in default comes with three types of output printers: specific-power, temperatures, and custom outputs. However to process the data later on it is important to combine all necessary data in one file. Therefore, a custom printer was added, which creates an output file that contains all data required to perform an LMP calculation.

In default, TRNLizard solely allows numerical input for key parameters in the setup, as for example the air change rate and the supply temperature of the mechanical ventilation system. However, the LMP calculation requires equations instead of a fixed numerical input to facilitate a presence-based minimum air change and a variable heating setpoint. A modification enables equation-based input in addition to numerical-input for the variables mentioned above.

The internal mass in TRNLizard is set to a fixed ratio that depends on the airnode volume. As internal mass is an important parameter in LMP calculation (see [Hausladen, 2014]), the code is adapted to allow for user-defined internal mass.

Except for the above mentioned modifications, no changes have been made to the original TRNLizard code. All other supplementation is implemented as independent components, that only interact with TRNLizard through the predefined interfaces. These extension are explained in the section 6.2.3 - 6.2.8.

6.2.3 CSV-Interface

Model definition in TRNLizard is prone to errors, as settings have to be done on different locations on the canvas. Therefore, a CSV-interface is created to externalize all relevant settings to a single CSV-file. This filetype can be understood as a text-based spreadsheet and can easily be read and written in Python. The parameters are stored in the different rows of a column. The row header represents the parameter name in the CSV-interface component. The columns stand for different base-variants (e.g., different energy standards). In Grasshopper, the base-variant is selected by the column header name. This allows for an error-free and automated way to change parameters or variants.

In the case of this study, additionally to variants, certain parameters are changed in the parametric-study. A naming system has been introduced to allow for the change of individual parameters (see section 6.2.5) that identifies the parameter and assigned level. The CSV-interface component decodes and processes the variant-name and replaces the selected parameters automatically.

6.2.4 PreProcessing

The pre-processing component fulfills the central task in the LMP calculation. It is furthermore the main point of interaction for the user as it integrates all important settings. Its task is to write a pre-processing file that stores all simulation data required to run the study. Variants are written according to the approach described in section 6.1, depending on the initial settings. These are:

- **Start time:** sets the start time of the study; allows for a list of inputs if several days are considered.
- **Stop time:** sets the stop time of the study; allows for a list of inputs if several days are considered.
- **Initial temperature:** sets the initial setpoint temperature at which the base-simulations are operated.
- **Comfortband:** defines the range of operative temperatures that are deemed comfortable by giving a lower and upper threshold.

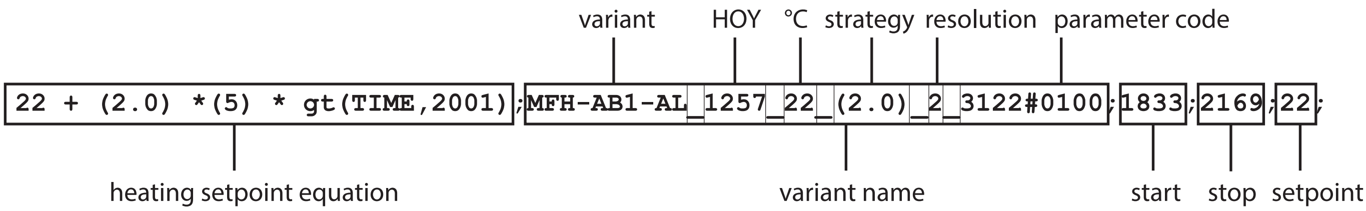

Figure 6.3 Exemplary line in the pre-processing file

- **Resolution:** sets the temperature increment at which LMP will be assessed. For each step, LMP will be independently assessed.
- **Base-variant:** specifies the base-variant; corresponds to the column headers of the CSV-file. Originating from this variant subsequent modifications will be made.
- **Design parameters:** set the design parameters in the robust optimization.
- **Uncertainty parameters:** set the uncertainty parameters in the robust optimization.

The algorithm within the pre-processing component computes all parameter combinations, then applies them to each step of the LMP calculation. Each line in the pre-processing file represents a simulation run. Semicolons separate the individual data items. Figure 6.3 illustrates the data stored in each line. Following data can be extracted from the pre-processing file:

- **Heating setpoint equation:** This equation is used to control the LMP-strategy as described in 6.1.
- **Variant name:** It defines the name of the simulated variant and contains all data necessary for post-processing. It includes the used variant, the considered hour of the year, the setpoint temperature, the applied strategy, the resolution, and the parameter code.
- **Start:** Start moment of the LMP-simulation.
- **Stop:** Stop moment of the LMP-simulation.
- **Setpoint:** Initial temperature of the LMP-simulation.

6.2.5 Parameter-study

Integrated into the pre-processing component is the parameter-study for the full factorial robust optimization. It computes all necessary parameter combinations in the form of abstracted parameter-codes. Each parameter is represented by one digit in the parameter code. As shown in figure 6.4, design and uncertainty parameters are separated by a hashtag. The value of each digit stands for the parameter level. The

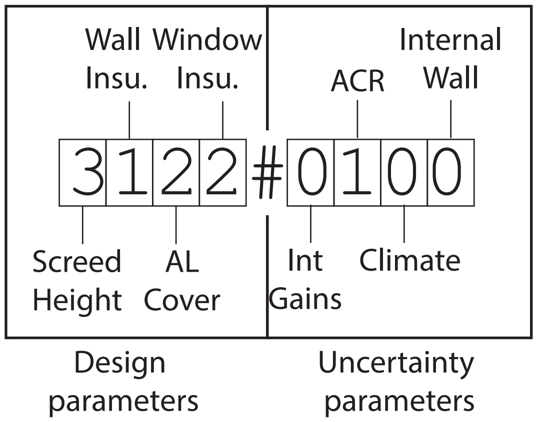

Figure 6.4 Exemplary parameter code

study combines a full-factorial analysis of design-parameters with an one-at-a-time analysis of uncertainty-scenarios.

An auxiliary file storing the digit parameters and values is saved in order to later be able to decode the parameter-code. It is utilized in the CSV-interface component to adapt the necessary parameters, as well as in post-processing.

6.2.6 Iterator

Avoiding external libraries other than TRNLizard and Python makes it necessary to develop an own solution for iterating over the pre-processing file. The correct identification of the completion of the thermal simulation is crucial to time the start of the next run. A dummy-file is introduced, which is edited after the simulation has commenced. The iteration component constantly monitors the dummy-file and at change, a new step is initiated. The current step is stored in an external file since Grasshopper does not allow internal programming loops. Utilizing external files has the added benefit of being able to abort the simulations by deleting either of the dummy-files.

6.2.7 Type day calculator

The type-day scheme of [Hausladen, 2014] is adopted for this study, as stated in section 5.8.2. In [Hausladen, 2014] the type-days have been determined manually for one location. However, since the process should be applicable for different locations, it has been automated in this study.

The type-day calculator is implemented in Python. It requires the weather data as well as the temperature boundaries to retrieve the start and the stop hour of each type-day. The temperature boundaries can be freely specified. In this case, the boundaries, as defined in figure 2.1, are used. The type day is determined by dividing the given weather data into the specified temperature groups. The average temperature of each group is computed, and a typical day is chosen, which matches the average most closely. This process is repeated for each specified temperature band. After completion, the type day calculator provides a list of start and stop moments that can be directly connected to the pre-processing component.

6.2.8 System-capacity

Defining the maximum capcity of the heating system individually for each variant is crucial, since it has decisive influence on the activation potential.

An algorithm is introduced, which computes the maximum available heating power, depending on the infiltration and the thermal resistance of wall and windows. The implementation is based on the calculation method in DIN 12831, which is used to dimension heating systems. This is done by assessing the losses due to infiltration, ventilation and conduction on the coldest day of the year. The power required to balance these losses equals to the maximum capcity of the heating system.

The algorithm is integrated in the TRNLizard framework through a Python-component. It extracts the required data from the building components and the weatherfile. Based on these inputs a area specific heating power is calculated, which is transmitted to the active-layer-component. Thus, an individual capacity is used for every combination of wall- and window-insulation.

6.3 Design-parameters

The choice of design parameters is crucial in robust optimization. Without time and computational constraints, an optimization of all parameters would be preferable. However, due to limited resources, a preselection has to be made. This study conducts a parameter-screening in which the sensitivity of each parameter will be assessed. The most sensitive parameters will then be optimized in the robust optimization study.

6.3.1 Parameter screening

A parameter screening for optimization studies is proposed in [Nguyen et al., 2014a]. In this study a preliminary estimation of parameter sensitivity is conducted by an one-at-a-time (OAT) analysis. The parameters are selected according to the following constraints:

- Ensure comparability to the studies of [Hausladen, 2014] and [Auer et al., 2017]: No change of dimensions and geometries
- Only parameters that can be influenced by the planner: No change of thermophysical properties and usage-related parameters
- Ensure comparability between LMP calculations: No change of parameters that are used for the calculation (e.g., heating setpoint, night setup, heating schedule)
- Stay within the defined framework (section 5.8.2): No change of the heating system or building typology.

This set of constraints leads to following parameters and stages:

- External wall construction: the stages are following the four building energy levels defined in [Auer et al., 2017]. The insulation levels increase from 0 to 280mm, simultaneously the u-value decreases from 1.2 W/m^2K to 0.12 W/m^2K.
- Heat transmission coefficient of the windows: the stages cover the typically applied values from 2.2 W/m^2K to 0.6 W/m^2K.
- Solar heat gain coefficient of the windows: the stages cover the typically applied values from 0.6 to 0.2.
- External shading fraction: the stages cover values from 0% to 75%. The shading is assumed to be moveable and is controlled depending on the operative temperature and horizontal irradiation.
- Internal shading fraction: the stages cover values from 0% to 75%. The shading is assumed to be moveable and is controlled depending on the operative temperature and horizontal irradiation.
- Position of the insulation: insulation outside of the load-bearing structure and insulation inside of the load-bearing structure are the two stages.
- Thickness of the screed: the stages cover values from the minimum allow screed thickness of 3 cm to 9 cm.
- Position of the floor heating pipes: top or bottom installation are the two stages.
- Infiltration air change rate: the stages are following the four building energy levels defined in [Auer et al., 2017]. The infiltration air change rate decreases from 0.42 1/h to 0.15 1/h.

- Heat recovery factor: the stages are following the four building energy levels defined in [Auer et al., 2017]. The heat recovery factor increases from 0 % to 75 %.

The results of an OAT analysis are highly dependent on the chosen base-variant. The lowest and highest building energy levels are avoided to avoid distortions. Due to the significantly higher share of 27% compared to 3% [Auer et al., 2017], the energy level AB2 is chosen over NB1.

6.3.2 Sensitivity analysis

In the following, the sensitivity of energy demand and loadmanagement towards changing parameters is assessed.

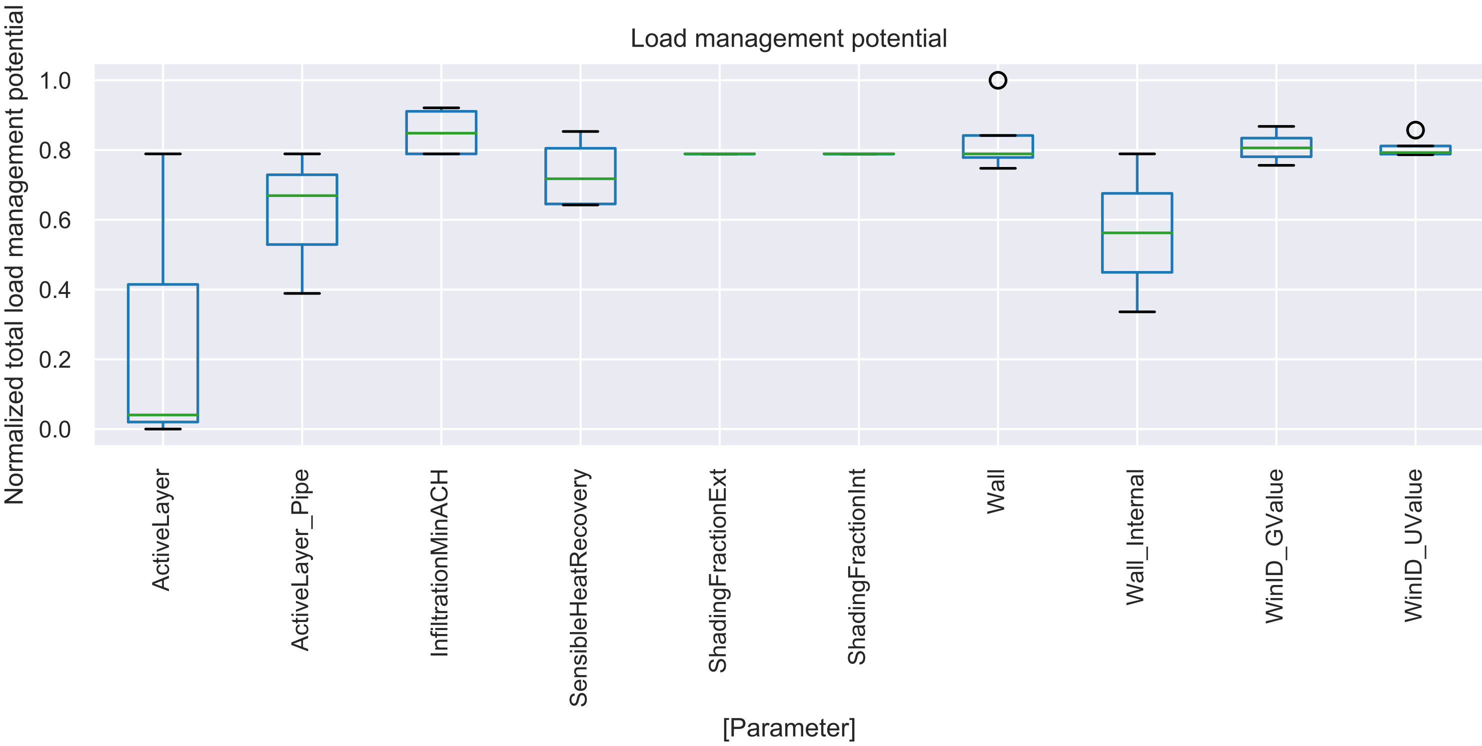

Figure 6.5 Sensitivity analysis total load management potential

Figure 6.5 visualizes the impact of the chosen parameters on LMP, the calculation of this metric is explained in section 8.3. The boxplot displays the range of values that are obtained by varying each parameter. The results have been normalized to allow for a comparison between LMP and energy demand. The green line represents the median of each group.

It can be initially determined that external- and internal-shading have no impact on LMP. This can be attributed to the shading control strategy, which priotizes solar gains over glare reduction during the heating period. It is most sensitive to screed-thickness, active-layer position, internal-insulation, and wall construction.

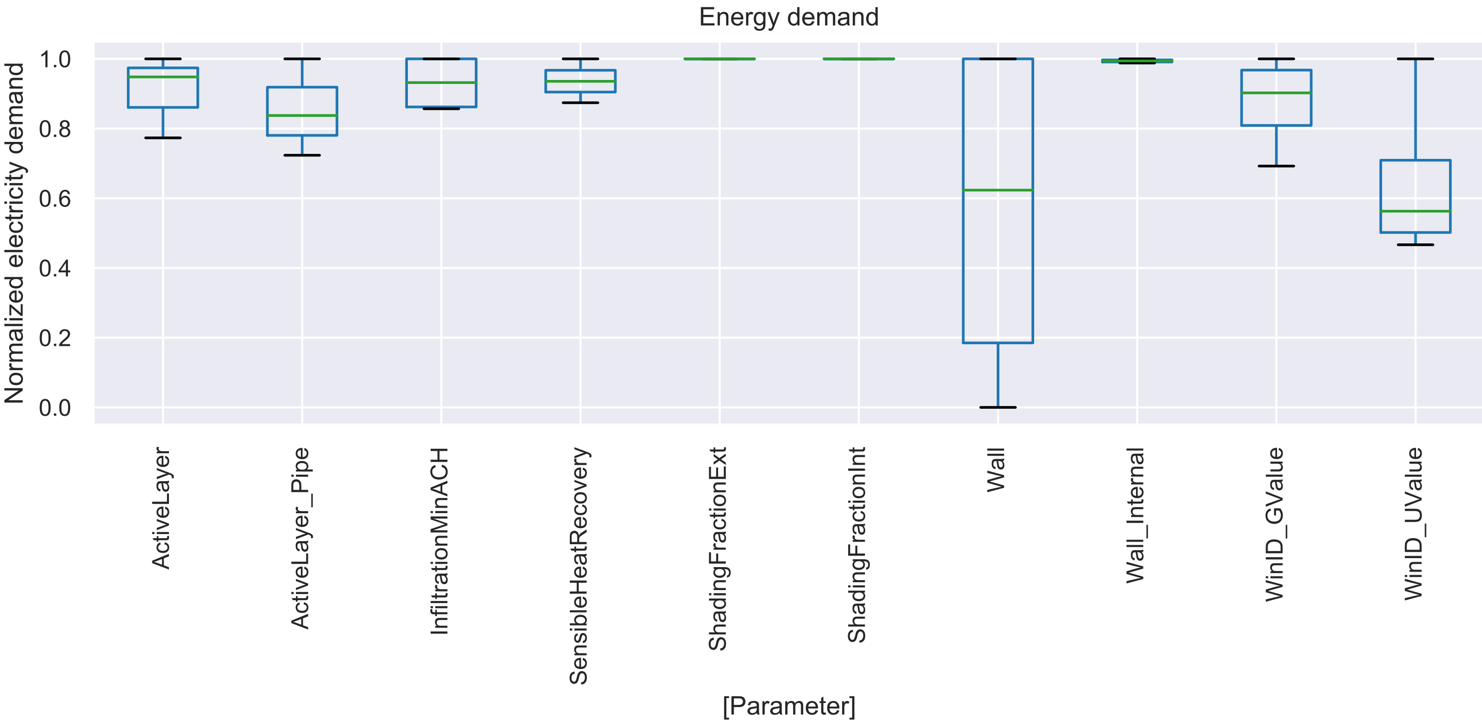

Figure 6.6 Sensitivity analysis energy demand

Figure 6.6 visualizes the impact of the chosen parameters on the normalized annual electricity demand. A neglegible influence is caused by internal- and external-shading, due to the reasons discussed above. Furthermore internal insulation has neglegible impact since it does not affect the thermal resistance of the wall. Energy demand is most sensitive to the type of wall-insulation, followed by window-inslation and the coverage of the active-layer.

Figure 6.7 visualizes the cumulative influence of the parameters on LMP and energy demand. The wall construction is predominant, since it has the foremost impact on energy demand and high impact on LMP. The screed-thickness is second in absolute influence, followed by the position of the active layer, both having significant impact on LMP and energy demand. These parameters are mainly influencing LMP. The window-insulation nearly exclusively impacts energy-demand. Internal insulation on the other side mainly

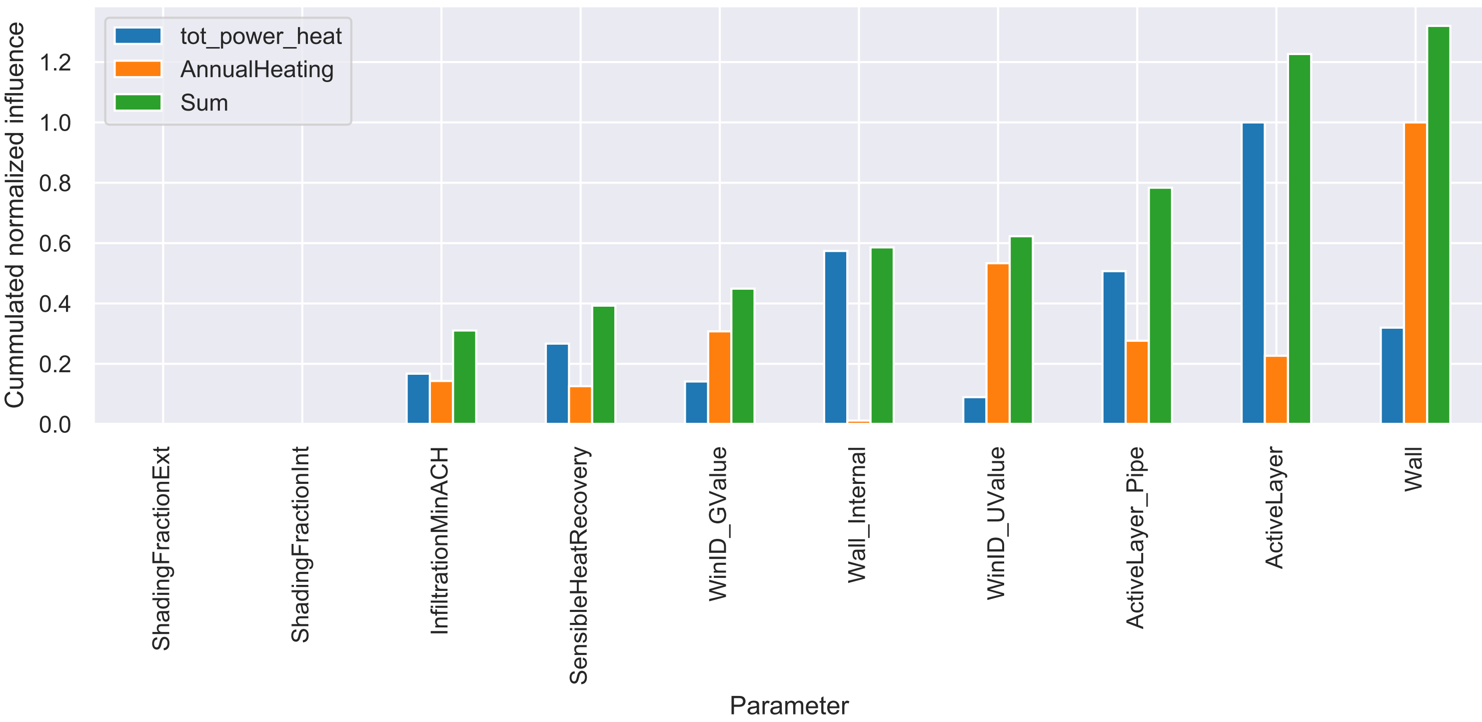

Figure 6.7 Cummulated sensitivity

impacts LMP. G-value, heat-recovery, and infiltration are only of minor influence. Internal-shading, and external-shading have no impact at all.

Since a preselection of parameters is necessary to keep simulation time in check, a cumulative sensitivity of at least 0.5 is chosen to rule out insignificant variants. Therefore following parameters are chosen for further examination: wall-construction, screed-thickness, active-layer position, window u-value as well as internal-insulation. Since internal-insulation is not a design-objective but rather induced by constraints, it is included in the study as a scenario, rather than a design-parameter.

6.4 Uncertainty-parameters

The uncertainty parameters define the scenarios in robust optimization. The selection of scenarios is explained in section 5.8.2. The assessed scenarios are a occupational-, usage-, climate- and technological-scenario. The implementation of each is described in the following section.

6.4.1 Occupational-uncertainty

The implementation of the occupational-scenario is adopted from [Auer et al., 2013]. An additional internal heat gain of 20 W/m^2 models unexpected user behavior or a higher number of occupants then intended. The heat gain is equal to five times the initial expected internal loads. An increase from 4 to 20 W/m^2 resembles the conversion of a living-space to an office space with ten people.

6.4.2 Usage-uncertainty

The implementation of the usage-scenario is created following [Auer et al., 2013]. Two potential user-types, who act outside of the expectations are assessed. On the one hand side a user, who does not ventilate at all is considered. On the other hand, a user who is constantly ventilating is assessed. The latter adds a constant airflow of 1.5 1/h on top of the infiltration rate which resembles an always tilted window. In the first scenario, the only air change is achieved through infiltration. Both scenarios are beyond the anticipated user behavior and are expected to have a major impact, due to the sensitivity of building performance to air change.

The usage-scenarios are implemented through a change of the air-change rate of mechanical ventilation. The infiltration rate remains unaffected from any modifications made.

6.4.3 Climate-uncertainty

Two climate scenarios are integrated into robust optimization. Climate change is taken into account over the typical lifespan of a residential building to assess future performance. A 2050- and 2080- climate scenario is used, covering the whole lifecycle of a building.

The weather files are generated based on a methodology developed in [Jentsch et al., 2008]. A morphing approach [Jentsch et al., 2008] is used to convert current epw-files to future scenarios based on projections by the IPCC. As reference case [Jentsch et al., 2008] recommends utilizing the medium-high emissions scenario. After all modifications are completed, the data is saved as a new epw-file, which can be used in TRNSYS.

With the above-mentioned process, weather-files for future climate conditions are created. Climate scenarios are implemented in the simulation framework by exchanging the weather file. One from three files (current, 2050, 2080) can be chosen.

6.4.4 Technological-uncertainty

The sensitivity analysis in section 6.3.2 showed that LMP is highly sensitive to the positioning of the insulation layer. Since refurbishment constraints, due to historical preservation, may require internal instead of external insulation, it is introduced as a technological-scenario.

The technological scenario is implemented through a second set of external wall definitions with internal instead of external positioned insulation.

6.5 Summary

Name	Description
CSV-interface	Allows to make all important settings externaly in a CSV-file.
Pre-processing	Setup of LMP-simulations and parametric-study.
Iterator	Automatically iterates over the pre-processing file.
Type-day	Outputs typicall days for given temperature bands.
System-capacity	Calculates the maximum available heating capacity.

Table 6.1 Overview of plugins developed for TRNLizard

The following section summarizes the setup of the model as well as the chosen parameters and scenarios. Table 6.1 summarizes the implemented additions to TRNLizard. Table 6.2 summarizes the chosen design- and uncertainty-parameters.

Design paramter							**Uncertainty paramter**					
		I	**II**	**III**	**IV**	**Unit**			**Scenario**	**I**	**II**	**Unit**
1	**Screed**	5	8	11	14	cm	5	**Gains**	Occ.	20	-	W/m^2
2	**Wall**	1.2	0.6	0.24	0.12	W/m^2K	6	**Vent.**	Usage	1.5	0	1/h
3	**Cover**	3	6	9	12	cm	7	**Weather**	Climate	2050	2080	-
4	**Win.**	2.2	1.1	0.9	0.6	W/m^2K	8	**Wall**	Tech.	Rev.	-	-

Table 6.2 Overview of design parameters and uncertainty parameters

The screed thickness and active layer coverage have been modified compared to the parameter screening. Both parameters are now assessed in continuous steps of 3 cm, allowing a better identification of trends in the data. Before, coverage varied depending on the screed-thickness. Furthermore, screed-thickness is modified in order to take the whole screed-height into account, including below and around the heating-pipes. In the case of the sensitivity analysis, solely the screed-height above the heating pipes was assessed.

Since screed coverage can not exceed screed-thickness only variants will be simulated, where the screed-thickness is at least 3cm bigger than the cover.

To summarize, the robust optimization study needs to be conducted for 160 parameter-combinations, seven scenarios, two load management strategies and four type-days. Each hour requires 2240 load-management-simulations, each type-day 53 760, and all type-days 215 040. Additionally, 1120 base-simulations need to be simulated. All in all four type days, a full factorial study of four parameters and a OAT-study of seven scenarios require a total of 216 160 simulations to be conducted.

7 Optimization run

The following chapter gives an overview of the procedures required to run the previously defined models in a time-optimized manner. The chapter is split into three sections. In section 7.1, three parallelization approaches are compared and assessed regarding their efficiency and reliability. The second section 7.2 deals with a method to detect errors during the simulation run. The final section 7.3 is comprised of a comparison of methods to monitor simulation progress and resource usage.

7.1 Parallelization

Since a large number of simulations will be conducted over several days, parallelization helps to mitigate simulation time. TRNLizard does not support parallelization in default. Therefore, different approaches have been implemented and tested to maximize time reduction. These are differentiated in external-parallelization (section 7.1.3), which outsources important task to a Python script, a hybrid-parallelization (section 7.1.2), where TRNLizard performs the writing, the simulation, however, is conducted externally, as well as internal-parallelization (section 7.1.1), where parallel TRNLizard instances perform the writing and simulation tasks. The developed methods are compared to the pre-implemented single-processing approach in regards to simulation-time and stability.

7.1.1 Internal-parallelization

In internal parallelization, all simulation related tasks are conducted in TRNLizard. Parallelization is achieved by launching multiple TRNLizard instances, each performing simulations on a fraction of the simulation-set. Every instance independently simulates their share of simulations. Internal parallelization is conducted in the following steps:

1. Creation of a Base Instance: A base TRNLizard model is needed that acts as a template for subsequent, automatically created instances.

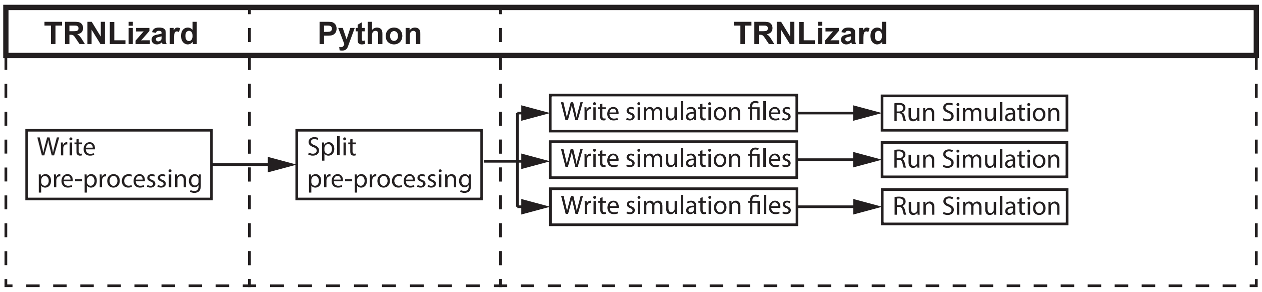

Figure 7.1 Internal-parallelization process

2. Creation of Parallel Instances: A Python script uses the base-template to initiate the TRNLizard instances by multiplying the template as often as parallel processes are needed. These are differentiated by their thread-number attached to their file-name.
3. Launching of Parallel Instances: The Python script launches the parallel instances. Each TRNLizard model fetches their assigned fraction of the simulations, depending on their thread-number. The models are set up in order to automatically start simulating.
4. Simulation Run: TRNSYS simulations are running in parallel. The iterator (see section 6.2) automatically starts subsequent simulations. No further action is required until all simulations are completed.

The key to the implementation of internal-parallelization is the starting of multiple TRNLizard instances and the correct assignment of simulation data. This is done in Python and comprised of the following major steps.

- Splitting of the simulation: The simulation period is a user-based input and equals to the start and stop moments defined in TRNLizard. The hours to be simulated are then split into equal blocks, their size depending on the number of processes. The divided start and stop moments are then saved to a files, which will later be read by the individual TRNLizard instances.
- Instances creation: The TRNLizard instances are created based on the template. They are copied and saved with the thread number included in their file-name (e.g., Model-3.gh). The previously created TRNLizard instances are launched through a command-line argument.
- Loading of the simulation data: A Python script within each instance loads the start and stop moments, required for the simulation. The data to load is derived from the assigned thread number. If all required data is available, the simulation starts automatically.

Internal-parallelization conducts TRNLizard simulations in parallel without changing the default procedure. It is applicable for simulations that focus on multiple short term simulations. However, the need to run multiple TRNLizard instances, each requiring Rhino and Grasshopper running in the background, creates a huge performance overhead.This poses a significant constraint on internal-parallelization, with a memory consumption of about 600 megabytes per instance. Furthermore, in certain circumstances, an interference between simulation instances is observed. This leads to the conclusion that even though TRNLizard is started separately, some interference between the instances takes place. Even though this error is fixed through reloading the template and files in TRNLizard for each simulation, this is a serious flaw and causes potential errors in the simulation results.

7.1.2 Hybrid-parallelization

In hybrid-parallelization, the workload is shared between TRNLizard, Python, and Batch-processing. TRNLizard is responsible for writing all simulation files. The written files are scanned and processed in Python, which creates a batch-file that orchestrates the parallel simulations.

Hybrid-parallelization is conducted in the following steps:

1. Model creation: The model is set up according to the steps in section 6.2
2. Writing of the pre-processing file: The pre-processing file is written.
3. Writing of the simulation-files: The TRNLizard simulation is set to write-only and iterates over the pre-processing file.
4. Writing of the batch-files: Python processes the simulation data. The simulations are partitioned according to the number of threads. The commands to start the individual simulations are stored in a batch-file for each thread, written by Python.
5. Simulation Run: All batch-files are started in parallel. The batch-files automatically iterate over the simulation-sets.

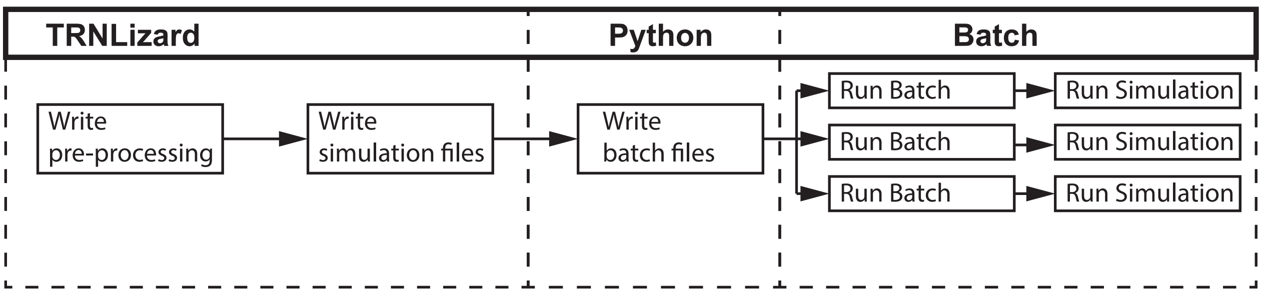

Figure 7.2 Hybrid-parallelization process

Hybrid-parallelization has already been applied in [Auer et al., 2013] and is modified for this study. In [Auer et al., 2013] it is implemented in a separate Grasshopper file, which conducts the aforementioned tasks. This implementation is modified for this study to run independent of Grasshopper and avoid its overhead.

The following modifications to the existing code from [Auer et al., 2013] have been made.

- Internalization of Grasshopper inputs: The inputs that have been formerly done in the Grasshopper interface, can now be done within the Python code.
- Error code output: Error codes, that are formerly output in Grasshopper, are now printed in the terminal.
- Automatic folder recognition: Simulation folders are automatically recognized in all subfolders of the location of the script.
- Randomized simulation order: The code implemented in [Auer et al., 2013] arranges the simulations according to their names and then splits the list into equal parts. In the case of this study, this leads to simulating all base files within one thread. Since base-simulations are conducted for the full year, they require significantly more time to finish. The execution of all base-variants in one thread leads to a major prolongation of the whole simulation. Therefore, the code is modified to randomize the variant order before the division and thus assign equal numbers of base-simulations to each batch-file.

The hybrid-parallelization approach is closest to the standard simulation methodology and least prone to errors. Furthermore, the setup effort is minimal. However, simulation files are not written in parallel, which has proven to be a major impact on simulation time. Therefore, hybrid-parallelization is best used for the parallelization of annual simulations or a small number of simulations,since in large-scale simulations, the time losses through non-parallelized file-writing outweighs the reduced setup effort.

7.1.3 External-parallelization

In external-parallelization, all simulation related tasks are conducted in Python. Solely the writing of the pre-processing file and generation of one base-variant is performed in TRNLizard. Python writes the simulation files and outputs batch-files needed to run the simulations. These start multiple simulations in parallel. The simulations are equally distributed between the batch-files, which equal to the number of parallel processes.

External-parallelization is conducted in the following steps:

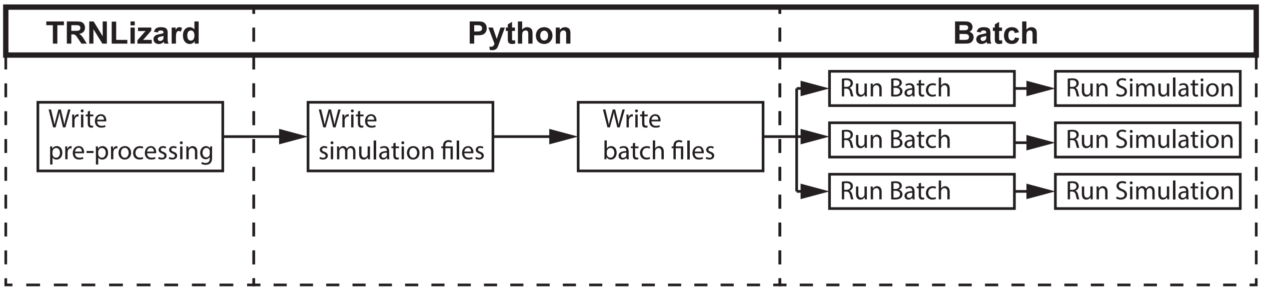

Figure 7.3 External-parallelization process

1. Writing of the pre-processing: After all settings have been adjusted, the pre-processing file is written in TRNLizard. Simultaneously, a set of simulation file templates is created.
2. Writing of the simulation-files: A Python script writes all simulation files by following the pre-processing file, using the templates.
3. Writing of the batch-files: Python processes the simulation data and partitiones them according to the number of threads. The commands to start the individual simulations are stored in a batch-file for each process.
4. Simulation Run: All batch-files are started in parallel and automatically iterate over the simulation-set.

The implementation of the external simulation file writing has been developed from scratch in Python. It is built to work with the data provided by the pre-processing file and simulation file templates. Basically, the code modifies the templates by the instructions given in the pre-processing file. The modified templates are then saved in separate folders. In order to be able to generate TRNSYS simulation files, a python-library of functions is developed. It allows us to read from the simulation-templates, find and modify individual lines, and write new simulation files.

- Reading: Since the TRNSYS-simulation files are non-standard files and not natively readable, dedicated functions are developed to read in the TRNSYS deck- and building-file.
- Modifying: A set of functions is developed, which allow to modify the template according to the preprocessing. These can be differentiated in multi-line operations, replacing several lines of the template-file, single-line operations, exchanging one line, or item operations, exchanging a single data item within a line.

- Writing functions: A certain file and folder structure has to be maintained to generate working simulation files. Therefore, a set of functions is dedicated to automate folder creation and writing of the files.

The developed library is used to write all variants according to the pre-processing file. In each iteration, a copy of the template files is created and modified according to the given instructions. The edited files are then stored in a folder corresponding to the variant-name.

Batch-writing and simulation is implemented in accordance with hybrid-parallelization and is explained in section 7.1.2.

Even though the writing process is signifantly more efficient than in other parallelization-methods, it can only facilitate minor modifications of a template file. It is not applicable for geometrical changes since this would require all 3D data to be rewritten. Furthermore, external-parallelization requires a time-intensive setup of the script since it needs to be individually modified for each parameter. It is, therefore, only applicable for large-scale simulations.

7.1.4 Comparison

A comparison is made to assess the different parallelization methods. One variant is simulated over the course of four type-days resulting in 193 individual simulations. These are conducted in 8 threads on the same processor. A single-process simulation acts as a benchmark.

Figure 7.4 shows the performance gain of parallel simulations compared to single-process simulation. A gain by at least 60% can be achieved. However, significant differences exist between the parallelization-methods. External-parallelization achieves the lowest runtimes per variant. In comparison to hybrid-parallelization, which performs worst, simulation times are more than halved. The performance differences can be attributed to the required writing-time of the different approaches. As seen in figure 7.4, simulation time performs equally well on all parallelized variants. However, writing-time significantly varies.

Figure 7.5 shows the share of writing time compared to total simulation time. The below-average performance of the hybrid-parallelization approach can be attributed to the fact that writing takes as long as in single-process simulation. This is owed to it not being parallelized and is responsible for over 50% of overall simulation time.

In internal simulation, a notable reduction of writing-time could be achieved, since TRNLizard instances are executed in parallel. Its share of about 20% equals that in single processing and marks the minimal achievable share in TRNLizard.

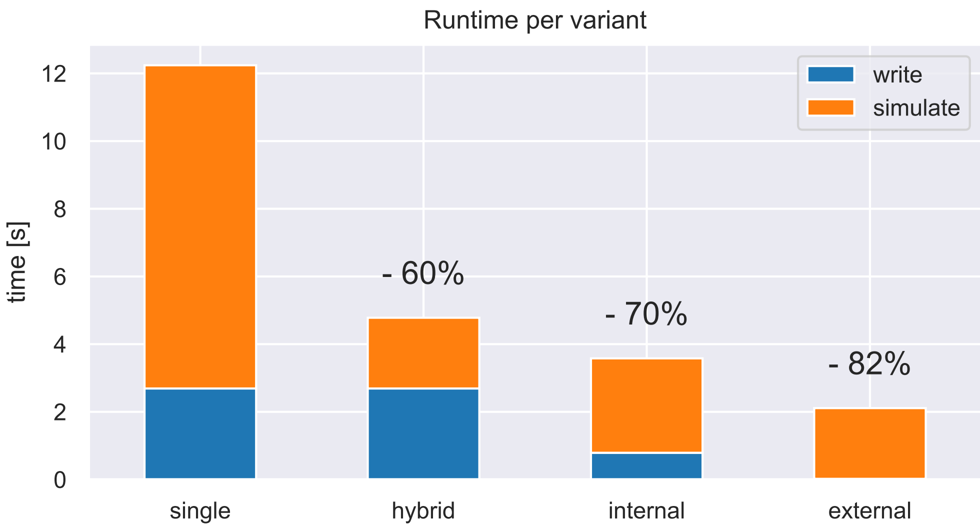

Figure 7.4 Runtime per variant

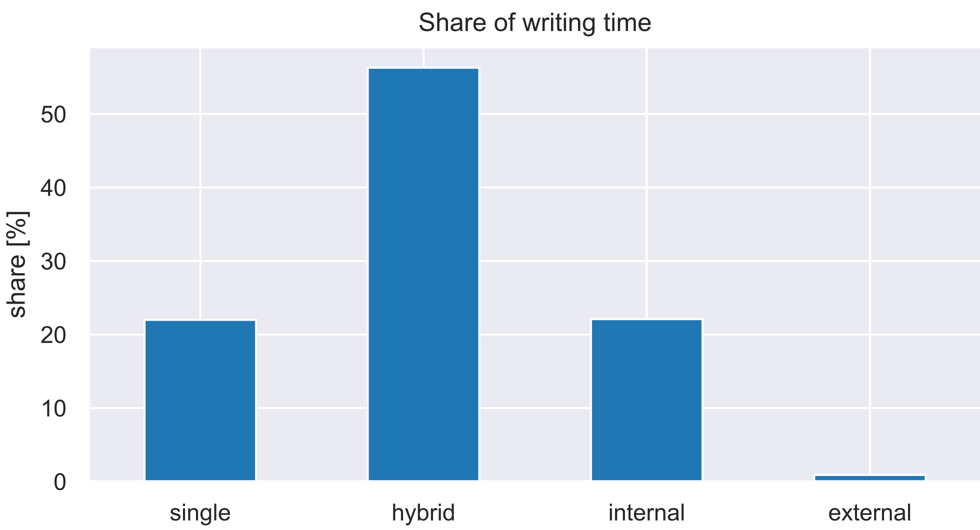

Figure 7.5 share of writing time

A further reduction of the share of writing-time is solely achievable through externalizing the writing of simulation files. In external-parallelization, the share could be reduced to under 1%, rendering it virtually negligible. Since no further reductions in simulation-time can be achieved, without modifications to the TRNSYS engine, external-parallelization is optimum in terms of parallelized simulation time.

The following simulation time is projected, for the total number of simulations:

- Single-simulation: 850 hours (35 days)
- Hybrid-parallelization: 333 hours (14 days)
- Internal-parallelization: 248 hours (10 days)
- External-parallelization: 145 hours (6 days)

To summarize, external-parallelization is most efficient if no geometrical changes are required. Internal-parallelization performs best if geometry needs to be taken into account. Since this study does not modify the geometry of the zone, external-parallelization will be applied.

7.2 Error detection

As noted in [Nguyen et al., 2014b], observing the simulation and detecting errors is key to mitigate errors in post-processing and optimize subsequent simulations. Therefore, a Python script is developed that observes the simulations, detects erroneous simulations and if required aborts them.

The error-detection is based on the assumption that a fixed time-span is required to perform a simulation successfully. If this time-span is undercut or exceeded, an error is assumed. Since simulations in LMP-calculation range from 336-hour LMP-simulations to full-year base-simulations, a wide range of time-spans is allowed. Including a margin of error time-spans between 5 and 240 seconds are regarded as successful, simulations that fall below this boundary most likely have a flawed setup and do not start at all. Simulations that exceed 240 seconds indicate an error during the simulations and need to be aborted to allow subsequent simulations to start.

The error-detection is implemented in Python using the psutil library, which allows for tracking and interacting with windows-processes. The simulations are identified by their process name "TrnEXE64.exe". Each simulation is distinguished by an individual process ID (PID), which is used to track simulation time. All simulations that do not perform as expected are saved in an output file with information about the occurred error.

7.3 Time estimation

Additionally, to the automatic error-detection, a second layer of monitoring is implemented through a progress-tracking script. It shows the percentage of concluded simulation as well as the projected finishing time.

Two approaches are implemented, the first is applicable to all three parallelization methods, the second is more time-efficient but only applicable for hybrid- or external-parallelization.

- Monitoring of .lst files: The LST-file is an output file generated by TRNSYS during the simulation run. It is, therefore, a suitable indicator if a variant was already simulated. Periodically Python checks all folders in the simulation directory for LST-files. The number of files is then compared to the total number of simulations, derived from the pre-processing file. However, if several thousand folders are checked, the scanning requires significant computational-effort, which negatively impacts the simulation efficiency.
- Monitoring of batch output: Alternative to using the LST-files is to monitor the output of the batch process. In the batch-file output, the start and stop time for each variant are stored. From this, the number of completed simulations can be derived and compared to the total number of simulations.

7.4 Summary

In the following section, the actual simulation time, the number of runs, as well as the storage required, is summarized.

A total of 216 160 simulations have been conducted. Every load-management-simulation required 4.25 MByte of storage, every base-simulation 32.3 MByte. In sum, 893 GByte of data were generated by all load-management-simulations, and 35 GByte by base-simulations.

A mean time of 1.8 seconds was required for each variant by executing ten-simulations in parallel. In total 108 hours, or 4.5 days were required to finish all simulations.

- Total number of simulations: 216 160
- Total storage: 928 Gbyte
- Total time: 108 hours
- Average time: 1.8 seconds

8 Post processing

The following chapter covers the post-processing steps that are performed in this study. In the following the process is divided in three major steps: compilation of simulation data (section 8.1), processing of the compiled data (section 8.2) and the visualization of the processed data (section 8.3). All post-processing steps are implemented in Python. The implementation is especially based on the Python library Pandas that allows for the analysis of big data sets.

8.1 Data compilation

This section covers the steps required to compile the result files to a single database. As the entire set of simulation data is close to one terabyte, the compilation is time-intensive. In order to enhance efficiency following measures are taken: a indexing of all simulation-result files (section 8.1.1), storing base-simulations in memory (section 8.1.2), and saving the results to a reloadable database (section 8.1.5).

8.1.1 Indexing

Initially, an index of result-file paths is constructed. Since the simulation data requires close to one terabyte of storage, reading and searching the entire simulation set is time-intensive. Therefore, all simulation folders are scanned and indexed. Based on this list of indices, all subsequent steps are performed in a programming-loop.

8.1.2 Processing result files

As stated in section 6.1, a base-simulation is needed to assess LMP. Since several load management simulations utilize a single base simulation, significant time gain is achievable if all base-simulations are initially stored in memory, which avoids rereading the same file. Base files are identified and found by the keyword 'base' in the filename. The heating power for every timestep is loaded and saved in a dictionary with the parameter code as a key and unique identifier. Since load management simulations are only needed once, these are read on demand, due to limited memory capacity. For each LMP simulation, operative temperature and power consumption are saved to a list.

8.1.3 Calculating load management potential

The calculation of load management potential is based on the theoretical approach by [Hausladen, 2014] and implemented according to the process described in section 6.1. The temperature of the LMP simulation is monitored originating from the action point. In a loop, each subsequent timestep is checked if it complies with comfort-conditions. The power difference between base-case and LMP-simulation is then calculated and appended to a list. If the operative temperature is not within comfort bounds, the loop is interrupted. The result data, including LMP and shutoff-time-span, are then appended to the database. The key to each data is the simulation filename.

8.1.4 Calculate annual energy consumption

The annual energy consumption is derived from the base-simulations. Since the base simulations are stored in memory, a rereading of the files is unnecessary. For each stored key of the dictionary, the sum of all data items is calculated. Since the resolution of the simulation is set to quarter-hourly and data is stored in W/m^2, it is necessary to divide the sum by 4000 in order to get results in kWh/m^2a.

8.1.5 Storage

Since data in memory is only stored as long as the program is running, it is necessary to develop a long term storage solution to avoid rerunning the time-consuming data compilation process. The Python library Pandas provides an inbuilt function that allows saving a database to a file. Beforehand, data types in the database are optimized in order to reduce storage size and facilitate fast loading times.

The entire compilation-process requires over 24 hours and scans nearly one terabyte of files. After the compilation-process is finished, the final result database is reduced to 700 megabytes of data. This database can later be reimported in seconds and is all that is required to perform subsequent post-processing tasks.

8.2 Data processing

In the following section all further tasks are described that are required to generate meaningful data from the previously created database. These include calculating the electrical energy consumption (section 8.2.1), extracting building data for each simulation (section 8.2.2), calculate robustness indicators (section 8.2.3), calculating pareto optima (section 8.2.4) and aggregate the results (section 8.2.5).

8.2.1 Electrical-energy calculation

For the sake of time-efficiency, building technology has not been modeled in detail. Therefore, simulations solely output usable energy demand. In order to be able to asses actual electricity consumption, a COP curve of a heat pump is used. The COP is calculated, based on the inlet temperature of the heating system and outdoor air temperatures. Having determined the COP, the usable energy demand can be converted to the electrical energy demand. Data from an air source heat pump of the company Wolf [Wolf, 2016] is used to estimate the COP. Wolf provides data on typical COP-curves depending on inlet temperature and outdoor air temperature. In this study, the curves are approximated by simplified functions displayed in red in figure 8.1. The COP and electrical energy demand are recalculated for each timestep of the annual simulations, depending on outdoor temperatures. Inlet temperature of 35 °C is assumed for underfloor heating systems and 55 °C for radiators.

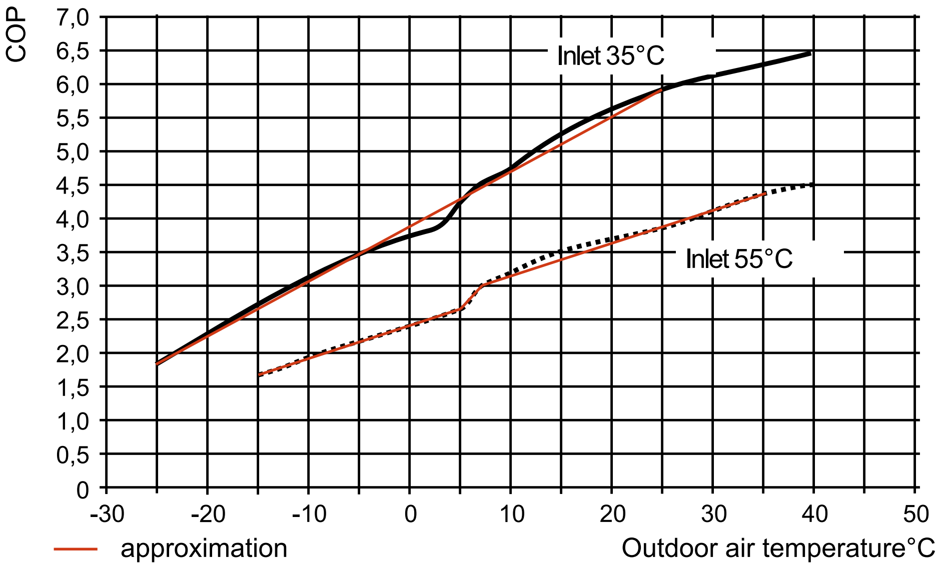

Figure 8.1 COP dependence on outdoor air temperature of air source heat pump under different inlet temperatures, adapted from [Wolf, 2016]

8.2.2 Extract simulation data

Building simulation data is extracted and added to the database to identify the effects of individual parameters and scenarios. It is decoded from the parameter-code and appended to the database. Each parameter and scenario is stored in individual database entries with their respective values. Therefore, variants can be filtered and selected according to their parameters and scenarios in the subsequent data processing.

8.2.3 Calculate robustness indicators

As stated in section 5.8.2, the min-max regret (MMR) and weighted-median-spread (WMS) indicators are chosen for this study. In the following, the implementation of both indicators is described. The MMR indicator is the sum of the differences to each local optimum of each scenario. The lower the sum, the smaller the regret under uncertain conditions. This procedure is repeated for each variant. Since two optimization objectives (energy consumption and LMP) are considered, a weighted objective function is applied.

The differences are normalized, in order to assess both objectives in a weighted function. Equation 8.1 shows the calculation method.

$$MMR = weight_{LMP} * MMR_{LMP} + (1 - weight_{LMP}) * MMR_{energy} \tag{8.1}$$

Weighted median-spread

In the WMS-indicator, median and spread are assessed for each variant. The results are then normalized and aggregated in an weighted sum. The results for each optimization objective (energy consumption and LMP) are again evaluated in a weighted objective function. Equation 8.2 shows the calculation method of WMS.

$$\begin{aligned} WMS = weight_{LMP} * [weight_{median} * (1 - \frac{median_{LMP}}{max(median_{LMP})}) + (1 - weight_{median}) * \frac{spread_{LMP}}{max(spread_{LMP})}] \\ + (1 - weight_{LMP}) * [weight_{median} * \frac{median_{energy}}{max(median_{energy})} + (1 - weight_{median}) * \frac{spread_{energy}}{max(spread_{energy})}] \end{aligned} \tag{8.2}$$

8.2.4 Calculate Pareto optima

An alternative to comparing to objectives with a weighted sum is a Pareto front. In it all non-dominated solutions in a result-set are included. Since the objective of this study is to generate different refurbishment strategies, the Pareto front provides a good indication of optimality in terms of energy demand and LMP.

In the case of this study, the Pareto-front is implemented through a programming-loop, which checks each variant of the result set if a variant with higher LMP or lower energy demand exists. If one or both of these conditions are true, the variant is no Pareto optimum. Else it is part of the Pareto front.

8.2.5 Aggregate results

Due to the size of the extracted raw data, aggregation is necessary to enhance readability. The aim is to decrease the overall number of datapoints without compromising the content. The different aggregation-methods applied in this study are explained below.

Projected annual load management potential

As simulation-time restraints make it unfeasible to perform a whole-year LMP simulation, only selected type-days are calculated. However, since each type-day represents for a certain time and temperature range with known occurence a projection of an annual LMP can be made. The annual LMP is calculated, as shown in equation 8.3.

$$LMP_{annual} = \sum n_{typeday} * LMP_{typeday} \tag{8.3}$$

LMP-metric

LMP is composed of activation potential and deactivation potential. However as examined in section 9.3, deactivation-potential tends to represent the maximum available LMP, activation potential, on the other hand, is rather underestimated, due to the calculation methodology. Therefore an aggregated LMP metric is introduced, which takes the mean of activation and deactivation potential. Its' estimation of LMP is asserted to be more realistic, than deactivation- or activation-potential individually

$$LMP_{total} = \frac{|LMP_{activation}| + |LMP_{deactivation}|}{2} \tag{8.4}$$

8.3 Data visualization

Visualizing the generated data is key to identify patterns. This is especially true, since the size and complexity of the dataset does not allow for drawing simple conclusions. Therefore a interactive-visualization methodology has been developed to support the data analysis in this study. It is implemented on basis of the python library Matplotlib and based on the previously processed data. Following section looks at the implementation of the interactive-visualization in detail. It covers the basic methodology in section 8.3.1, the creation of a scatterplot (section 8.3.2) and barplot (section 8.3.4), labelling of the scatter-plot (section 8.3.5), integration of the robustness indicator (section 8.3.3) and pareto-optima (section 8.3.6), a visualization of the parameter- (section 8.3.7) and scenario-impact (section 8.3.8) as well as a way to filter data (section 8.3.9).

8.3.1 Interactive visualization

Interactive-visualization is defined in this study as plots that react immediately to their inputs. For example, this allows visualizing the graduate change of the cumulated robustness indicator if the weight of the objective function is changed.

In this study, the interactive-visualizations are implemented through interactive-widgets provided by the Matplotlib library. A control panel in a separate window allows for live user interaction. The control panel is composed of switches, sliders, and text fields. The plots are refreshed each time the user changes an element.

8.3.2 Scatterplot

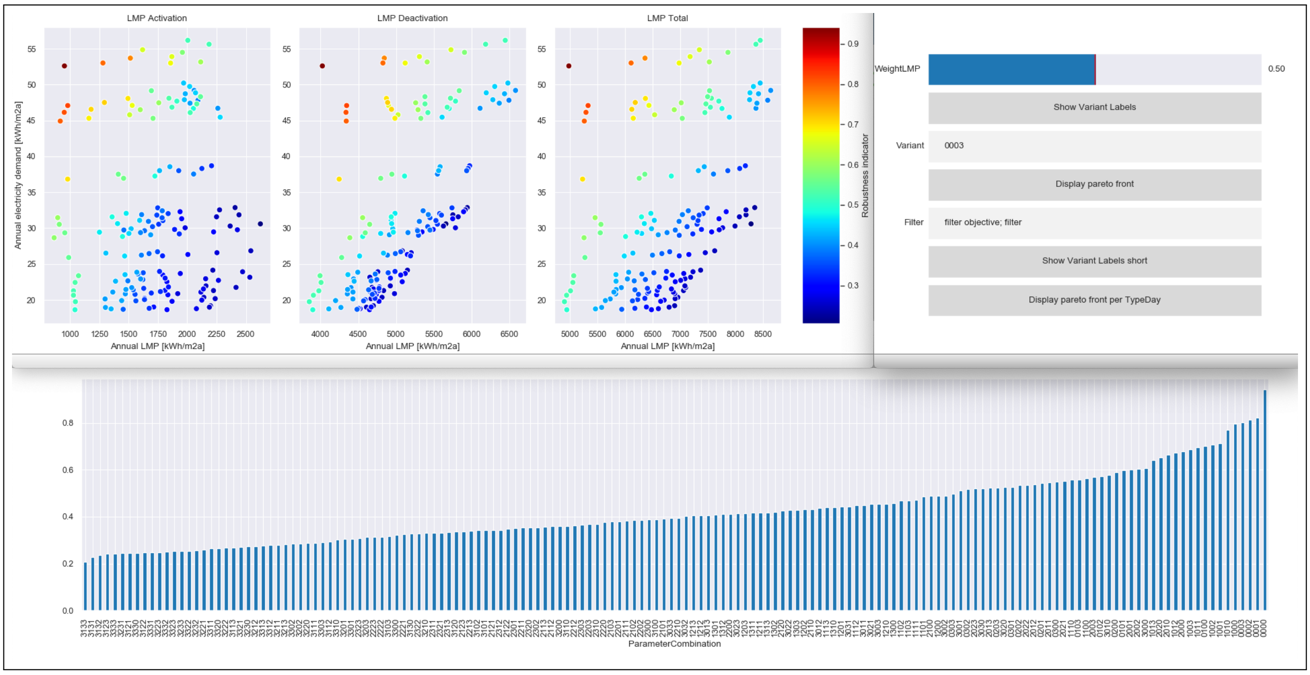

Figure 8.2 Interactive visualization interface

A scatter-plot is the most useful tool to visualize data with two performance objectives (energy-demand, LMP). In this case the x-axis represents mean-total-LMP, the y-axis mean annual energy-demand. Each scatter-point represents a variant and is colour-coded depending on their robustness-indicator. The color scale ranges from dark-blue (optimal robustness indicator) to dark red (worst robustness indicator).

Alternatively to plotting energy-demand and LMP, robustness indicators can be directly plotted to the x- and y-axis, since the mean values can be misleading. However, this has the disadvantage that the robustness indicators are normalized values between zero and one.

8.3.3 Robustness-indicator weight

The control panel allows to adapt the weight between LMP and energy demand for the MMR indicator and additionally the weight of median and spread in the case of the WMS indicator. Since the weighing is an integral part of the robustness indicator function, it has a significant influence on the result. The weight can

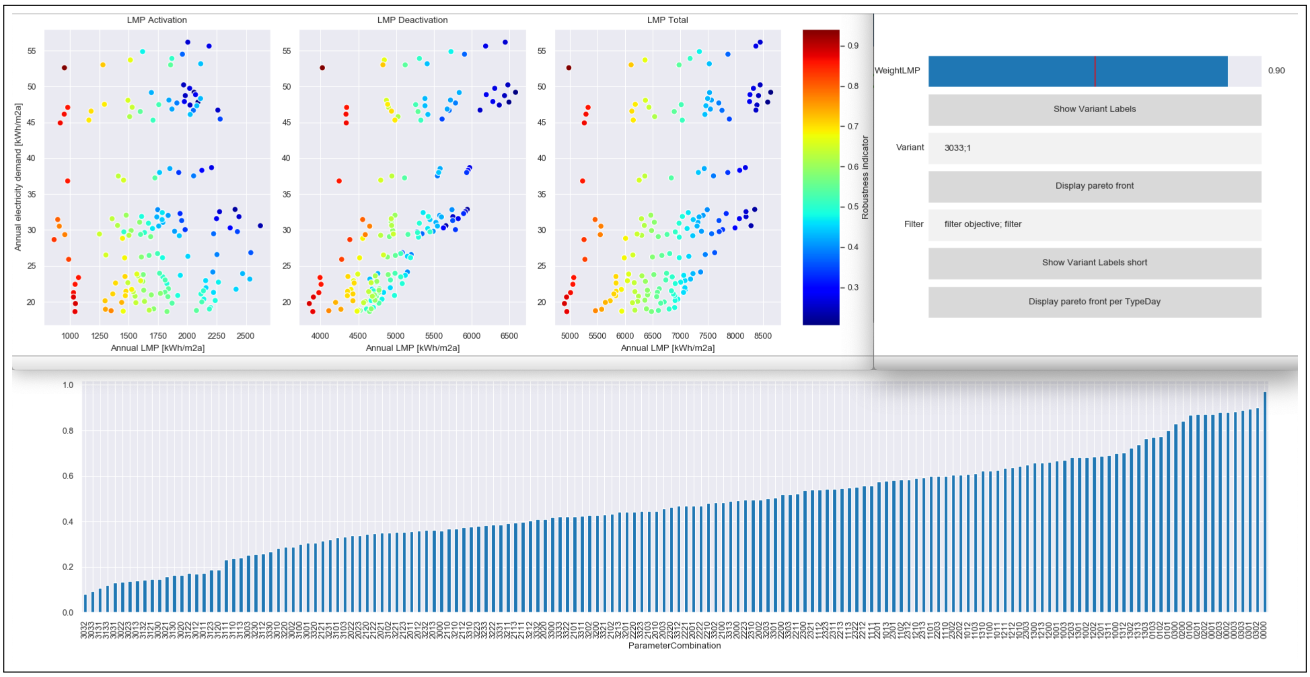

Figure 8.3 Interactive visualization interface LMP weighted 90%

be adapted via a slider that ranges from zero to one. In the case of LMP and energy demand zero means, that no focus is laid on LMP. If the median and spread are considered, zero stands for no influence of the median value.

8.3.4 Bar-plot robustness-indicator

The bar-plot visualizes the robustness indicator. The smaller the bars, the better the variant. The bars are automatically sorted depending on their value. The individual variant-codes can be retrieved from the x-axis labeling. The barplot automatically updates the bar-sizes if the weight is changed in the control panel. The variant with minimum bar size is optimum for the chosen weight.

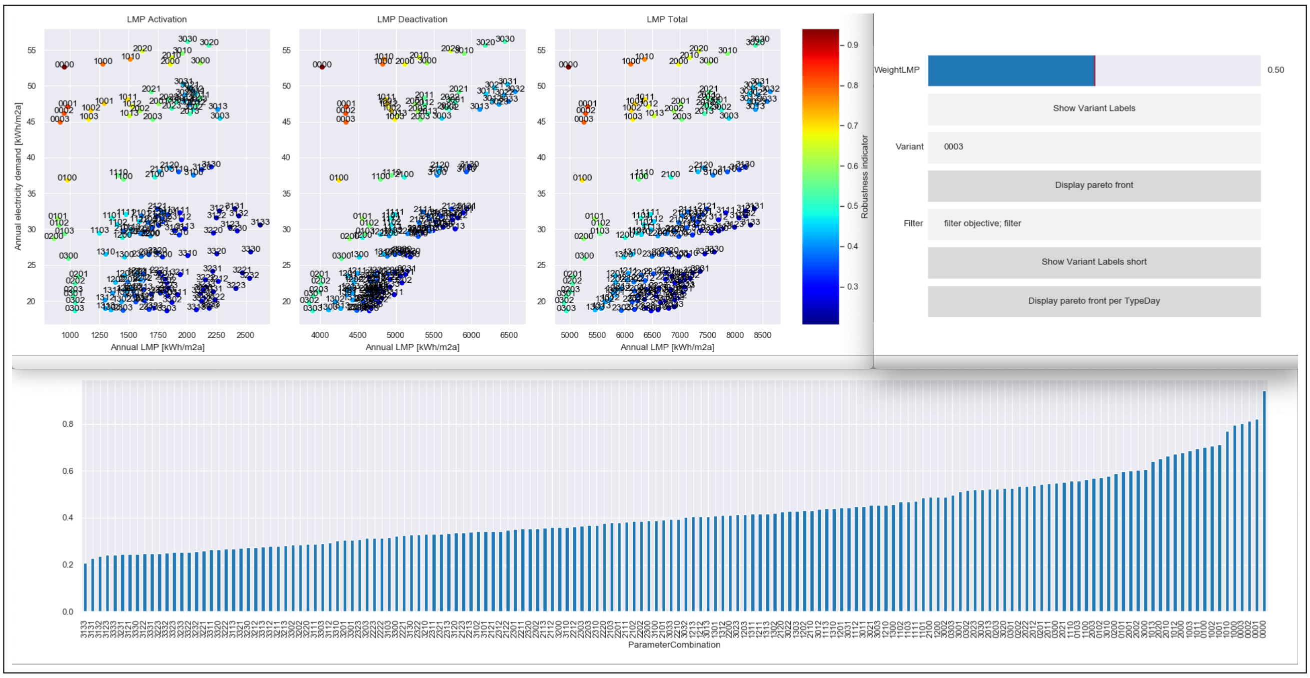

Figure 8.4 Interactive visualization interface scatter plot labels

8.3.5 Labelled scatter plot

As individual variants can not be discerned in the scatter-plot, an option to label individual points is integrated in the interactive-visualization. Depending on their x- and y-value point are labeled with their respective variant-codes (e.g., 3103). The label is expanded if raw data instead of aggregated values is plotted, to include all information (e.g.,'cold-0000#0000').

A loop over each variant conducts the labeling. It queries the x- and y-position and places the label on these coordinates.

8.3.6 Pareto-front

Since a Pareto-front is well suited to create potential refurbishment strategies by identifying non dominated solutions, it is visually implemented in the scatter-plot.

The calculation of the Pareto optimal variants follows the implementation explained in section 8.2.4. The coordinates of the determined optima are extracted from the database and connected in the scatter-plot.

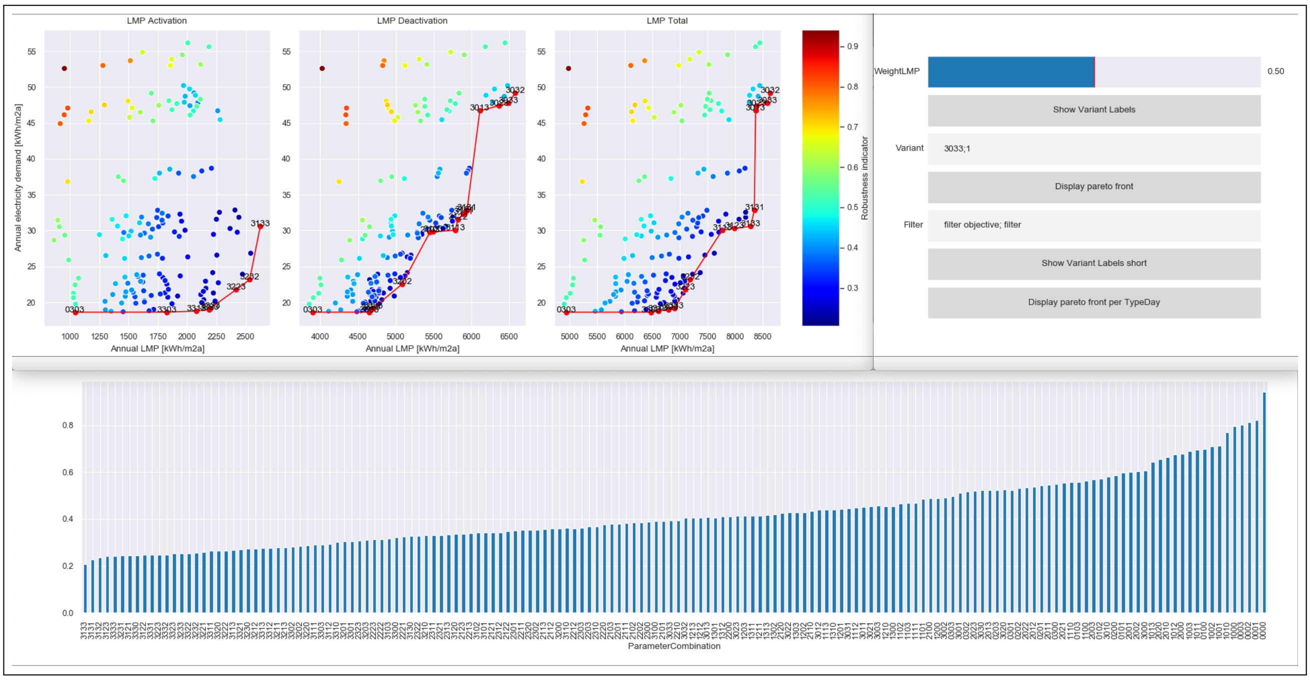

Figure 8.5 Interactive visualization interface Pareto-front

8.3.7 Visualize impact of parameters

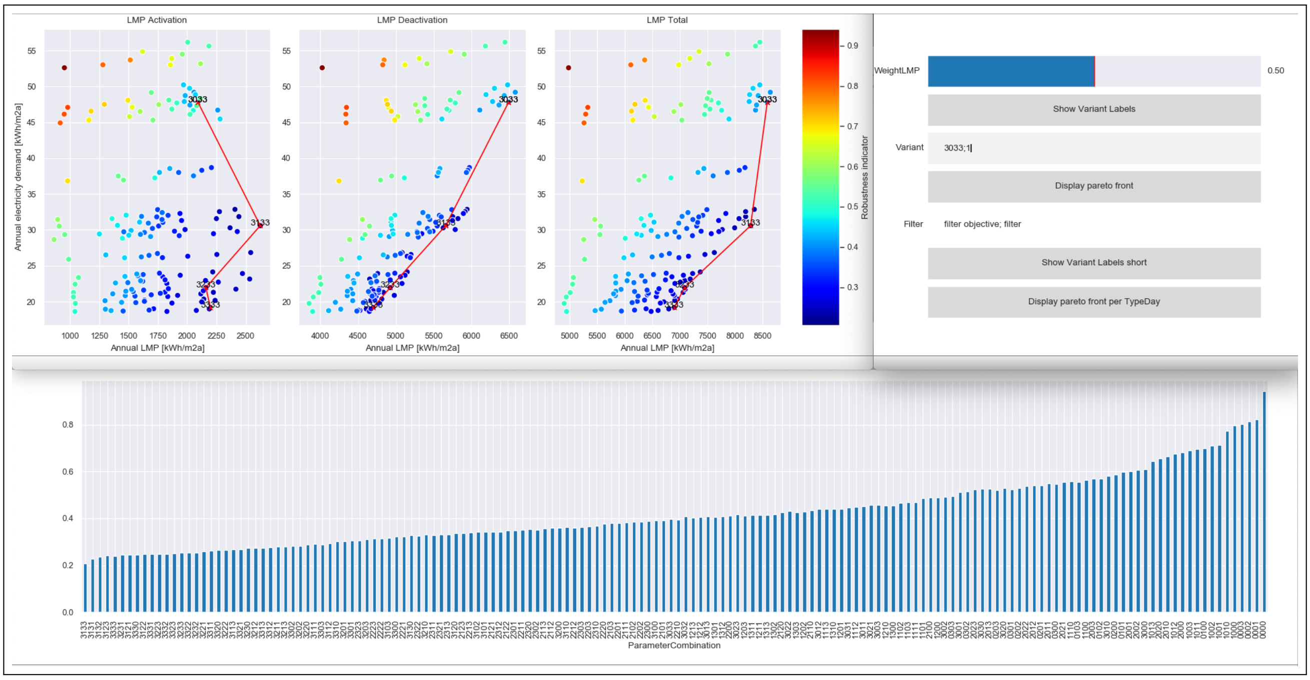

Figure 8.6 Interactive visualization interface parameter impact

The identification of parameter impact on the optimization objectives is key to this study. Therefore the impact of individual parameters can be visualized in the scatter-plot. The requested parameter and variant can be chosen through the control panel by entering the variant code and specifying the position of the parameter to be analyzed. For example, the entry "3033;1" searches the result database for the coordinates of the following variants: 3033, 3133, 3233, and 3333. Once all coordinates are retrieved, the points are connected and drawn on the scatter plot.

8.3.8 Visualize impact of scenarios

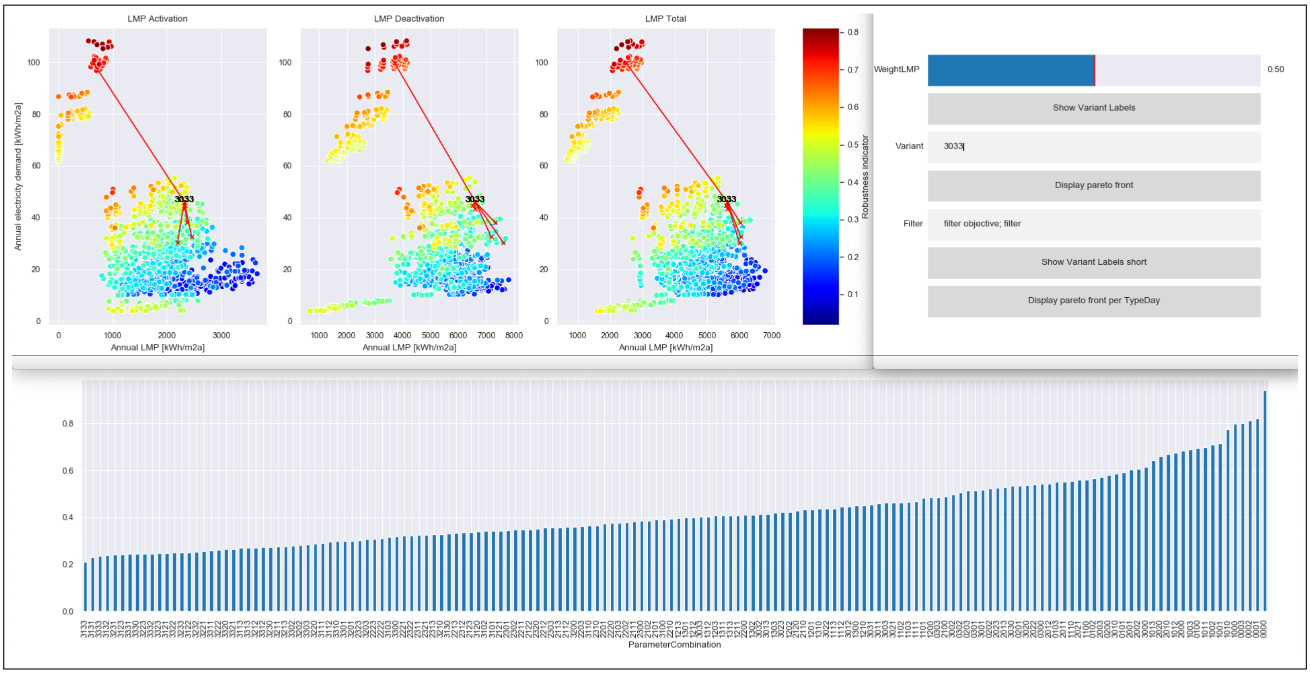

Figure 8.7 Interactive visualization interface scenario impact

Similarly to the visualization of parameter-impact, the impact of scenarios can be displayed. The variant for which the scenario-impact should be displayed can be chosen in the control panel by entering its variant code. For example, entering "3033" retrieves the coordinates of the base scenario 3033#0000 and the uncertainty scenarios: 3033#0100, 3033#0200, 3033#0010, 3033#0020, 3033#0001. A line is then drawn from the base scenario to each uncertainty scenario, thus displaying the amount of change caused by each scenario. However, this requires that the results are not aggregated.

8.3.9 Filter data

To fully explore the data and check its validity, it is helpful to work with the unaggregated, raw data. A filtering function is implemented in the control panel to help to explore the raw data. It allows visualizing only certain sections from the data. The implemented filter is flexible in its function. A filter objective, as well as a filter aim, needs to be specified. For example, the entry "ExternalWall; AW1" narrows the data-set to variants, which posses an external wall of the class "AW1". Other potential filter objectives are TypeDay, Scenario, Window, ActiveLayer and ScreedHeight. Each of these can be freely combined. For example, raw-data can be queried for variants from the very-cold type-day with passive-house standard external-walls and high screed-thickness. The filter box needs to be left empty in order to reset all filters and return to the whole data-set.

9 Results

This chapter discusses the generated and processed results. The chapter is subdivided in a fundamental categorization (section 9.1), an exploration of the differences between the two robustness indicators (section 9.2), an assessment of the differences between activation- and deactivation-potential (section 9.3),an analysis of the impact of the different parameters (section 9.4) and scenarios (section 9.5). Furthermore, the course of the pareto-fronts is regarded in section 9.6, section 9.7 merges the individual findings to create refurbishment strategies.

9.1 Categorization

A general categorization of the result allows us to initially explore the impact of parameters and scenarios on energy demand and load management potential. In the following, the discernible categories are described. The section is subdivided in an interpretation of the aggregated results data (section 9.1), separate type-days (section 9.2) and separate uncertainties (section 9.1.3).

9.1.1 Aggregated results

Figure 9.1 shows the mean values for LMP and electricity demand for all scenarios. Furthermore, the results of the individual type-days are aggregated to a projected annual LMP.

The categorization shows that the different insulation-levels of the external wall are easily discernible. Moreover, the activation potential plot allows differentiating between different screed heights.

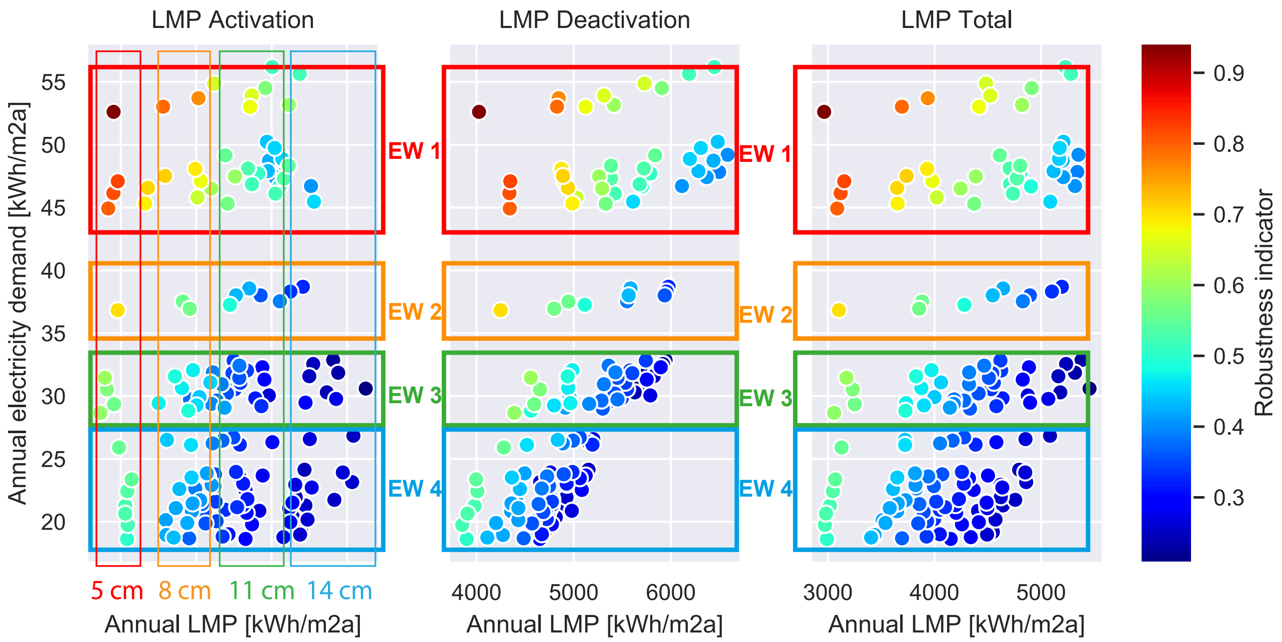

Figure 9.1 Classification | aggregated results

9.1.2 Seperate typedays

In figure 9.2, mean values for LMP and energy demand are plotted. However, the result data for each type-day is displayed as an individual data point. Therefore the LMP result is that of a single day and is not comparable. Since the energy demand is based on an annual calculation, type-days can only be differentiated by the LMP.

If activation-potential is considered, a division into three groups can be seen. The lowest activation-potential is achieved during the very-cold type-day. During it the heating system operates close to full-load, thus minimizing activation-power. The center is taken up by the type-days cool and moderate. These allow a high activation-power, since the heating-system only operates in part-load. However, higher outdoor temperatures cause the activation-time to be the smallest among the compared. The highest activation-potential can be achieved during the cold type-day. As the heating system is no longer operating close to full load, a substantial activation-power is available. Furthermore, the low outside temperatures allow for a long activation-time.

In the case of deactivation-potential, the correlation as seen in activation potential is reversed. During the cold-type-day, the worst results are reached. This can be attributed to the mediocre heating-power that is available for deactivation, as well as small deactivation-time since external temperatures are low. The

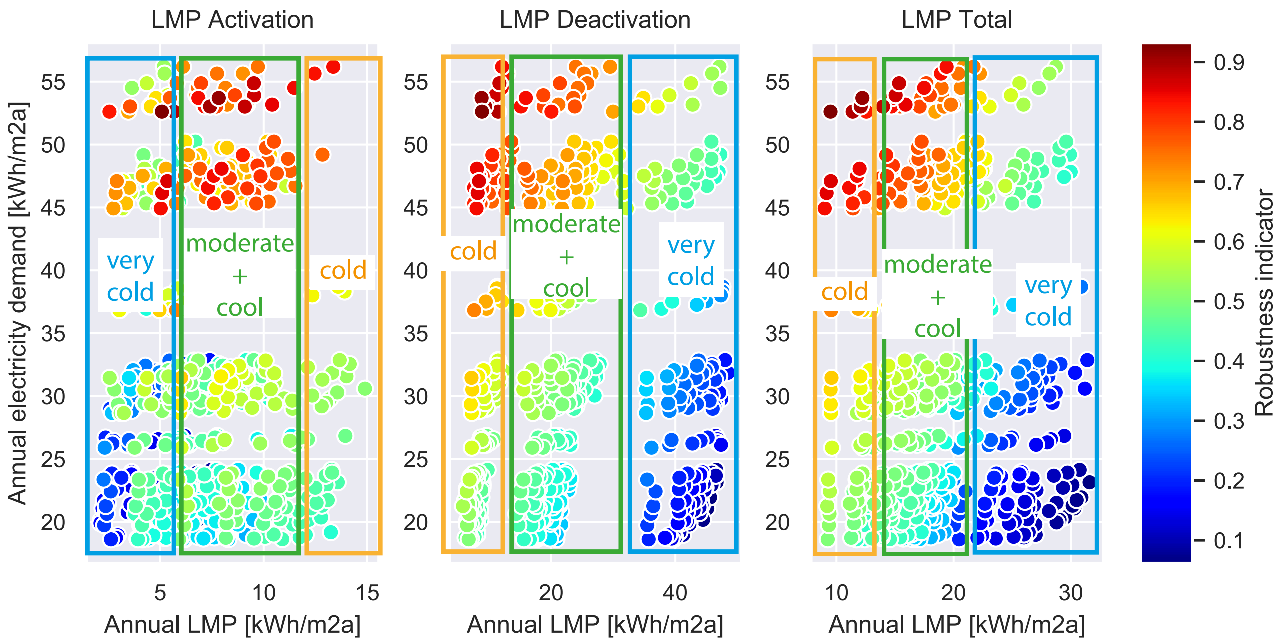

Figure 9.2 Classification | seperate typedays

type-days moderate and cool form again the center of the plot. Even though their deactivation-power is low, long-lasting deactivation-times result in average deactivation-potential. Very-cold external conditions are best in terms of deactivation-potential. Even though the deactivation time is short, the deactivation-power is high as the heating system operates close to full-load.

9.1.3 Seperate scenarios

In figure 9.3 annual results are plotted, however without aggregating the individual scenarios to a mean-value. Two outliers can be immediately identified. In the top-left corner of each plot, a group of variants with very high energy demand, as well as low LMP can be identified. These are exclusively comprised of variants operating under the constant-ventilation scenario. High ventilation-losses, due to the constant air-change rate, is the reason. A smaller sub-group can be seen in the bottom-left corner of the deactivation-potential plot. It is comprised of highly insulated variants in the occupational scenario. Due to increased internal gains, these variants require next to no heating energy and allow only minimal deactivation-potential. All remaining scenarios form a main group, that is not distinguishable.

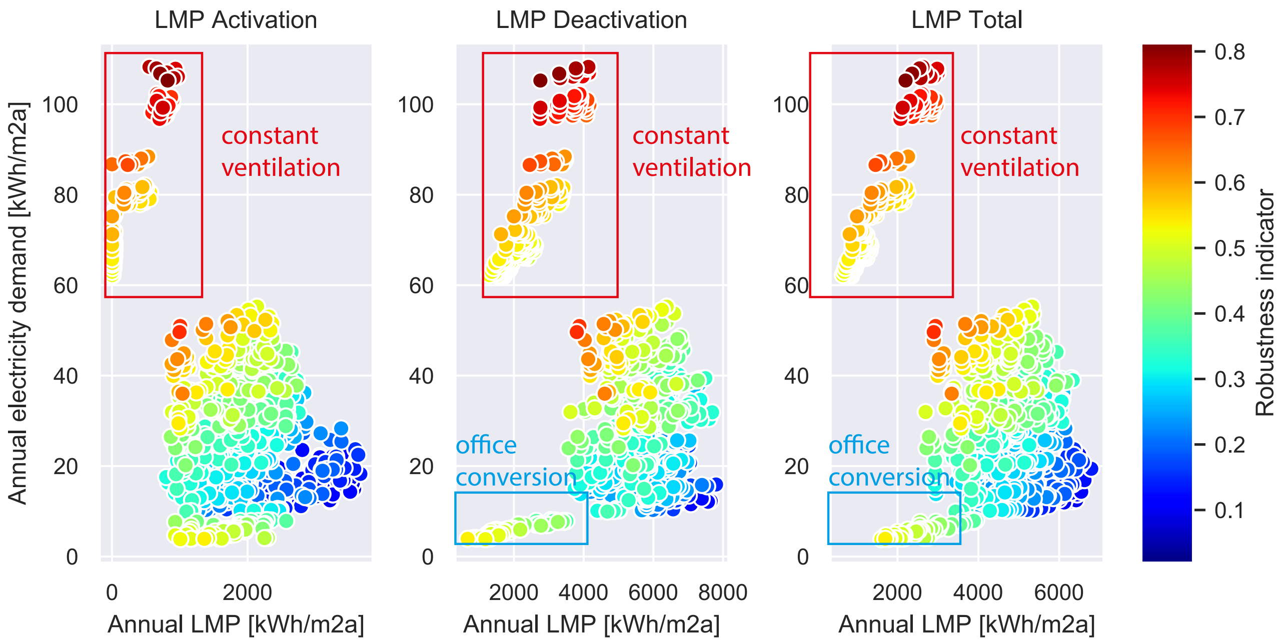

Figure 9.3 Classification | seperate scenarios

9.2 Differences between indicators

The following section examines the difference between the used robustness indicators. The MMR indicator, as developed in [Kotireddy, 2018], is compared to the MWS indicator as used in [Maderspacher, 2017]. The comparison is conducted regarding to the ranking of optima under differnt weights, as well as the robustness of the results.

In figure 9.4, WMS and MMR are compared to each other. The three columns represent the LMP weight of the objective functions. The first and second row shows the results of the twenty best performing variants for each indicator. The third row indicates the impact of the weighing of the median on the correspondence between the two indicators. The last row visualizes the robustness of each indicator regarding to changes in the weighing-factor.

WMS and MMR are contrasted, by comparing the best performing variants. Espescially in the case of 50% weight differences become evident. The overall insulation level tends to be higher with the WMS-indicator. If MMR is considered, the six best performing variants all have a medium insulated external wall in common, compared to high and very high insulation in the case of WMS. Furthermore, significant differences are notable regarding the building technology of the variants. WMS leads to a medium screed thickness with minimum coverage. MMR, however, leads to variants with very high screed thickness and high coverage.

A critical distinction can also be seen in the difference between each rank of the result data. The distances that differentiate each variant are minute in the case of WMS, implicating a high sensitivity to change. In comparison, the distances in MMR are more pronounced. Especially the top-ranking variants are well distinguished and therefore less prone to change.

The correlation between WMS and MMR, is shown in the third row of figure 9.4. The x-coordinates represent the weight of the median-value in the WMS indicator. The blue line shows the share of overlap in best-performing variants. The orange line shows the share of variants with the same rank. Maximum correspondence between the indicators is reached if the focus is put on LMP and median. In this case, over 85% of the top 20 match. A peak in rank-correspondence can be identified at 75% median-weight and reaches a maximum of 45 %.

The last row in figure 9.4 shows the sensitivity of the indicators towards change of weight. The y-axis signifies the share of optimum-variants that remain unchanged even though the weight is modified. The bigger the area under the curve, the higher the share of unchanged variants, which indicates robust solutions that perform well under a range of expectations.

MMR proves to be more robust, especially if the focus is led on LMP. With MMR a large share of variants remain the same at change.

It can be summarized that the robustness indicators behave differently depending on the weight of LMP and median. Generally, a high correspondence is achieved if the focus is led on LMP and median instead of energy and spread. The analysis shows that MMR produces more robust results than WMS. In other words, WMS is better in finding optimal solutions for specific cases, optima determined by MMR however, perform well under a broad range of expectations and are more robust to change. Since this study aims to find robust refurbishment strategies, all subsequent examinations will be solely based on the MMR indicator.

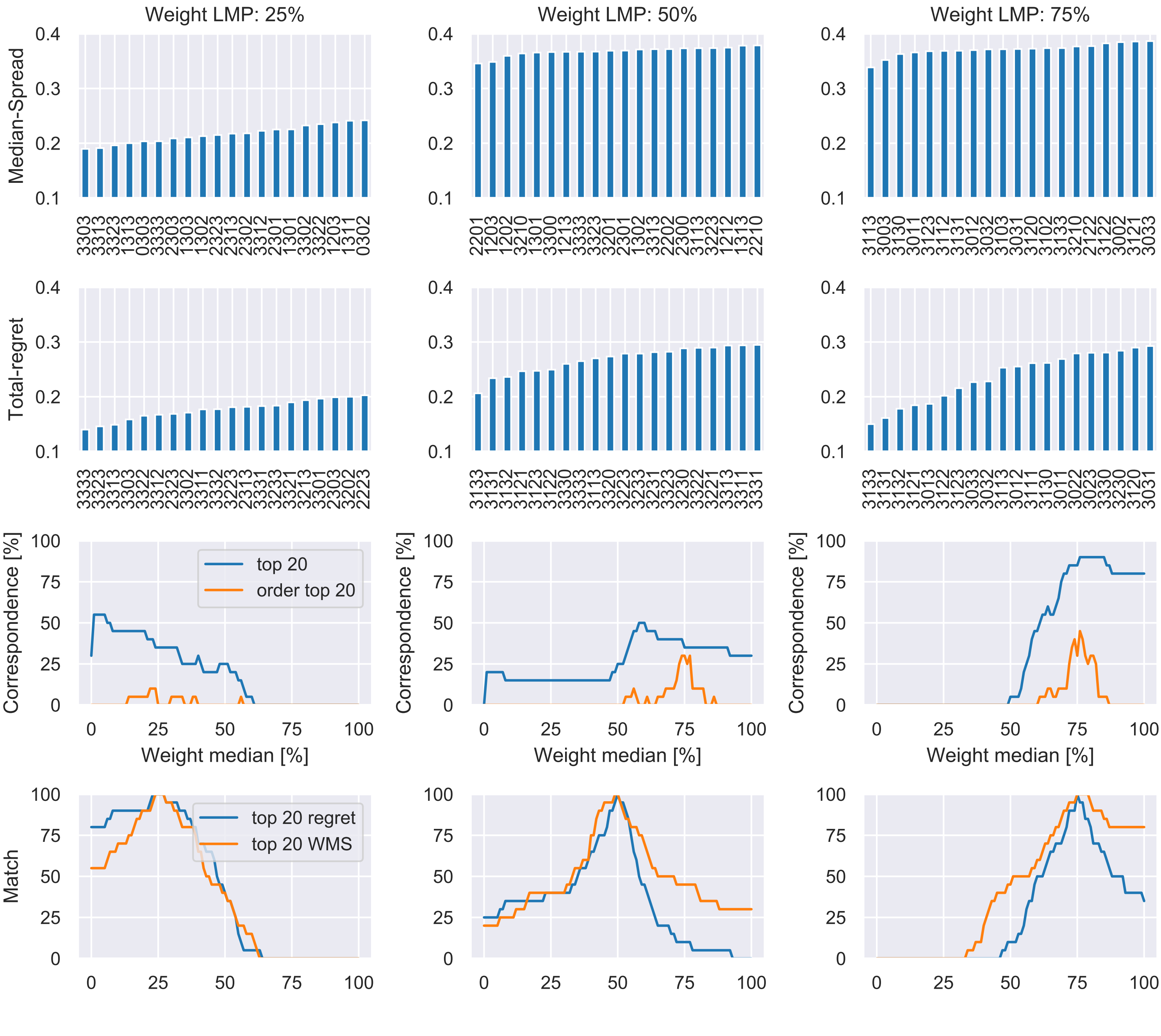

Figure 9.4 Comparison of robustness indicators

9.3 Activation- and deactivation-potential

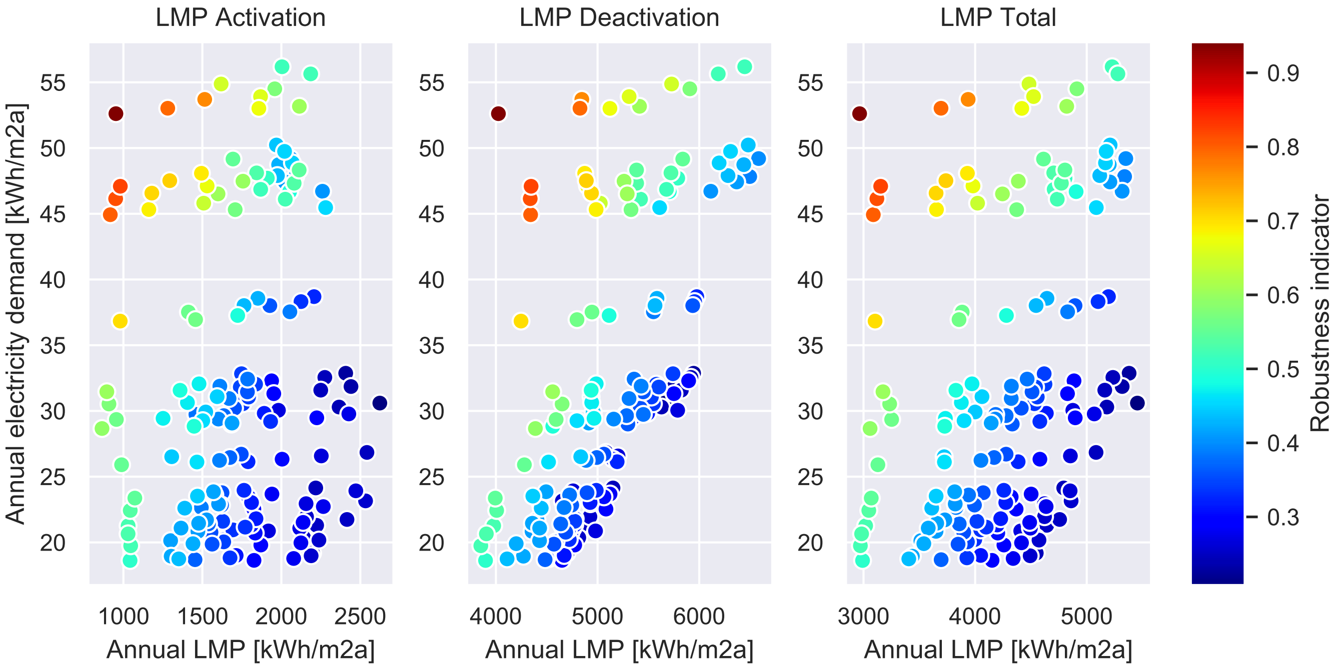

Figure 9.5 Comparison of activation and deactivation potential

Figure 9.5 shows the difference between annual activation-potential, deactivation-potential and combined-potential. Even though both strategies are performed over the same temperature difference of two Kelvin, values vary significantly. Deactivation-potential manages to achieve more than double of the activation potential. At first glance, this seems to highlight a inconsistency of the result-data. However, the effect can be attributed to the LMP calculation methodology. In the case of deactivation potential, the thermal-mass is precharged for the duration of two-weeks, before the heating power is deactivated, therefore, providing ideal conditions. However, if activation potential is considered, the pre-charged thermal mass becomes a disadvantage since the additional absorption capacity is severly reduced and the comfort limits reached quicker. This effect is additionally intensified, if heat transmission system with convective heat transfer and low response times are used.

These assumptions have also been proven in the simulation, where radiators perform much worse than underfloor heating in terms of activation-potential, due to their faster response time and higher share of convective heat transfer.

Therefore both values are consistent within their methodology. Due to the fully charged thermal-masses, deactivation-potential demonstrates the maximum exploitable LMP. Activation potential on the other hand is often unable to fully exploit the its potential. Therfore, the aggregated LMP-metric (see section 8.2.5) is deemed to be the best approach to actual LMP.

9.4 Impact of parameters

Identifying the impact of parameters is key in this study. The next section will look at each parameter individually and assess its impact. A sensitivity analysis will compare the parameters among each other and determine the parameter with the foremost impact.

9.4.1 External-wall

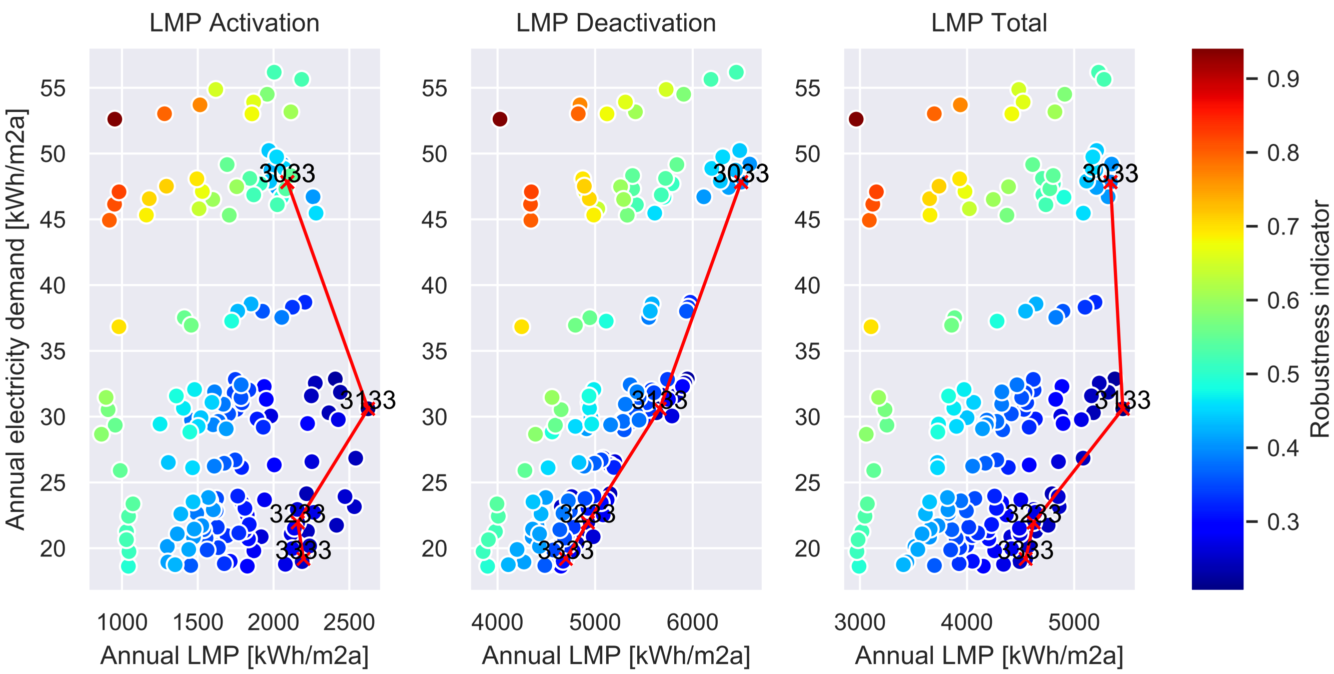

Figure 9.6 Parameter impact | wall insulation

Figure 9.6 visualizes the impact, that the change of the external wall has on the result at otherwise identical conditions. The shown variant is representative and displays the typical course.

The impact on energy demand is significant. A maximum reduction of over 60% can be achieved due to the increased thermal resistance of the external wall. Maximum energy reduction is registered between the first and second stage. The reduction between the third and fourth stage is insignificant.

The effect of wall-construction on LMP is less clear than on energy demand. Overall, higher quality of the external wall reduces the LMP. Especially the deactivation potential is steadily falling with increasing thermal resistance. This can be mainly ascribed to the reduced energy demand, which leads to less deactivation power. The activation potential, however, initially increases from the first to the second stage, to fall back short above the initial level for the third and fourth stage. This initial increase can be attributed to the reduced heating power required, which leaves more capacity for activation. The effect is declining for the third and fourth stage since the reduced activation-time predominates the reduced base-capacity. In total LMP, the overall decline in the deactivation-potential is balanced by the increase in activation potential. Therefore only a minor reduction between the first and second stages can be registered, followed by a substantial decline of total LMP in the third and fourth stages.

All in all, the external wall is a crucial parameter that has a significant influence on energy demand as well as LMP. The highest decrease in energy demand and the lowest reduction of LMP can be achieved from stage one to two. All subsequent stages decrease energy demand as well as LMP significantly.

9.4.2 Window

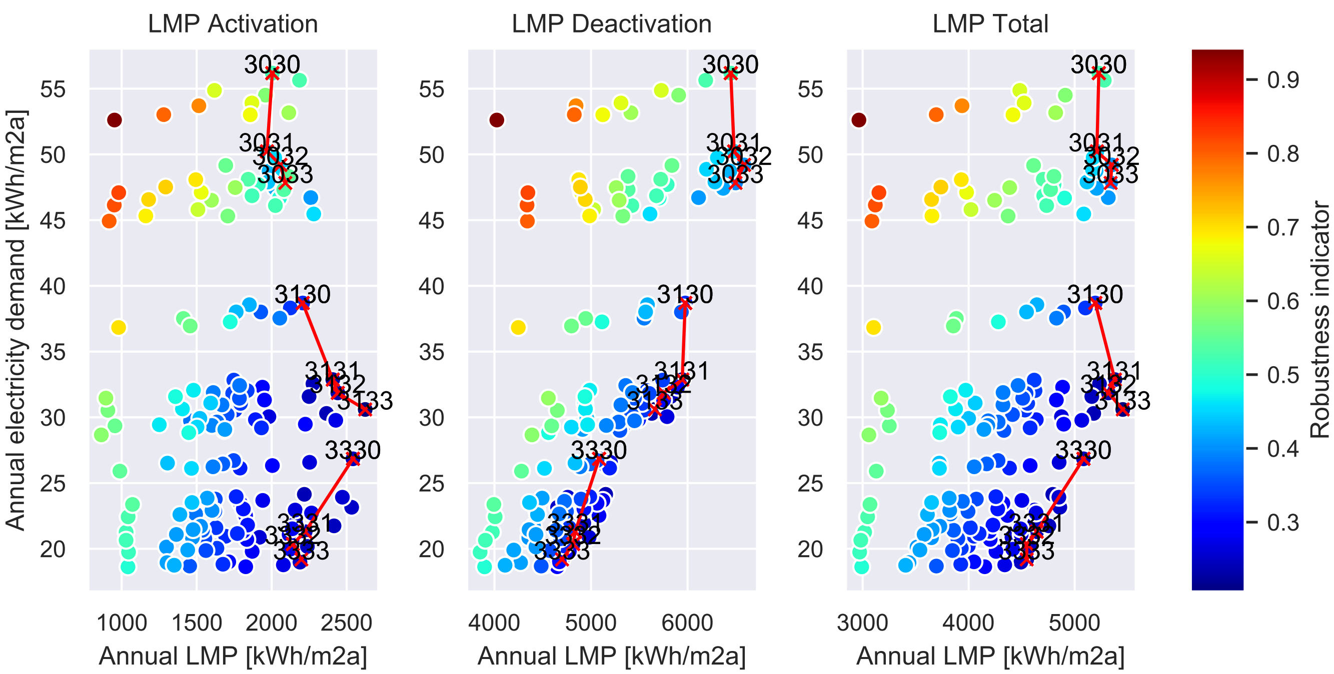

Figure 9.7 Parameter impact | window insulation

Figure 9.7 visualizes the impact of different window-qualities on LMP and energy demand. The shown variants (low, medium, and high wall insulation) are representative of the effects caused by different windows.

The window quality has a significant impact on energy demand. With an increasing stage, energy demand decreases due to increased thermal resistance. The overall reduction of energy demand by window-replacement is up to 30 %. The highest energy reduction can be achieved from stage one to two. Further improvements only deliver small performance gains.

The influence on LMP is ambiguous and depends on the insulation-level of the external-wall.

In low-insulated buildings, the window quality has next to no impact on LMP. The activation-potential shows a small increase due to a higher activation capacity. Deactivation-potential, as well as total-LMP, show no discernible impact.

In medium-insulated buildings, an increase of activation potential, and decrease of deactivation potential is registered.

In highly insulated-buildings, the quality of windows has a significant impact on LMP. No matter if activation- or deactivation-potential are considered, increased window quality causes a steady decrease of LMP. The decrease of LMP is in proportion to the decrease in energy demand.

9.4.3 Screed thickness

Figure 9.8 visualizes the impact of the screed thickness on LMP and energy demand. The shown variants represent the range of insulation qualities considered in this study with maximum coverage of the active-layer.

The screed thickness has minimal influence on energy demand. A negligible rise in energy demand can be recorded in the low- and medium-insulated building, due to the increased thermal mass that needs to be heated and is partially lost. In the high- and very-high insulated buildings, energy demand remains constant.

On the other hand, screed thickness has a strong influence on LMP. The effect is evident for all age classes, as well as for activation and deactivation potential.

In all except the low-insulated building, the first to the second stage is most influential in regards to activation-potential, followed closely by the third to the fourth stage. This effect is attributed to the reaction speed of the underfloor-heating. The first stage is only supplied by minimum screed coverage, which leads to an immediate reaction to changes in the heating power. The step from the first to the second

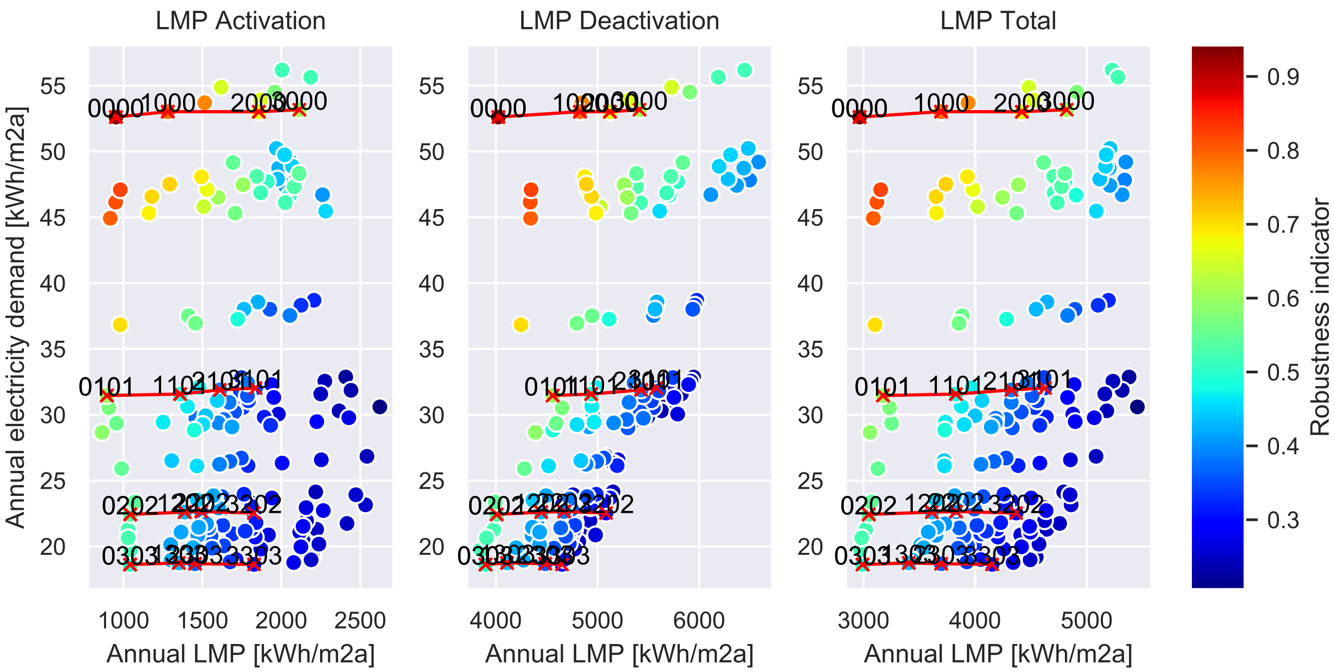

Figure 9.8 Parameter impact | screed thickness

stage means a doubling of coverage, resulting in much higher thermal inertia and thus higher activation potential. Stepping up from the third stage to the maximum screed-thickness causes an overall change of behavior of the heat transmission system in highly insulated buildings. Due to the very high thermal inertia, the underfloor-heating is operated continuously with low power, resembling a component-activation system. This results in very long activation times and high activation potential.

9.4.4 Active-layer coverage

Figure 9.9 visualizes the impact of the active-layer position on energy-demand and LMP. The shown variants represent the range of insulation qualities considered in this study.

The impact on energy demand is mainly dependent on the insulation-quality of the considered building. The higher the overall insulation-level, the lower the impact on energy demand. Generally, energy demand increases with increasing coverage. This can be attributed to the share of heating-power lost before it can be supplied to the zone. Since the coverage stands in correlation to the time the heat takes to spread through the screed, a higher potential for heat loss exists in buildings with high thermal inertia. This effect is predominant in buildings with poor thermal insulation.

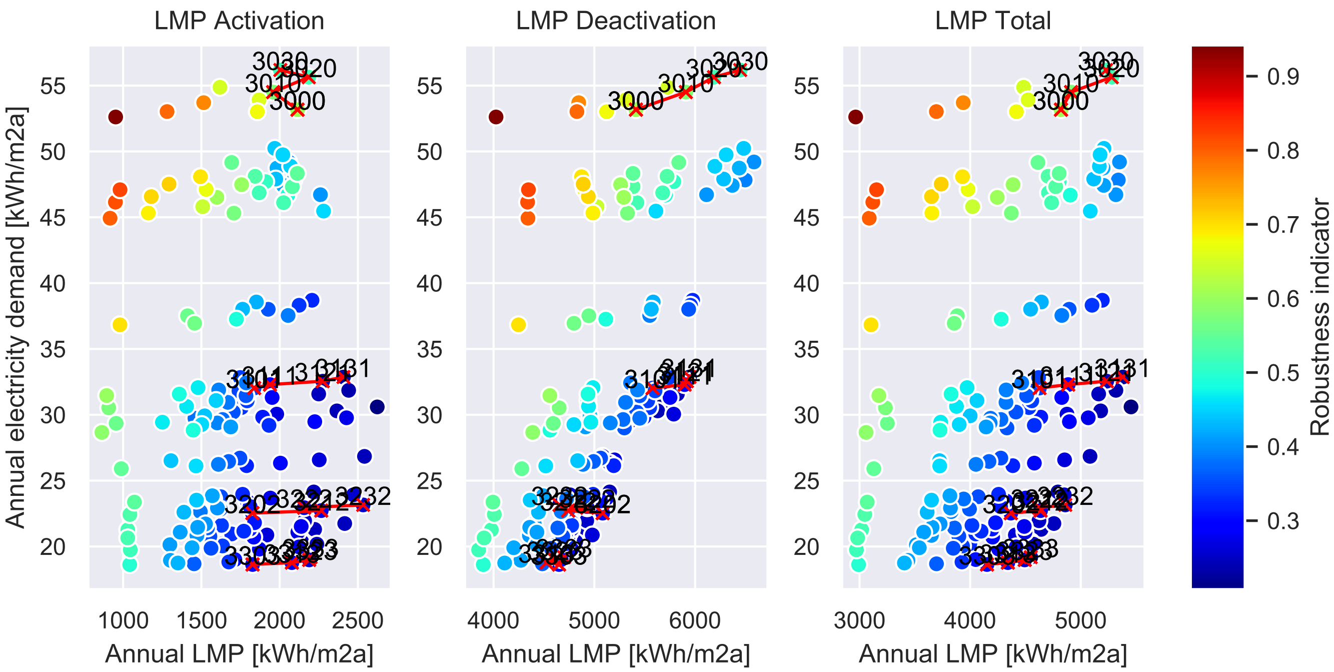

Figure 9.9 Parameter impact | active-layer coverage

In terms of LMP, the impact of the active-layer position is significant for all insulation-levels. For low insulated buildings, deactivation potential increases most due to the rise in energy-demand with higher coverage. In the case of higher insulation levels, LMP is mainly driven through activation-potential, due to higher thermal inertia. Higher thermal inertia allows for longer activation-times and thus higher total activation power. Gains in deactivation-potential through higher coverage can be mainly attributed to the increased energy demand.

9.4.5 Sensitivity-analysis

In the following, the previous findings are summarized in a sensitivity analysis of the parameter-impact. A typical boxplot is not applicable since all possible parameter combinations are evaluated, which would result in 256 separate boxplots. Therefore a method is developed that allows us to consider only the impact of one parameter for various starting situations. The parameter impact is implemented as the maximum difference for LMP and energy demand for each starting situation. The resulting data is then visualized in a boxplot. In general, a high mean corresponds to a major impact of the parameter on the given optimization-objective. Widespread results indicate a significant dependence on the starting conditions. Consequently,

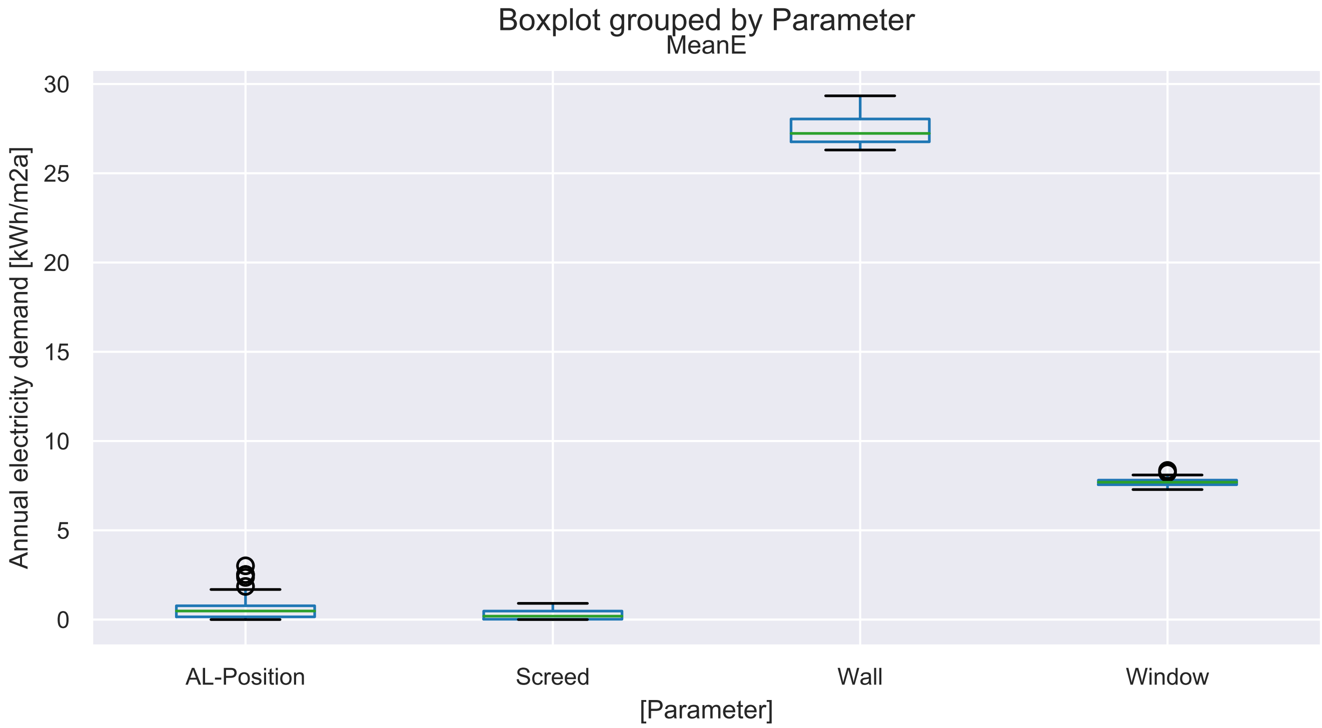

Figure 9.10 Parameter sensitivity energy demand

a small spread indicates an independent parameter. In the following section, the sensitivity is analyzed for energy-demand, as well as LMP.

Figure 9.10 visualizes the impact of the four parameters on energy demand. The wall-construction is predominant. However, the spread of results indicates a significant dependence on other parameters. Second in impact on energy demand is the window-quality. Contrary to the wall-construction, it exhibits next to no spread and is therefore independent of other parameters. The position of the active layer has only a minor influence. Its impact is prone to major variations. A negligible impact is registered for the screed thickness.

Figure 9.11 visualizes the impact of the four parameters on LMP. The highest impact can be attributed to screed thickness as well as the construction of the wall. The impact of screed-thickness, however, is more sensitive to other parameters and shows a high spread of results. The window-type, as well as the position of the active layer, are second in impact. An adaption of the window leads to a predictable amount of change, which is only subject to minor fluctuations. The coverage of the active layer, on the other hand, is significantly dependent on other variables.

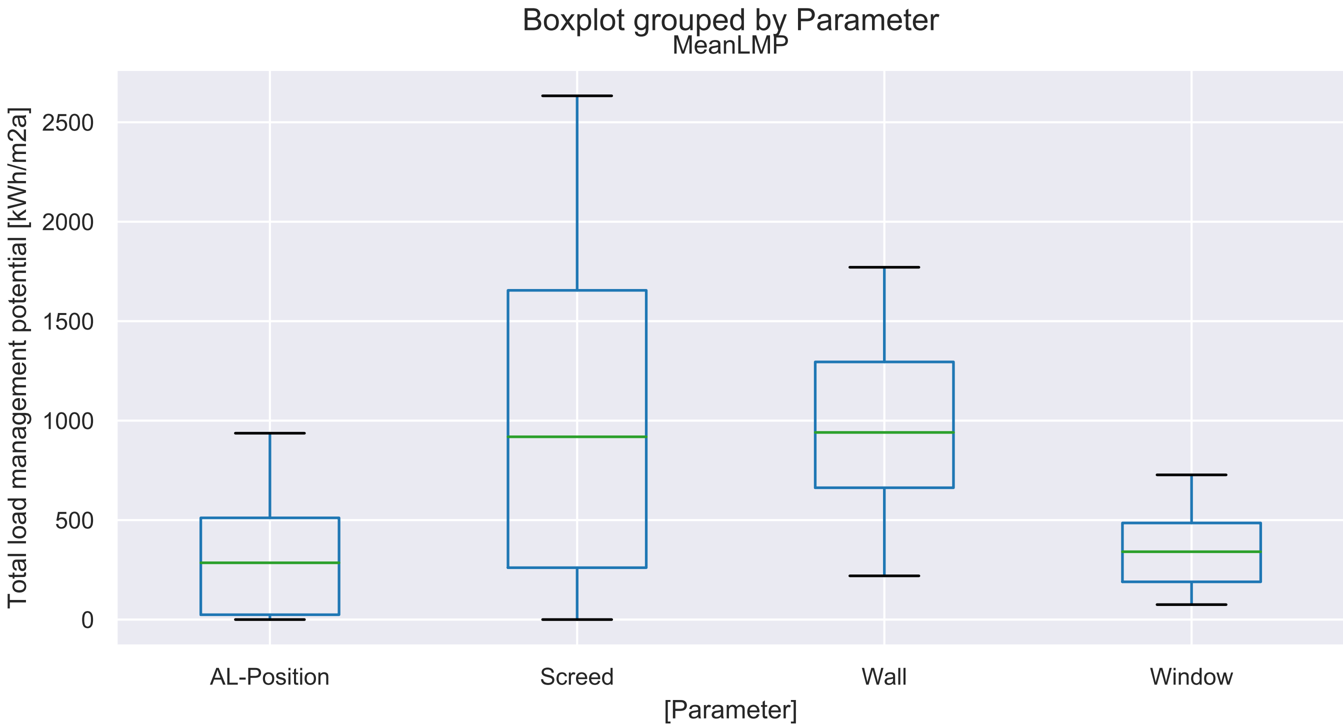

Figure 9.11 Parameter sensitivity load management potential

9.5 Impact of scenarios

The impact of scenarios is crucial for the robust optimization. The following section will analyze the effect of each scenario. A sensitivity analysis will identify the most influential scenarios.

9.5.1 Occupational-scenario

Figure 9.12 visualizes the impact of occupational uncertainty on LMP and energy demand. Occupational uncertainty is modelled through increased internal gains, representing the additional load caused by converting a living space to an office space. The exemplary variants cover the whole input range. The determined impact is representative of all variants.

The increased internal gains positively impact energy demand. The reduction is independent of other parameters and accounts for about 5 kWh/m^2a. The reduction can be attributed to the reduced heating load since increased internal gains replace it.

The effect on LMP is less ambigous. In the case of activation potential, the effect on LMP is strongly dependent on the thermal-inertia and insulation-level of a building. Generally, no decisive influence can be

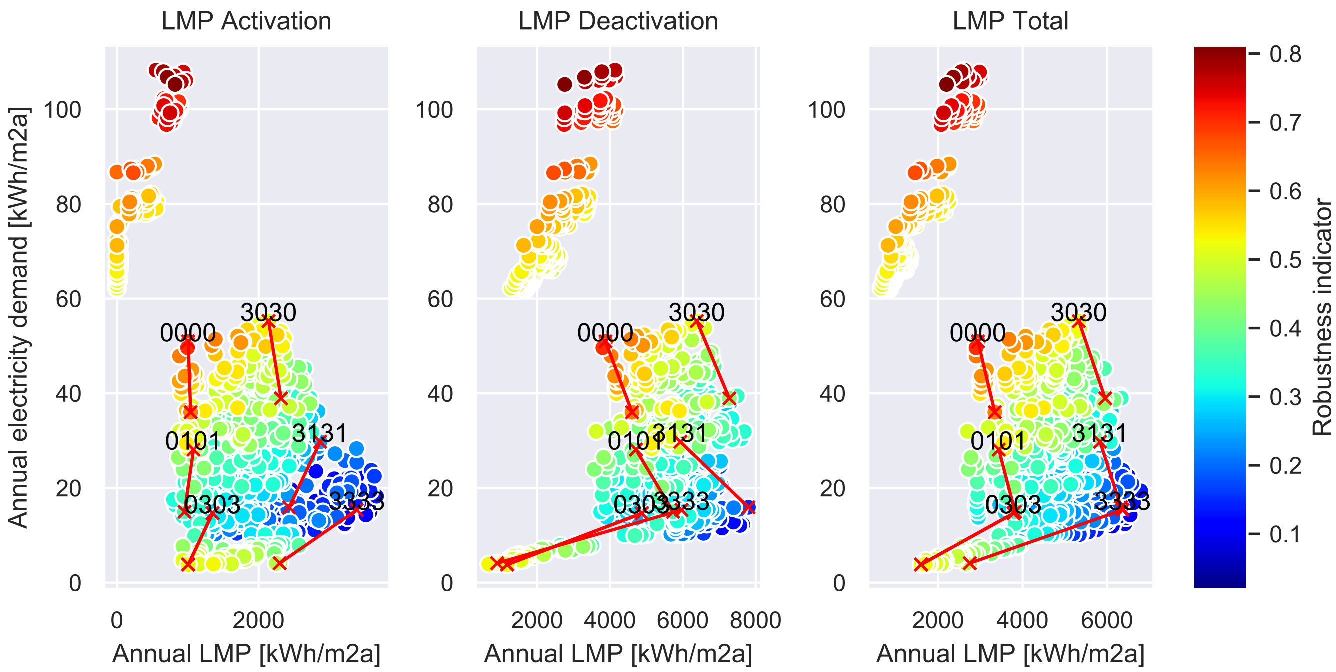

Figure 9.12 Occupational scenario impact

detected in the case of low insulation level. However, considering highly insulated buildings, a decrease in activation-potential in proportion to its thermal inertia is registered. This is due to the additional heat-gain, which reduces the activation time in highly insulated buildings crucially.

In the case of deactivation-potential, the impact is mainly dependent on the insulation level. Low to medium insulated buildings show an increase, due to the prolonged deactivation-time. In the case of highly-insulated buildings, LMP decreases significantly, since the internal gains provide nearly all required heating power. Therefore, no power to deactivate is available.

9.5.2 Usage-scenarios

In the following section the usage scenarios are assessed. Two scenarios have been implemented in this study, the first checks the effect of a constant air change rate through permanent ventilation, in the second case the absence of user ventilation and its impact on load management potential and energy demand is examined.

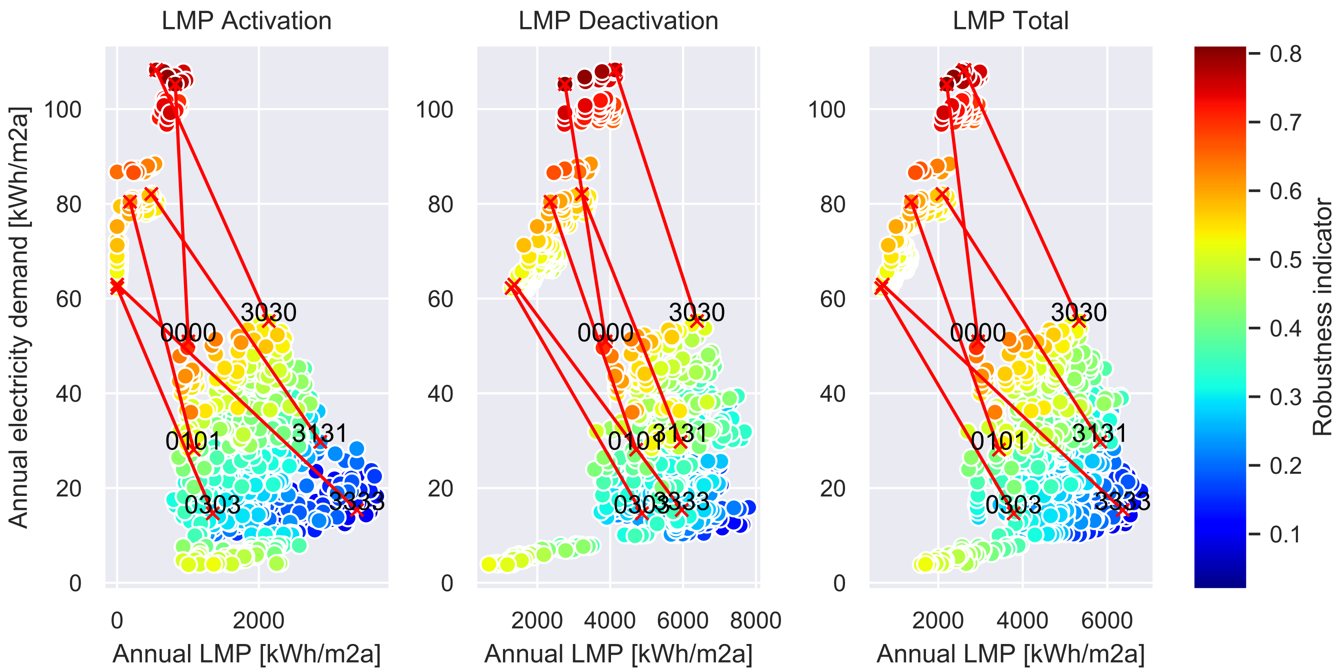

Figure 9.13 Usage scenario impact | constant ventilation

Constant ventilation

Figure 9.13 visualizes the impact of constant ventilation on energy demand and LMP. The exemplary variants cover the whole input range and are representative of all variants.

Constant-ventilation proves to be the most impactful scenario to energy demand. It results in an up to a five-times increase of about 20 kWh/m^2a, is independent of thermal-inertia or insulation level. The increased heating demand can be attributed to increased ventilation losses.

Constant ventilation has a major impact on LMP. Especially, the activation potential of medium and high insulated buildings is close to zero since the heating system can not deliver enough power to compensate for the ventilation losses and is therefore continuously operating at 100 %. The thermal-inertia has next to no impact on activation energy.

Deactivation-potential is strongly reduced in this scenario. Even though more power can be deactivated, it is dominated by the significantly reduced deactivation-time.

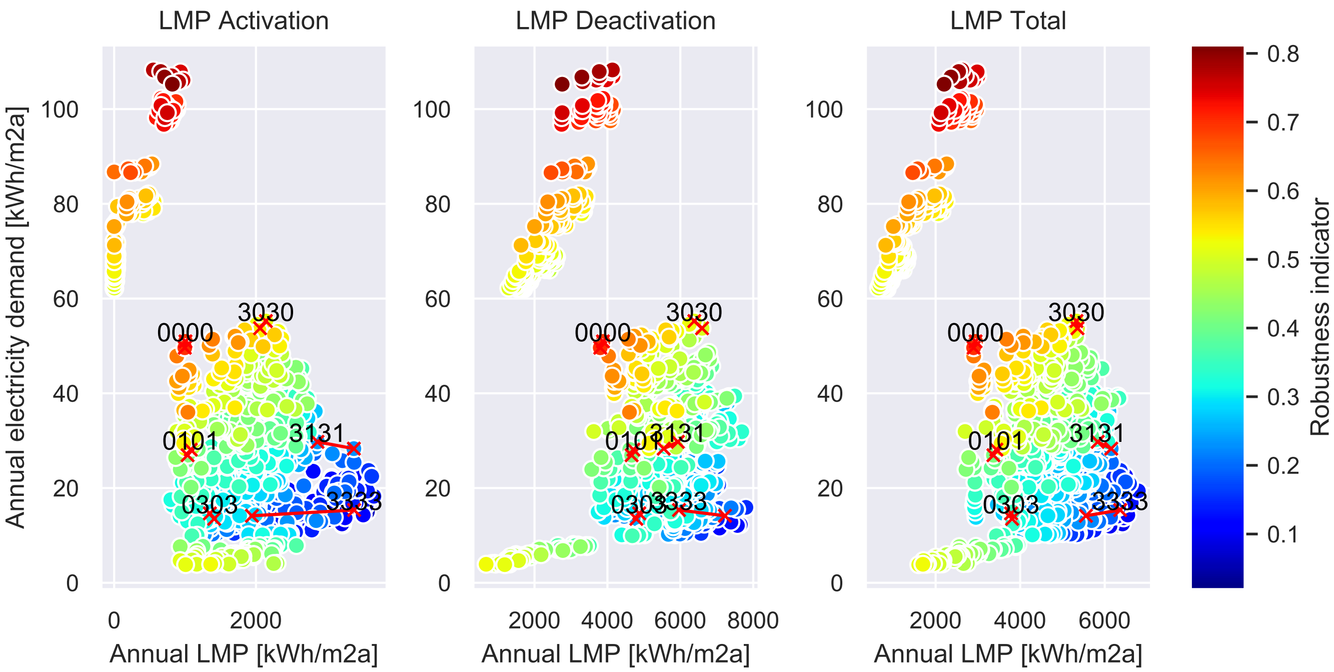

Figure 9.14 Usage scenario impact | no ventilation

No ventilation

Figure 9.14 visualizes the impact that no-ventilation has on the results. As this study only provides the legally required minimum air change rate, the difference in air-change is marginal. In practice, a higher impact can be expected.

The effects of no-ventilation on energy demand are minimal. All scenarios register a constant decrease by about 0.5 kWh/m^2a. This can be fully attributed to the reduced ventilation losses.

In most cases, the effect on LMP is negligible as well. Highly insulated variants with high thermal inertia make an exception. These react strongly, even to this minor change in the air-change rate. Considering activation-potential, the reduction of air-change causes a strong decrease due to the reduced activation time. Deactivation potential, on the other hand, increases, since deactivation-time is prolonged. Considering the total LMP, the effects are counterbalancing each other, leading to hardly any impact.

9.5.3 Climate-scenarios

Figure 9.15 visualizes the impact of climate change (2050) on LMP and energy demand.

Due to increased average temperatures, energy demand is reduced for all variants. The reduction is higher in the cases of lower insulated buildings since these have a less thermal resistance.

Activation-potential is negatively affected only in the case of medium and high insulated buildings with high thermal inertia. As explained in the previous section, these variants are sensitive to additional heating loads during activation (higher average temperatures), which significantly shortens activation time.

In deactivation potential, only an insignificant correlation to insulation-level and thermal inertia can be detected. The increased average temperature results in a much longer deactivation-times. Together with a reduced deactivation-power, a slight increase in deactivation-potential is the result.

Figure 9.16 visualizes the impact of climate change (2080), to uphold comparability, the same variants as used in the 2050- scenario are chosen.

Since the average temperatures in the 2080 scenario are even higher, the trend of reduced energy demand shown in figure 9.15 is continued, and even lower energy-demand is achieved.

Results for activation and deactivation for variants with low-thermal inertia are as expected and ar in line to the trends examined in the 2050 scenario. An exception to this are the results achieved for the activation-potential of medium-insulated, high-inertia variants. Instead of a reduction of activation-potential an increase is registered. Higher external temperatures cause the activation-time to further decrease. Therefore, the rise can be attributed to a higher available activation-power, due to lower base-load. Furthermore, the reduced base-load leads to a higher available storage capacity of the thermal mass. This retarding effect does not take place in very high insulated buildings, due to the low heating power available.

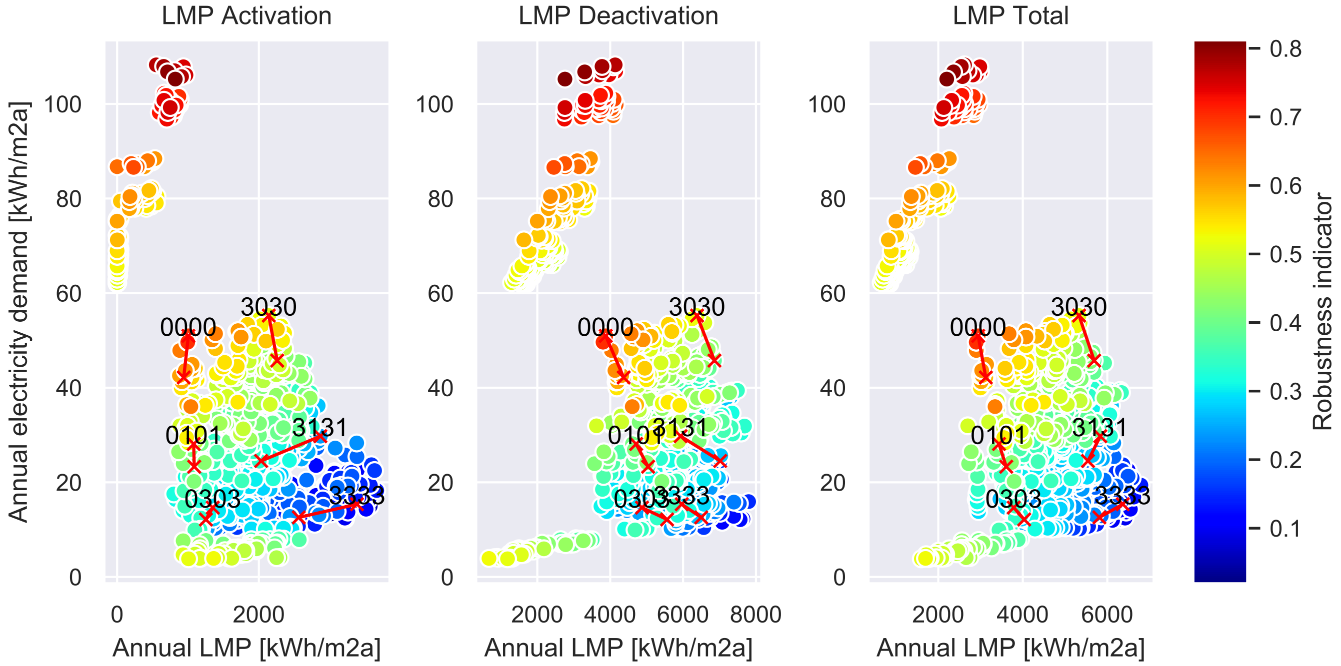

Figure 9.15 Climate scenario impact | 2050

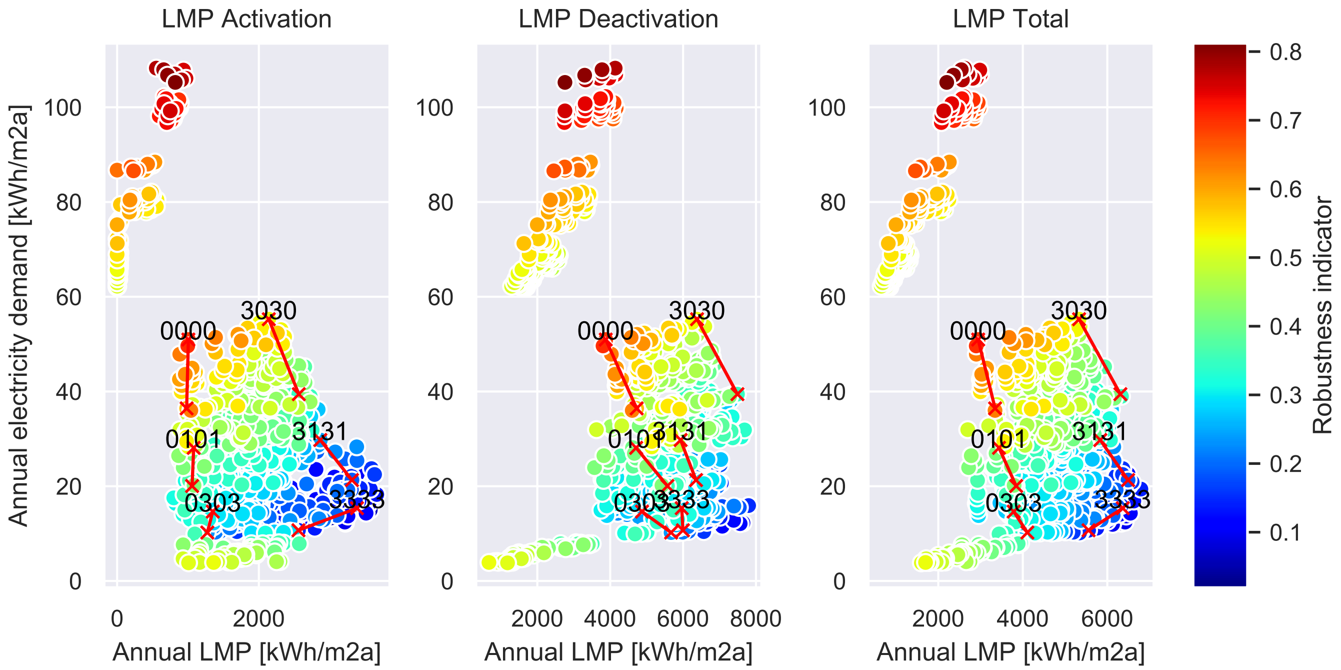

Figure 9.16 Climate scenario impact | 2080

9.5.4 Technological-scenario

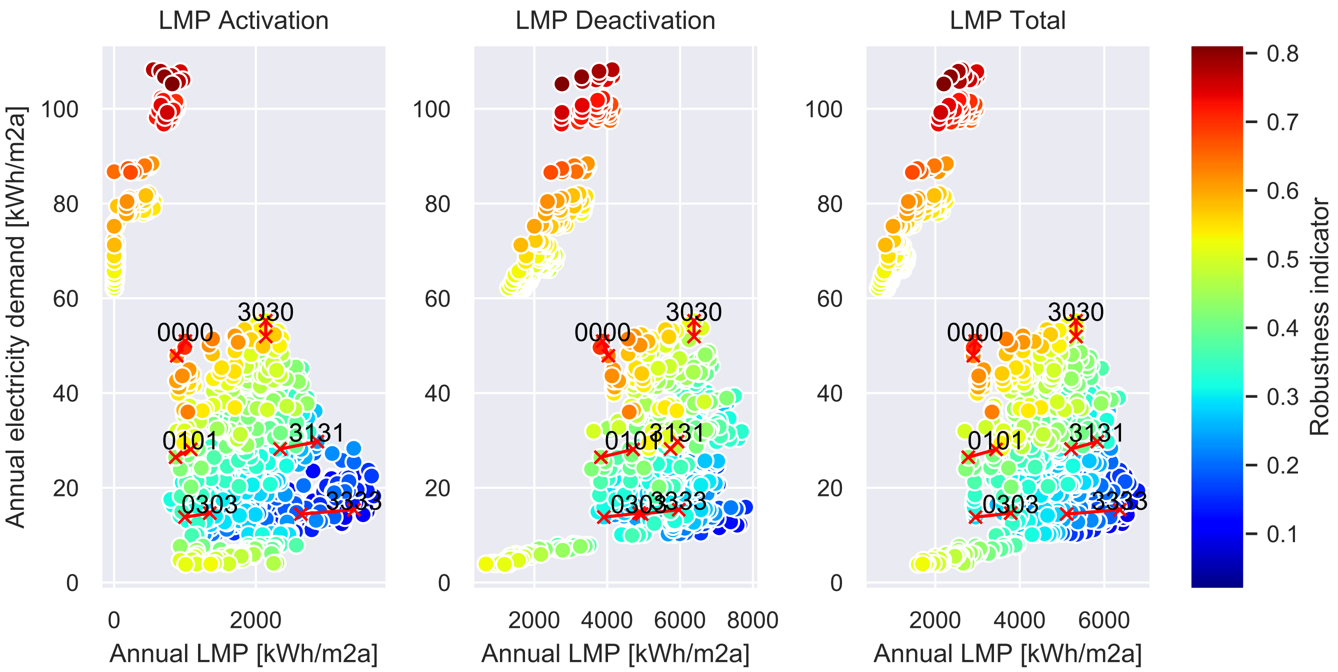

Figure 9.17 Technological scenario impact

Figure 9.17 visualizes the impact of utilizing internal- instead of external-insulation.

An energy-reduction is registered, which is disproportional to the insulation-level of the building. This can be attributed to the energy required to heat the thermal mass of the external walls. As some of this heat is lost, additional heating demand is disproportional to the thermal resistance of the envelope.

Internal-insulation causes a reduction of activation- and deactivation-potential, proportional to the insulation-level. This is due to the amount of power that can no longer be stored during activation or released during deactivation.

9.5.5 Sensitivity-analysis

The impact, which the individual scenarios have on the optimization-parameters is compared in the following sensitivity analysis. The methodology introduced in section 9.4.5 is applied below.

Figure 9.18 visualizes the impact, which each scenario poses on LMP. Constant-ventilation is most impactful and strongly reduces LMP. However its impact is dependent on other parameters. Second in impacts is the occupational scenario. Depending on the boundary conditions, it may lead to a slight increase of LMP, in the case of low-insulated buildings, or a major decrease, if buildings with high insulation

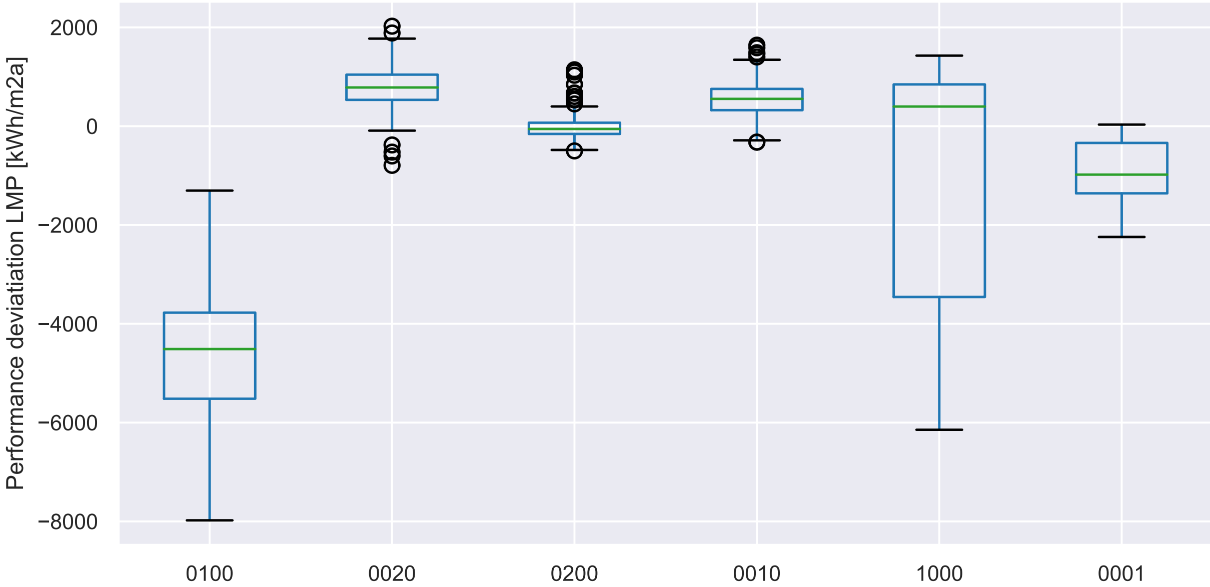

Figure 9.18 Scenario sensitivity | LMP

and thermal inertia are considered. Third in impact is the technological-scenario. It is responsible for a drop in LMP. Both climate scenarios affect LMP positively. No-ventilation has next to no impact.

Figure 9.19 visualizes the impact each scenario has on electricity consumption. Inline to previous findings, the constant air-change rate is most impactful. It exhibits by far the highest deterioration of energy demand and is nearly independent of other parameters. A positive impact is registered for the occupational scenario and both climate-scenarios due to reduced heating-energy. Each of these scenarios is only prone to minor fluctuations. Internal-insulation and no-ventilation have next to no influence on electricity consumption.

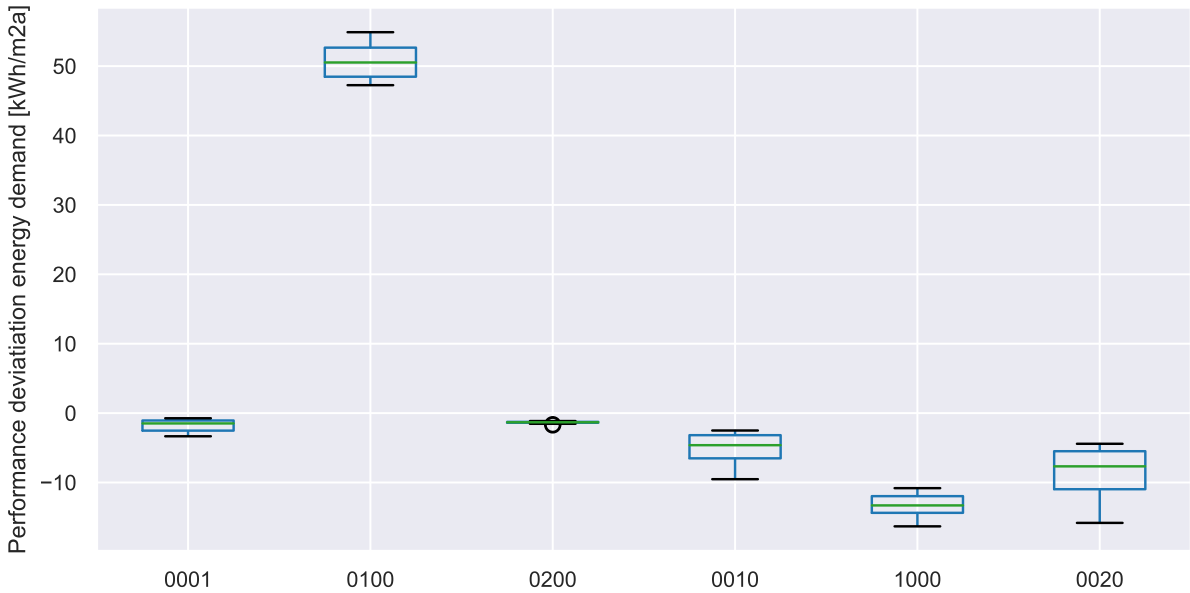

Figure 9.19 Scenario sensitivity | energy demand

9.6 Pareto front

The Pareto-front identifies non-dominated solutions in a result-set of two or more optimization objectives. An analysis of the pareto-optima is conducted in the following section.

Figure 9.20 visualizes the Pareto-front for the aggregated data-set. Significant differences can be identified between the course of deactivation-potential and activation-potential. The latter only includes high insulated buildings, all variants, that require more than 30 kWh/m^2a are dominated by variant 3133. It is noticeable that except variant 0303, with the overall lowest energy consumption, all Pareto-optima are comprised of variants with maximum screed-thickness since these allow achieving maximum LMP. Coverage tends to be very-high in the case of low- and medium insulated buildings and decreases with increasing insulation level.

In the case of deactivation-potential, the Pareto front extends up to low-insulated buildings. All except two optima show maximum screed thickness.

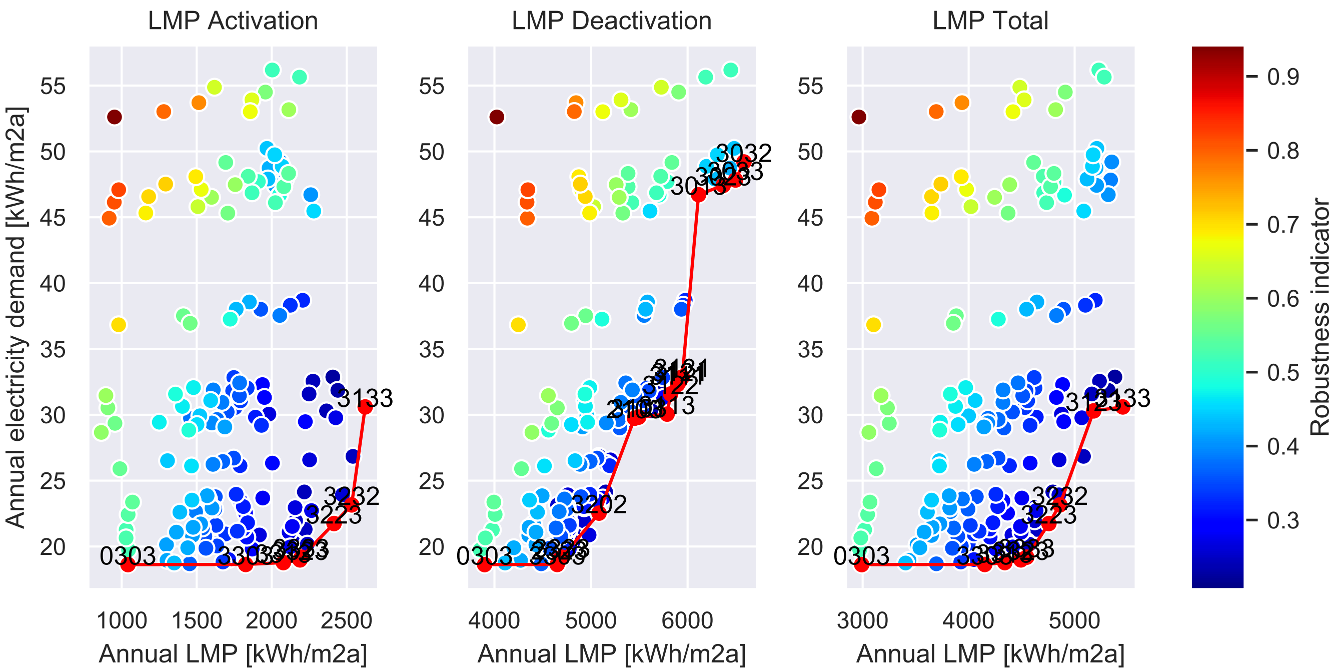

Figure 9.20 Pareto front

9.7 Refurbishment strategies

The following section brings together all previously identified results to create robust refurbishment strategies. The section is subdivided in a general description of the methodology (section 9.7.1), the definition of the boundary conditions (section 9.7.2), the refurbishment-measures (section 9.7.3), refurbishment-focus (section 9.7.4), the considered base-cases and their modelling (section 9.7.5), the final strategies (section 9.7.6) as well as an interpretation of the derived strategies (section 9.7.7).

9.7.1 Methodology

Since each existing building is different, refurbishment strategies need to be applicable to a range of different starting conditions. The developed methodology is based on the assumption that for each starting point, different approaches may be applicable. It is not the aim to develope a "one-fits-all" solution but rather find individual for different energy-standards.

Therefore, the refurbishment strategies are individually developed for each starting condition. The various base cases aim to represent the different building types in the building stock.

Three refurbishment-measures are available for each base-case distinguished by the required effort. Finally, for each of these methods, a focus can be chosen that determines the weight between energy demand and LMP.

9.7.2 Boundary conditions

Following boundary conditions are defined to sort out infeasible refurbishment strategies and select an optimum.

- **Wall insulation > window insulation**: A wall insulation level exceeding the energy standard of the window is not allowed since it takes more effort and expenses to refurbish the wall than the windows.
- **Downgrade**: A decrease of the energy standard is not allowed, even if it results in a higher LMP.
- **Pareto-optima**: If possible, optimized variants have to be on the Pareto-front.
- **Lower expense**: If the difference between the two variants is negligible, the variant with lower refurbishment steps is taken.
- **No optimization**: If the variant is already part of the Pareto-front, no optimization is necessary.

9.7.3 Refurbishment measures

The chosen refurbishment measures aim to represent the different depths of interventions, usually applied in practice. The different measures may be constricted by the required expenses, effort, or regulations. Each subsequent measure integrates the previous ones.

- Building technology: Since this study seeks to optimize energy demand and LMP, the minimum measure required is a change in building technology. The parameters regarding building technology are screed-thickness, active layer coverage, as well as a change to an electricity based heating system.
- Window: The second refurbishment measure is focused on enhancing the insulation-level of the windows. It is performed simultaneously to an exchange of the building-technology. The adapted parameters are window insulation-level, as well as a replacement of the building technology.
- Envelope: The third refurbishment measure is a comprehensive refurbishment of a building. It is comprised of an upgrade of the external-wall, a window replacement, and an exchange of the building technology. Therefore, all available parameters are optimized.

9.7.4 Refurbishment focus

For each refurbishment strategy, the final variants are chosen based on individual requirements, with regards to LMP and electricity-consumption. Choosing the balance between these optimization objectives is key in selecting a suitable variant. Therefore a focus can be chosen for each refurbishment-measure:

- 25% energy: The weights of the objective function are distributed 75% in favor of LMP and 25% to energy demand. Therefore, LMP dominates the choice of optimal variants.
- 50% energy: The weights of the objective function are equally distributed between energy demand and LMP. The variants represent a balanced optimum between LMP and energy consumption.
- 75% energy: The weights of the objective function are distributed 75% in favor of energy demand and 25% for LMP. Therefore, the required electricity dominates the selection of the variables.

Since it has been shown in figure 9.10 that building-technology has a negligible impact on energy demand, a weighing will only be conducted for the window and envelope refurbishment.

9.7.5 Base-cases

In the following section, the definition of the base-model is conducted. Furthermore, the steps required to model and simulate the base-models are elaborated.

Base-models are selected by generating all combinations of window- and wall-insulation-levels within the boundary conditions defined in section 9.7.2. This results in a set of ten base-models that represent each energy-standard present in the building stock.

For each of these base-models, a LMP simulation is conducted to set the improvements through refurbishment in context. Base-cases are modeled with radiators instead of underfloor-heating since these are the most widespread heating transmission system in the building-stock [Auer et al., 2017]. The implementation of the system is based on the type 1231 of the TESS-library for TRNSYS. Since the type is not available in TRNLizard by default, it has been implemented as a plugin to TRNLizard. A heat-pump is chosen as a heating-system in order to be able to compare LMP between the base-cases and optimized-variants. Energy consumption is then calculated according to the approach described in section 8.2.1 with an assumed inlet-temperature of 55℃. Apart from these modifications, the process resembles that in section 6.1.

9.7.6 Strategies

The derived refurbishment strategies, as well as their performance gains compared to the base-model, are illustrated in the table in the following two pages. A symbolic representation of the parameter combinations is chosen to enhance readability. The improvements shown in the second table correspond to the order of the first. Each cell is subdivided to facilitate a separate consideration of energy demand and LMP. Improvements are given as percentual-gains (LMP) or percentual-reduction(energy) compared to the base-case. All compared values are mean values over all scenarios. The cells are color-coded to identify variants with the highest refurbishment potential. If no refurbishment is possible since the base-case has already reached an optimum, it is greyed out. If one variant is applicable for more than one refurbishment-focus or -measures, the cells are joined to highlight especially versatile variants.

The individual variants are chosen based on the boundary conditions defined in section 9.7.2. Selection is based on the MMR robustness-indicator. The weight between LMP and energy demand corresponds to the refurbishment-focus. The variant, which performs best and fulfills all conditions, is chosen. This process is repeated for each base-case, refurbishment-measure, and refurbishment-focus.

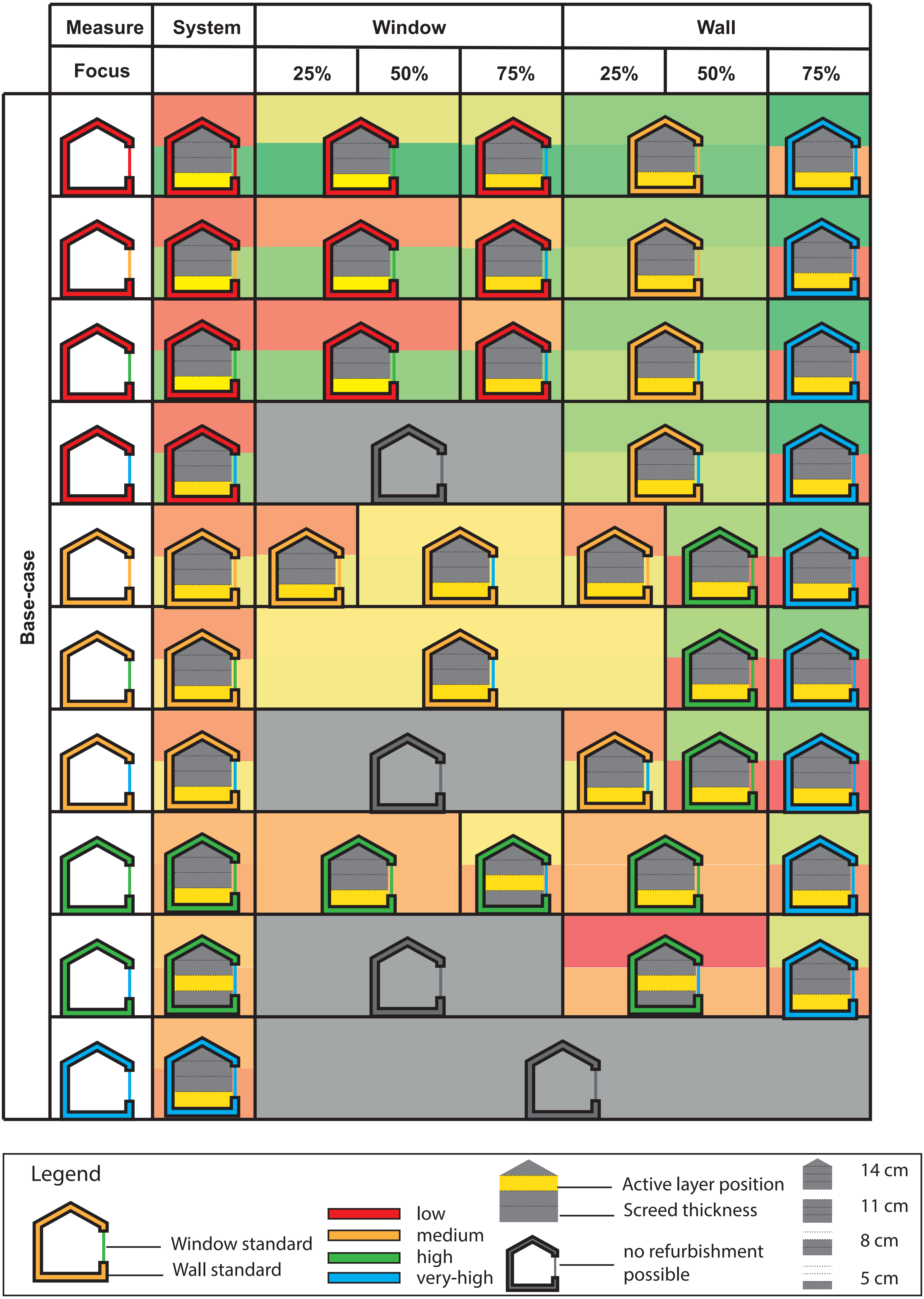
Measure
System
Window
Wall
Focus
25%
50%
75%
25%
50%
75%
Base-case
Legend
Window standard
Wall standard
low
medium
high
very-high
Active layer position
Screed thickness
no refurbishment possible
14 cm
11 cm
8 cm
5 cm

<table>
<tr><th>Measure</th><th>System</th><th colspan="3">Window</th><th colspan="3">Wall</th></tr>
<tr><th>Focus</th><th></th><th>25%</th><th>50%</th><th>75%</th><th>25%</th><th>50%</th><th>75%</th></tr>
<tr><td>Energy</td><td>- 25 %</td><td colspan="2">- 35 %</td><td>- 37 %</td><td colspan="2">- 56 %</td><td>- 75 %</td></tr>
<tr><td>LMP</td><td>+ 124 %</td><td colspan="2">+ 129 %</td><td>+ 128 %</td><td colspan="2">+ 122 %</td><td>+ 83 %</td></tr>
<tr><td>Energy</td><td>- 26 %</td><td colspan="2">- 27 %</td><td>- 29 %</td><td colspan="2">- 51 %</td><td>- 72 %</td></tr>
<tr><td>LMP</td><td>+ 111 %</td><td colspan="2">+ 115 %</td><td>+ 114 %</td><td colspan="2">+ 108 %</td><td>+ 72 %</td></tr>
<tr><td>Energy</td><td>- 26 %</td><td colspan="2">- 26 %</td><td>- 28 %</td><td colspan="2">- 54 %</td><td>- 71 %</td></tr>
<tr><td>LMP</td><td>+ 115 %</td><td colspan="2">+ 115 %</td><td>+ 114 %</td><td colspan="2">+ 106 %</td><td>+ 72 %</td></tr>
<tr><td>Energy</td><td>- 26 %</td><td colspan="3" rowspan="2"></td><td colspan="2">- 52 %</td><td>- 70 %</td></tr>
<tr><td>LMP</td><td>+ 112 %</td><td colspan="2">+ 105 %</td><td>+ 70 %</td></tr>
<tr><td>Energy</td><td>- 27 %</td><td>- 27 %</td><td colspan="2">- 32 %</td><td>- 27 %</td><td>- 48 %</td><td>- 57 %</td></tr>
<tr><td>LMP</td><td>+ 98 %</td><td>+ 98 %</td><td colspan="2">+ 97 %</td><td>+ 98 %</td><td>+ 71 %</td><td>+ 64 %</td></tr>
<tr><td>Energy</td><td>- 27 %</td><td colspan="4">- 30 %</td><td>- 47 %</td><td>- 56 %</td></tr>
<tr><td>LMP</td><td>+ 93 %</td><td colspan="4">+ 96 %</td><td>+ 70 %</td><td>+ 63 %</td></tr>
<tr><td>Energy</td><td>- 27 %</td><td colspan="3" rowspan="2"></td><td>- 27 %</td><td>- 45 %</td><td>- 54 %</td></tr>
<tr><td>LMP</td><td>+ 96 %</td><td>+ 96 %</td><td>+ 70 %</td><td>+ 64 %</td></tr>
<tr><td>Energy</td><td>- 28 %</td><td colspan="2">- 28 %</td><td>- 32 %</td><td colspan="2">- 28 %</td><td>- 40 %</td></tr>
<tr><td>LMP</td><td>+ 83 %</td><td colspan="2">+ 85 %</td><td>+ 83 %</td><td colspan="2">+ 85 %</td><td>+ 78 %</td></tr>
<tr><td>Energy</td><td>- 29 %</td><td colspan="3" rowspan="2"></td><td colspan="2">- 24 %</td><td>- 37 %</td></tr>
<tr><td>LMP</td><td>+ 85 %</td><td colspan="2">+ 85 %</td><td>+ 78 %</td></tr>
<tr><td>Energy</td><td>- 28 %</td><td colspan="6" rowspan="2"></td></tr>
<tr><td>LMP</td><td>+ 79 %</td></tr>
</table>

9.7.7 Interpretation

In the following, the refurbishment scenarios are interpreted. Generally, a significant improvement is registered for energy demand and LMP in all variants. This can be attributed to the replacement of radiators by underfloor-heating, which improves LMP through incorporated thermal mass and lowers energy consumption since higher COPs are achievable, due to lower inlet-flow temperatures. Therefore, only the switch from radiators to underfloor heating reduces electricity demand by 24% and increases LMP by 63% in the worst-case.

The highest individual improvements of LMP and energy demand can be achieved in the base-case with low insulation on the windows and walls. Already a replacement of the heat transmission system improves LMP by 124%. The overall maximum LMP increase of 129% is accomplished by improving the window standard to high-insulation level and replacing the radiators by underfloor heating with very high thermal inertia. A maximum energy reduction of 75% can be reached by upgrading windows and walls to the highest insulation-level.

The most significant improvements for energy demand and LMP together can be made by conducting an envelope-refurbishment for low insulated base-cases. A balanced focus leads to medium-insulated external walls with high-insulated windows. These variants manage to improve LMP up to 122% and reduce energy-demand by about 53%. If a full envelope refurbishment is not feasible (e.g., historical preservation), a sole upgrade of the windows to high insulation-levels is second in overall efficiency and achieves a improvement of 129% in LMP and 35% in energy demand.

A pattern can be identified that variants with a focus on LMP are often also optimal for balanced focus. This is in line to the findings in section 9.2, attributing a high robustness to MMR if LMP focused variants are assessed. In comparison, energy-focused variants are less robust and only perform optimal in a narrow field of application. Medium wall insulation and very-high window insulation is the most chosen variant, being valid in twelve cases as good performance in both objectives make it universaly applicable. Second to this is maximum insulation level for both windows and walls. However, except for the last base-case, it is exclusively present in the energy-focused envelope refurbishment strategy and does not demonstrate a high versatility. Overall, assessing all refurbishment-strategies, medium wall insulation is the most applied envelope refurbishment. Very-high insulation is the most chosen refurbishment strategy, if windows are considered. Maximum screed-thickness and -coverage are preferred in the case of building technolgy parameters.

It can be concluded that high thermal mass is crucial in refurbishment. The position of the active-layer is near as unambiguous. Maximum coverage performs best for all except one variant. The combination of both traits makes for a building system with very high thermal inertia.

Assessing the color-code in the second table, a proportional decrease of refurbishment-efficiency to base-insulation-level is evident. Therefore most potential in terms of LMP increase and energy reduction can be unlocked in low insulated buildings. Diminishing returns at increasing expenses are the result; the higher the energy standard of the existing building. Therefore, refurbishment should start at the lowest insulation level and work its way up in order to unlock the maximum-potential efficiently.

Part III

Summary

10 Discussion

The following chapter discusses the results and sets them into relation to previous studies. Section 10.1 lists all findings that have been made. These are then compared in section 10.2 to previous results in literature. An exemplary application in section 10.3 illustrates the achieved improvements. An assessment of the limitations and restrictions of the study is performed in section 10.4.

10.1 Findings

The following section lists all findings that have been made in this study.

The chosen methodology has been proven to be well implementable in the existing TRNSYS and TRN-Lizard framework. However, it has been shown to be very computational intensive in terms of storage and computing time.

The external-parallelization approach is best suited to minimize total simulation time for this study and achieves a time-reduction of 83% compared to single-process simulations.

The implemented interactive visualization approach eases result analysis and allows for a better comprehension of the data.

The pre-screening of different parameters identified following most impactful parameters: wall-insulation, screed-thickness, active-layer-coverage, window-insulation, as well as internal instead of external insulation.

The evaluation of the refurbishment-strategies indicates that maximum refurbishment efficiency can be unlocked in uninsulated buildings. Upgrading the walls with an insulation layer of 4cm, installing double glazed windows and exchanging the heating system by underfloor heating unlocks the maximum potential.

The highest improvements of load management potential can be achieved in uninsulated buildings if double glazed windows and a heating system with high thermal inertia is used. This identifies espescially listed buildings as target group.

Choosing the balanced or LMP-focused refurbishment strategy leads to more robust variants. Energy-focused solutions solely perform well in predefined cases.

The comparison showed that replacing radiators by underfloor heating unlocks significant improvements in LMP and energy demand.

Analyzing the variants on the Pareto-front showed that very high thermal inertia through maximum screed-thickness and high coverage delivers optimum results. This dependence has also been proven in the analysis of the impact of screed-thickness and coverage.

The min-max-regret indicator creates more robust optima compared to the weighted median-spread indicator.

The constant-ventilation scenario was most impairing on LMP and energy demand. The occupational and technological scenario impact LMP heavily if very high insulated buildings are considered. The climate scenarios have a slightly beneficial impact on LMP and energy demand.

Energy demand is most sensitive to the wall- and window-insulation. LMP is sensitive to all parameters. However, screed-thickness has the foremost impact.

An evaluation of the parameter-courses showed that an increase of insulation-level from low to medium causes a minor decrease in LMP and a high decrease in energy demand. However, all further increase causes a high decrease of LMP and a regressing decrease in energy demand.

Screed-thickness and active-layer position mainly influence LMP. A higher coverage and higher screed-thickness always increases LMP.

The detailed examination of the scenario-impacts show that variants with high-thermal inertia and high-insulation level react strongly to changing conditions. However, even though results are impaired, they still outperform variants with lower thermal-inertia.

The course of the Pareto-fronts show, that activation-potential performs best, only if medium- to very-high insulation levels are chosen. Deactivation potential, however, achieves the highest LMP in the case of low insulated buildings.

In direct comparison, a discrepancy between activation- and deactivation-potential is shown. The calculation methodology leads to deactivation-potential being assessed under ideal conditions, whereas activation-potential is examined under slightly disadvantageous circumstances. Therefore, comparability is given only within each metric. This is mitigated by an aggregated metric, which includes activation- as well as deactivation-potential.

Medium wall insulation, high window-insulation and very-high thermal inertia achieves the best balance between LMP and energy demand.

10.2 Comparison to previous studies

In the following section, the findings are compared to previous studies in this field and how the new results add value. Its main predecessors are the studies of [Hausladen, 2014] and [Auer et al., 2017].

[Hausladen, 2014] assessed LMP under static conditions and first introduced the load-management-potential calculation methodology. The study conducted an encompassing assessment of impacting factors on LMP and derived recommendations based on a parameter study. Fixed parameter sets were defined differntiating in building typology and age-class. Neither did [Hausladen, 2014] take energy consumption into account, nor uncertain conditions or conduct an optimization.

[Auer et al., 2017] assessed LMP under dynamic conditions. The study examined the integration of buildings in the electricity grid in detail. However, only fixed parameter sets were assessed depending on typology and age-class. It evaluated load-management-potential on a national scale rather than on building scale. Uncertain conditions were only introduced in regards to refurbishment scenarios and renewable energy coverage.

This study assesses LMP and energy consumption simultaneously under dynamic conditions. Furthermore, it does not work with fixed parameter sets but rather parametrizes the most sensitive parameters in order to optimize them. The studies' focus is on individual buildings and seeks to provide optimized refurbishment strategies. Optimization is conducted under uncertain future conditions in order to receive the most robust parameter configuration.

To summarize, this study adds value to existing research by assessing LMP and energy demand in a multiobjective optimization under uncertain conditions, by which actual robust refurbishment strategies are derived.

10.3 Exemplary application

In the following section, the benefits of the developed refurbishment strategies will be demonstrated in an exemplary case. A conversion of 10% of the building-stock, built before 1978, is considered, in order to unlock load-management-potentials. The assessed floor area equals to about 102 million square meters, which is about 1.6% of the total floor area in Germany [Auer et al., 2017]. The optimized refurbishment strategies will be compared to the sole replacement of the heating system. It is assumed that all of the considered buildings have the lowest insulation standard for windows- and walls.

By replacing fossil-fuel based heating-systems by heat-pumps, an increase in the electricity demand of the domestic-sector is the result. A replacement of the heating systems, without further refurbishment measures, causes an additional electricity demand of 4.74 TWh/a. Compared to Germany's total domestic sector consumption of 129 TWh/a [AG Energiebilanzen e.V., 2018], this equals to a rise of 4%. In average, a load-management-capacity of 137 GWh is available during the heating-period, which is about 3.4 times the storage capacity available through water-storage-power-plants (40 GWh [Faulstich et al., 2013]).

Choosing an optimized refurbishment strategy significantly increases the load-management-capacity and simultaneously lowers the electricity consumption. Only by replacing the radiators by an optimized underfloor heating system, an increase of the storage-capacity to 313 GWh (= 7.8 times water-storage-power-plants capacity) can be achieved. Furthermore, it lowers the electricity consumption of the domestic sector by 1% compared to the base-case. Further improvements in energy demand can be achieved by replacing the windows and the envelope. If a LMP focused strategy is chosen, load management potential is not compromised and remains at 313 GWh. If only windows are replaced, 1.6% less electricity is required. A full envelope-refurbishment results in a 2.6% reduction compared to the base-case. If minimizing the additional electricity is vital, choosing the energy-focused envelope-refurbishment causes an increase of 1.2 TWh electricity-consumption (1% of domestic electricity consumption; 3.5% reduction). However, this is paid for by a lowered load-management-capacity of 263 GWh (= 6.6 times the water-storage-power-plants capacity).

To summarize, by applying the robust refurbishment strategies in this exemplary-case, the load-management-capacity can be more than doubled even though less additional electricity is required. Therefore, to reach the same load-management-capacity, less than half of the floor-area has to be converted. Together with the lower electricity consumption, this outweighs the higher initial effort by far.

10.4 Limitations and restrictions

The following limitations have been identified for this study.

The load-management-potential calculation methodology applied in this study is focused on providing equal starting conditions by pre-charging the thermal mass previous to simulation. However, this does not take dynamic effects of subsequently conducted load management measures into accout. Therefore, the resulting LMP resembles more a maximum potential for each hour. This is especially relevant since the projected annual load management potential does not represent the actual available storage capacity since individual load management measures would interfere with each other. Therefore, the given methodology proved well in making an objective comparison between different variants and assess their overall load management potential. However, it was not able to determine the actual available LMP under dynamic conditions.

A further limitation is induced by basing the optimization on a full-factorial-study, which is computational extensive. Therefore, limitations to the number of parameters, parameter steps, and assessed time frame had to be made to keep the number of simulations in check. Even though parameters and type-days have been carefully chosen to provide maximum coverage of the design-space, simplifications have been made, which will impact the results.

The decision to focus this study solely on one building typology in the domestic sector has been made due to simulation and time constraints. Even though the typology has been carefully chosen and sufficiently represents the domestic sector, non-domestic buildings have been neglected. This is especially relevant since non-domestic buildings could provide an LMP during summer, due to cooling-power being available. Therefore, the conducted study can only assess load management potential during the heating-period.

11 Conclusion

The final chapter concludes this study and summarizes the key arguments. It restates the research question and hypothesis and verifies if all objectives have been met. Furthermore, the most important findings and contribution of this study are repeated. A final recommendation for the future direction of research concludes this study.

Three research questions have been defined in the introduction of the study. Each of these was successfully answered. Several Pareto-optima have been found for energy demand and load management potential through conducting a multiobjective optimization of both objectives simultaneously. These optima have proven to perform best, even under uncertain conditions, which has been checked in seven scenarios. Furthermore, the impacts on LMP and energy demand have been analyzed in detail in the result chapter, and all key correlations have been identified.

The hypothesis has been made, that robust refurbishment strategies can be defined for load management potential and energy consumption through a robust optimization. This is proven true since detailed refurbishment strategies have been created based on the findings of the robust optimization study. Significant improvements have been ascertained compared to unoptimized variants.

All set research objectives could be achieved. Robust optimization was conducted by choosing the optimization framework by a literature review. A full-factorial optimization was chosen, which includes scenarios to assess robustness. Two different robustness indicators evaluate the results. The boundary-conditions, and LMP calculation methodology, have been adpoted from previous studies to uphold comparability. The TRNSYS implementation was successfully created through extensions to the grasshopper-TRNSYS interface TRNLizard. Its efficiency was further increased by developing an optimized multiprocessing-procedure for this study. A custom post-processing gathered, processed, and visualized the data. Based on this data, refurbishment strategies have been successfully developed. The last objective to assess the improvements was also met by comparing the optimized variants to base-cases.

The most important findings from this study are as follows. The replacement of radiators by underfloor heating unlocks significant improvements in LMP and energy demand, which outweigh the required additional effort. Choosing balanced or LMP-focused refurbishment strategies lead to more robust results than energy-focused refurbishment. Maximum refurbishment efficiency can be unlocked in uninsulated buildings. Upgrading the walls with an insulation layer of 4cm, installing double glazed windows and exchanging the heating system by underfloor heating unlocks the maximum potential. An even higher load management potential can be achieved at the costs of energy demand if no refurbishment of the facade is conducted. This identifies espescially listed buildings as target group.

The following key limitations have been identified in this study. Due to the calculation methodology, the annual potential is not equal to actual storage capacity, and dynamic effects are not taken into account. Furthermore, the parameter-steps, as well as the assessment of only one typology, is owed to the restrictions caused by the required number of simulations in a full-factorial study.

Based on the findings and restrictions of this study, following future directions of research can be recommended.

Conducting a robust optimization of LMP and energy demand with a mathematical optimization instead of a full factorial study would facilitate a higher resolution of individual parameters. This would allow for a more detailed analysis of parameter impact and even more precise refurbishment strategies.

Furthermore, conducting a full-year study and integrating non-residential buildings would enable us to assess heating- as well as cooling demand and evaluate LMP during summer. This would provide a holistic picture of load management potential.

Finally, a dynamic assessment of LMP with continuous simulation would facilitate a more realistic estimation of load-management potential and allows for a direct evaluation of annual storage capacity compared to other energy-storage technologies.

A Appendix

A.1 Glossary

Term	Explanation
Load-management-potential	Integrated shiftable power over a certaint time-frame
Load-management-simulation	Simulation to assess the load management potential
Action-point	Analyzed hour in a load management-simulation
Start- / Stop-moment	Absolute start and stop time of each simulation
Deactivation-time	Duration, in which temperatures are within the comfortband during the deactivation-strategy
Activation-time	Duration, in which temperatures are within the comfortband during the activation-strategy
Resolution	Temperature increment at which load management potential will be assessed
Comfort-band	Range of comfortable operative temperatures in which LMP simulations are allowed
Initial-temperature	The initial setpoint temperature at which the base-simulations are operated
Load-management-strategy	Measures to shift loads over a certain timespan

Term	Explanation
Base-simulation	Annual simulations with constant setpoints; needed to assess LMP
Deactivation-strategy	Perform load management through deactivation of the heating system
Activation-strategy	Perform load management through activation of the remaining capcity of the heating system
Hour of year	Absolute hour of the year, ranges from 0 to 8760
Variant	Unique combination of design-parameters
Parameter	Modifiable simulation-setting, which is integrated in the robust optimization study
Variant-name	Unique identifier of a variant
Parameter-stage	Discretized parameter steps used in the robust optimization study
Uncertainty-parameter	Parameter, which is used in order to model uncertain future conditions
Design-parameter	Parameter, which is optimizated
Activation-potential	Load-management-potential if solely the activation-strategy is regarded
Deactivation-potential	Load-management-potential if solely the deactivation-strategy is regarded
Total-potential	Average load-management-potential derived from activation- and deactivation-potential
Type-day	Representative day for a defined temperature-band
Single-processing	Non parallelized conduction of thermal simulations
Thread	Individual process on a multi-core processor
Instance	Individual simulation in a set of parallelized simulations
Processor	Processing unit of a computer

Table A.1 Glossary

A.2 Additional data

Office (new / concrete core activation)	very hot	hot	warm	moderate	cool	cold	very cold
activation potential daytime	++	++	++	++	++	+	+
activation potential nighttime	++	++	++	++	+	+	+
deactivation potential daytime	o	o	o	o	o	o	+
deactivation potential nighttime	o	o	o	o	+	+	++

Table A.2 Load management potential Office (new/concrete core activation), data sourche: [Hausladen, 2014]

Office (new)	very hot	hot	warm	moderate	cool	cold	very cold
activation potential daytime	o	+	+	o	+	+	++
activation potential nighttime	o	o	o	++	+	+	o
deactivation potential daytime	++	+	+	o	o	o	o
deactivation potential nighttime	o	o	o	o	+	+	++

Table A.3 Load management potential Office (new), data sourche: [Hausladen, 2014]

Office (old)

	very hot	hot	warm	moderate	cool	cold	very cold
activation potential daytime	o	+	+	o	o	+	++
activation potential nighttime	o	o	o	+	++	++	+
deactivation potential daytime	++	+	o	o	o	+	+
deactivation potential nighttime	o	o	o	+	++	+	o

Table A.4 Load management potential Office (old), data sourche: [Hausladen, 2014]

Apartment house (new)

	very hot	hot	warm	moderate	cool	cold	very cold
activation potential daytime	o	o	o	+	o	o	o
activation potential nighttime	o	o	o	o	o	o	o
deactivation potential daytime	o	o	o	o	o	o	+
deactivation potential nighttime	o	o	o	o	o	o	+

Table A.5 Load management potential Apartment house (new), data sourche: [Hausladen, 2014]

Apartment house (old)

	very hot	hot	warm	moderate	cool	cold	very cold
activation potential daytime	o	o	o	+	++	o	o
activation potential nighttime	o	o	o	++	o	o	o
deactivation potential daytime	o	o	o	o	+	o	o
deactivation potential nighttime	o	o	o	o	o	o	o

Table A.6 Load management potential Apartment house (old), data sourche: [Hausladen, 2014]

Single Family home (new)

	very hot	hot	warm	moderate	cool	cold	very cold
activation potential daytime	o	o	o	++	o	+	o
activation potential nighttime	o	o	o	o	+	o	o
deactivation potential daytime	o	o	o	o	+	o	++
deactivation potential nighttime	o	o	o	+	o	+	++

Table A.7 Load management potential single family home (new), data sourche: [Hausladen, 2014]

Single Family home (old)

	very hot	hot	warm	moderate	cool	cold	very cold
activation potential daytime	o	o	o	o	++	o	o
activation potential nighttime	o	o	o	o	o	+	o
deactivation potential daytime	o	o	o	+	o	+	o
deactivation potential nighttime	o	o	o	o	o	o	o

Table A.8 Load management potential single family home (old), data sourche: [Hausladen, 2014]

Bibliography

[Adamski, 2007] Adamski, M. (2007). Optimization of the form of a building on an oval base. *Building and Environment*.

[AG Energiebilanzen e.V., 2018] AG Energiebilanzen e.V. (2018). Auswertungstabellen zur Energiebilanz Deutschland. 1990 bis 2017 (Stand Juli 2018). (030).

[Al-Homoud, 2005] Al-Homoud, M. S. (2005). A Systematic Approach for the Thermal Design Optimization of Building Envelopes. *Journal of Thermal Envelope and Building Science*.

[Al-Homoud, 2009] Al-Homoud, M. S. (2009). Envelope thermal design optimization of buildings with intermittent occupancy. *Journal of Building Physics*.

[Anderies, 2014] Anderies, J. M. (2014). Embedding built environments in social-ecological systems: Resilience-based design principles. *Building Research and Information*.

[Andersson, 1997] Andersson, P. (1997). Robustness of technical systems in relation to quality, reliability and associated concepts. *Journal of Engineering Design*.

[Auer and Endres, 2017] Auer, T. and Endres, M.-e. (2017). Parameterstudie Low-Tech Bürogebäude.

[Auer et al., 2013] Auer, T., Franke, L., Kaufmann, H., Winter, S., Ott, S., Krechel, M., Gehlen, C., and Thiel, C. (2013). Einfach Bauen. *Einfach Bauen*.

[Auer et al., 2017] Auer, T., Hamacher, T., Wagner, U., and Atabay, D. (2017). Gebäude als intelligenter Baustein im Energiesystem. Lastmanagement-Potenziale von Gebäuden im Kontext der zukünftigen Energieversorgungsstruktur in.

[Bandara and Attalage, 2012] Bandara, R. M. P. S. and Attalage, R. a. (2012). Optimization Methodologies for Building Performance Modelling and Optimization. *National Engineering Conference, 18th ERU Symposium*, pages 32–37.

[Ben-Tal et al., 2009] Ben-Tal, A., El Ghaoui, L., and Nemirovski, A. (2009). *Robust optimization. Princeton series in applied mathematics*. Princeton University Press.

[Bettis and Hitt, 1995] Bettis, R. A. and Hitt, M. A. (1995). The new competitive landscape. *Strategic Management Journal*.

[BMU, 2019] BMU (2019). Klimaschutz in Zahlen : Der Sektor Gebäude. page 150.

[BMVBS, 2009] BMVBS (2009). Bekanntmachung der Regeln für Energieverbrauchskennwerte und der Vergleichswerte im Nichtwohngebäudebestand. *Bundesministerium für Verkehr, Bau und Stadtentwicklung, BMVBS*.

[Bouchlaghem and Letherman, 1990] Bouchlaghem, N. M. and Letherman, K. M. (1990). Numerical optimization applied to the thermal design of buildings. *Building and Environment*.

[Burhenne et al., 2010] Burhenne, S., Jacob, D., and Henze, G. P. (2010). Uncertainty Analysis in Building Simulation With Monte Carlo Techniques. In *SimBuild 2010*.

[Buso et al., 2015a] Buso, T., Fabi, V., Andersen, R. K., and Corgnati, S. P. (2015a). Occupant behaviour and robustness of building design. *Building and Environment*.

[Buso et al., 2015b] Buso, T., Fabi, V., Andersen, R. K., and Corgnati, S. P. (2015b). Occupant behaviour and robustness of building design. *Building and Environment*, 94:694–703.

[Castro-Lacouture et al., 2009] Castro-Lacouture, D., Sefair, J. A., Flórez, L., and Medaglia, A. L. (2009). Optimization model for the selection of materials using the leed green building rating system. In *Building a Sustainable Future - Proceedings of the 2009 Construction Research Congress*.

[Chalupnik et al., 2013] Chalupnik, M. J., Wynn, D. C., and Clarkson, P. J. (2013). Comparison of ilities for protection against uncertainty in system design. *Journal of Engineering Design*.

[Chinazzo et al., 2015a] Chinazzo, G., Rastogi, P., and Andersen, M. (2015a). Assessing robustness regarding weather uncertainties for energy-efficiency-driven building refurbishments. In *Energy Procedia*, volume 78, pages 931–936.

[Chinazzo et al., 2015b] Chinazzo, G., Rastogi, P., and Andersen, M. (2015b). Assessing robustness regarding weather uncertainties for energy-efficiency-driven building refurbishments. In *Energy Procedia*.

[Chlela et al., 2007] Chlela, F., Husaunndee, A., Riederer, P., and Inard, C. (2007). A statistical method to improve the energy efficiency of an office building. In *IBPSA 2007 - International Building Performance Simulation Association 2007*, pages 1756–1764.

[D'Cruz and Radford, 1987] D'Cruz, N. A. and Radford, A. D. (1987). A multicriteria model for building performance and design. *Building and Environment*.

[de Wilde and Tian, 2009] de Wilde, P. and Tian, W. (2009). Identification of key factors for uncertainty in the prediction of the thermal performance of an office building under climate change. *Building Simulation*.

[De Wit, 1997] De Wit, M. S. (1997). Identification of the important parameters in thermal building simulation models. *Journal of Statistical Computation and Simulation*, 57(1-4):305–320.

[Deutsche Energie-Agentur GmbH (dena), 2012] Deutsche Energie-Agentur GmbH (dena) (2012). Handbuch Lastmanagement.

[Dirlich et al., 2011] Dirlich, S., Gruhler, K., Deilmann, C., Petereit, R., Petereit, K., Kunz, C., Hempel, A., and Markfort, D. (2011). Typologie und Bestand beheizter Nichtwohngebäude in Deutschland. *BMVBS-Online-Publikation*, 16:2011.

[Discher et al., 2010] Discher, H., Hinz, E., and Enseling, A. (2010). „Wirtschaftlichkeit energetischer Modernisierung im Mietwohnungsbestand,". *Deutsche Energie-Agentur GmbH (dena), Berlin*, 9.

[Druitt and Früh, 2012] Druitt, J. and Früh, W. G. (2012). Simulation of demand management and grid balancing with electric vehicles. *Journal of Power Sources*.

[Endres et al., 2019] Endres, M.-e., Franke, L., Dong, M. S., and Neubert, L. (2019). Parameters to Design Low-Tech Strategies. *JANUARY 17TH 2019 – MUNICH POWERSKIN CONFERENCE | PROCEEDINGS,*, pages 1–11.

[Evins, 2013] Evins, R. (2013). A review of computational optimisation methods applied to sustainable building design.

[Faulstich et al., 2013] Faulstich, M., Foth, H., Calliess, C., Hohmeyer, O., Holm-Müller, K., Niekisch, M., and Schreurs, M. (2013). 100% erneuerbare Stromversorgung bis 2050: klimaverträglich, sicher, bezahlbar. Sachverständigenrat für Umweltfragen (SRU), Berlin, 2010.

[Frenzel and Hiller, 2014] Frenzel, C. and Hiller, M. (2014). TRNSYSLIZARD – Open Source Tool Für Rhinocerus – Grasshopper. *Fifth German-Austrian IBPSA Conference*, pages 490–496.

[Goldberg, 1989] Goldberg, D. (1989). Genetic algorithms in search, optimization, and machine learning. *Choice Reviews Online*.

[Hamby, 1995] Hamby, D. M. (1995). A comparison of sensitivity analysis techniques. *Health Physics*.

[Hamdy et al., 2009] Hamdy, M., Hasan, A., and Siren, K. (2009). Combination of optimisation algorithms for a multi-objective building design problem. In *IBPSA 2009 - International Building Performance Simulation Association 2009*.

[Hamdy et al., 2011] Hamdy, M., Hasan, A., and Siren, K. (2011). Applying a multi-objective optimization approach for Design of low-emission cost-effective dwellings. *Building and Environment*.

[Hasan et al., 2008] Hasan, A., Vuolle, M., and Sirén, K. (2008). Minimisation of life cycle cost of a detached house using combined simulation and optimisation. *Building and Environment*.

[Hausladen, 2014] Hausladen, G. (2014). Lastverhalten von Gebäuden unter Berücksichtigung unterschiedlicher Bauweisen und technischer Systeme Speicher- und Lastmanagementpotenziale in Gebäuden. page 113.

[Hooke and Jeeves, 1961] Hooke, R. and Jeeves, T. A. (1961). Direct search solution of numerical and statistical problems. *Journal of the ACM (JACM)*.

[Hopfe and Hensen, 2011] Hopfe, C. J. and Hensen, J. L. (2011). Uncertainty analysis in building performance simulation for design support. *Energy and Buildings*, 43(10):2798–2805.

[(IEA) International Energy Agency, 2013] (IEA) International Energy Agency (2013). Annex 55 Reliability of Energy Efficient Building Retrofitting - Probability Assessment of Performance & Cost (RAP-RETRO) - Probabilistic Tools. *Energy Conservation in Buildings and Community Systems*.

[Jentsch et al., 2008] Jentsch, M. F., Bahaj, A. B. S., and James, P. A. (2008). Climate change future proofing of buildings-Generation and assessment of building simulation weather files. *Energy and Buildings*, 40(12):2148–2168.

[Jungwirth, 2014] Jungwirth, J. (2014). Lastmanagement in Gebäuden. Entwicklung einer modellprädiktiven Regelung mit einem adaptiven Gebäudemodell zur Flexibilisierung der Wärme- und Kälteversorgung von Gebäuden. *Dissertation TU München*.

[Keane and Nair, 2005] Keane, A. J. and Nair, P. B. (2005). *Computational approaches for aerospace design: The pursuit of excellence*.

[Klobasa, 2007] Klobasa, M. (2007). *Dynamische Simulation eines Lastmanagements und Integration von Windenergie in ein Elektrizitätsnetz*. PhD thesis.

[Kotireddy, 2018] Kotireddy, R. (2018). *Towards Robust Low-Energy Houses -A Computational Approach for Performance Robustness Assessment using Scenario Analysis*.

[Kotireddy et al., 2017] Kotireddy, R., Hoes, P., and Hensen, J. L. (2017). Simulation-based comparison of robustness assessment methods to identify robust low energy building designs. *Proceedings of 15th IBPSA conference, SanFrancisco, CA, USA*, (Proceedings of 15th IBPSA conference, Sanfransisco, USA):892–901.

[Kotireddy et al., 2015] Kotireddy, R., Hoes, P. J., and Hensen, J. L. (2015). Optimal balance between energy demand and onsite energy generation for robust net zero energy buildings considering future scenarios. In *14th International Conference of IBPSA - Building Simulation 2015, BS 2015, Conference Proceedings*, pages 1970–1977.

[Kotireddy et al., 2019] Kotireddy, R., Hoes, P. J., and Hensen, J. L. (2019). Integrating robustness indicators into multi-objective optimization to find robust optimal low-energy building designs. *Journal of Building Performance Simulation*, 12(5):546–565.

[Loga et al., 2015] Loga, T., Stein, B., Diefenbach, N., and Born, R. (2015). *Deutsche Wohngebäudetypologie - Beispielhafte Maßnahmen zur Verbesserung der Energieeffizienz von typischen Wohngebauden*.

[Macdonald, 2002] Macdonald, I. (2002). Quantifying the Effects of Uncertainty in Building Simulation. *Regulation*, Ph D(July):267.

[Macdonald, 2009] Macdonald, I. A. (2009). Comparison of sampling techniques on the performance of monte-carlo based sensitivity analysis. In *IBPSA 2009 - International Building Performance Simulation Association 2009*.

[Macdonald et al., 1999] Macdonald, I. A., Clarke, J. A., and Strachan, P. A. (1999). Assessing Uncertainty in Building Simulation. *Sixth International IBPSA conference*, pages 683–690.

[Machairas et al., 2014] Machairas, V., Tsangrassoulis, A., and Axarli, K. (2014). Algorithms for optimization of building design: A review.

[Maderspacher, 2017] Maderspacher, J. (2017). *Robuste Optimierung in der Gebäudesimulation: Entwicklung einer Methode zur robusten Optimierung für die energetische Sanierung von Gebäuden unter unsicheren Randbedingungen*. PhD thesis.

[Magnier and Haghighat, 2010] Magnier, L. and Haghighat, F. (2010). Multiobjective optimization of building design using TRNSYS simulations, genetic algorithm, and Artificial Neural Network. *Building and Environment*.

[Marks, 1997] Marks, W. (1997). Multicriteria optimisation of shape of energy-saving buildings. *Building and Environment*.

[Nguyen et al., 2014a] Nguyen, A. T., Reiter, S., and Rigo, P. (2014a). A review on simulation-based optimization methods applied to building performance analysis.

[Nguyen et al., 2014b] Nguyen, A.-t., Reiter, S., and Rigo, P. (2014b). Bpa Nguyen. *Elsevier*, 113:1043–1058.

[Nitsch et al., 2011] Nitsch, J., Pregger, T., Naegler, T., Heide, D., de Tena, D. L., Trieb, F., Scholz, Y., Nienhaus, K., Gerhardt, N., Sterner, M., Trost, T., von Oehsen, A., Schwinn, R., Pape, C., Hahn, H., Wickert, M., and Wenzel, B. (2011). Langfristszenarien und Strategien für den Ausbau der erneuerbaren Energien in Deutschland bei Berücksichtigung der Entwicklung in Europa und global. Technical report.

[O'brien, 2013] O'brien, W. (2013). Occupant-proof buildings: Can we design buildings that are robust against occupant behaviour? In *Proceedings of BS 2013: 13th Conference of the International Building Performance Simulation Association*, pages 1746–1754.

[Olewnik et al., 2004] Olewnik, A., Brauen, T., Ferguson, S., and Lewis, K. (2004). A framework for flexible systems and its implementation in multiattribute decision making. *Journal of Mechanical Design, Transactions of the ASME*.

[Paulus and Borggrefe, 2011] Paulus, M. and Borggrefe, F. (2011). The potential of demand-side management in energy-intensive industries for electricity markets in Germany. *Applied Energy*.

[Ren et al., 2009] Ren, H., Gao, W., and Ruan, Y. (2009). Economic optimization and sensitivity analysis of photovoltaic system in residential buildings. *Renewable Energy*.

[Rhein, 2014] Rhein, B. (2014). Robuste Optimierung mit Quantilmaßen auf globalen Metamodellen.

[Roy et al., 2008] Roy, R., Hinduja, S., and Teti, R. (2008). Recent advances in engineering design optimisation: Challenges and future trends. *CIRP Annals - Manufacturing Technology*.

[Sahab et al., 2013] Sahab, M. G., Toropov, V. V., and Gandomi, A. H. (2013). A Review on Traditional and Modern Structural Optimization: Problems and Techniques. In *Metaheuristic Applications in Structures and Infrastructures*.

[Sahu et al., 2012] Sahu, M., Bhattacharjee, B., and Kaushik, S. C. (2012). Thermal design of air-conditioned building for tropical climate using admittance method and genetic algorithm. *Energy and Buildings*.

[Sarran et al., 2017] Sarran, L., Foteinaki, K., Gianniou, P., and Rode, C. (2017). Impact of Building Design Parameters on Thermal Energy Flexibility in a Low-Energy Building Impact of Building Design Parameters on Thermal Energy Flexibility in a Low-Energy Building. In *15th IBPSA Conference*, pages 239–248.

[T Rössel, F Sänger, 2012] T Rössel, F Sänger, J. S. (2012). SmartBuildings-Implementierung von Lastmanagementsystemen. *VDE-Kongress 2012 - Intelligente Energieversorgung der Zukunft*.

[Tuhus-Dubrow and Krarti, 2010] Tuhus-Dubrow, D. and Krarti, M. (2010). Genetic-algorithm based approach to optimize building envelope design for residential buildings. *Building and Environment*.

[Van Gelder et al., 2014] Van Gelder, L., Janssen, H., and Roels, S. (2014). Probabilistic design and analysis of building performances: Methodology and application example. *Energy and Buildings*, 79:202–211.

[Wang et al., 2005] Wang, W., Zmeureanu, R., and Rivard, H. (2005). Applying multi-objective genetic algorithms in green building design optimization. *Building and Environment*.

[Wei, 2013] Wei, T. (2013). A review of sensitivity analysis methods in building energy analysis.

[Wetter and Wright, 2004] Wetter, M. and Wright, J. (2004). A comparison of deterministic and probabilistic optimization algorithms for nonsmooth simulation-based optimization. In *Building and Environment*.

[Wolf, 2016] Wolf (2016). Hocheffizienz-Wärmepumpen. Technical report.

[Wong et al., 2010] Wong, S. L., Wan, K. K., and Lam, T. N. (2010). Artificial neural networks for energy analysis of office buildings with daylighting. *Applied Energy*.

[Yu and Jin, 2012] Yu, H. X. and Jin, L. (2012). An brief introduction to robust optimization approach. *International Journal of Pure and Applied Mathematics*, 74(1):121–124.

[Zemella et al., 2011] Zemella, G., De March, D., Borrotti, M., and Poli, I. (2011). Optimised design of energy efficient building façades via Evolutionary Neural Networks.

List of Figures

List of Tables

Klimaneutral
Druckprodukt
ClimatePartner.com/12518-1907-1001